The effect of tubulin acetylation and detyrosination on the *in vitro* motility of kinesin-1

by

Neha Kaul

A dissertation submitted in partial fulfillment
of the requirements for the degree of
Doctor of Philosophy
(Mechanical Engineering)
in The University of Michigan
2012

Doctoral Committee:
Professor Edgar Meyhofer, Chair
Professor Ellen M. Arruda
Associate Professor Katsuo Kurabayashi
Associate Professor Kristen J. Verhey

ACKNOWLEDGEMENTS

Binding assays were performed by Virupakshi Soppina, research scientist in the Verhey Lab. COS cell lysates were prepared by him and Steve Norris from the same lab. I have been fortunate in closely collaborating with Viru and I would like to thank both him and Steve for their continued support. I am also grateful to Lynne Blasius and other members of the Verhey lab for valuable guidance with biochemistry and cell biology techniques.

My development as a graduate student would not have been the same without the influence of Kristen Verhey, collaborator and mentor. Her approach to experiments opened up a whole new world to my initially engineering-oriented one-track mind.

Committee members Ellen Arruda and Katsuo Kurabayashi have been highly supportive of my work throughout. I am extremely thankful to them for their time, which they have never hesitated to share with me, be it in discussing my research directly, or in advising me about graduate school and beyond.

I would like to thank my labmates, Chang Jiang and Jenna Campbell for making the lab a great place to be at all times, including 5am for tubulin preps. Being in the mechanical engineering department has brought with it the fortune of working with some very kind people in the staff and I am thankful to them for being themselves.

I am especially thankful to my adviser, Edgar Meyhofer for his continued support and patience as my mentor.

Finally, I would like to thank my family and friends from the bottom of my heart for their love and support without which none of this would have been possible.

CONTENTS

LIST OF TABLES

TABLE

LIST OF FIGURES

GLOSSARY

AMPPNP	adenylyl-imidodiphosphate
ATP	adenosine triphosphate
BDNF	brain-derived neurotrophic factor
BME	beta-mercaptoethanol
BSA	bovine serum albumin
ccd	charged coupled device
CLEP	chymostatin, leupeptin, eastatinal, pepstatin
CO_2	carbon dioxide
CPA	carboxypeptidase A
CTT	C-terminal tail
DTT	dithiothrietol
EGFP	enhanced green fluorescent protein
EGTA	ethylene glycol tetraacetic acid
FBS	fetal bovine serum
GTP	guanosine triphosphate
HEPES	4-(2-hydroxyethyl)-1-piperazineethanesulfonic acid
IPTG	isopropyl beta-D-1-thiogalactopyranoside
KCl	potassium chloride
KOAc	potassium acetate
MAPs	microtubule-associated proteins
$MgCl_2$	magnesium chloride
NAD	nicotinamide adenine dinucleotide
NaOAc	sodium acetate
Ni-NTA	nickel-nitriloacetic acid
pen/strep	penicillin/ streptomycin
PIPES	piperazine-N,N′-bis(2-ethanesulfonic acid)
PMSF	phenylmethanesulfonylfluoride
SDS-PAGE	sodium dodecyl sulfate- polyacrylamide gel electrophoresis
siRNA	small-interference ribonucleic acid
TPI	threads per inch

CHAPTER 1

Introduction

With the first chapter of this dissertation, I would like to introduce to the reader relevant concepts and share my appreciation for the complex intra-cellular transport process. An ensuing discussion of the current literature will lead us to open questions in the field, some of which are addressed in this thesis. Questions I hope to answer in this section are:
What is intra-cellular transport and why is it important?
What do we know about cargo-carrying motor proteins?
What do we know about microtubules, the cytoskeletal highways?
What do we know about post-translational modifications (PTMs) of microtubules

What is Intra-Cellular Transport and Why is it Important?

Every cell requires a targeted transport system in order to efficiently transport proteins, vesicles and organelles to specific locations through its dense and crowded cytoplasm. This targeted transport is achieved by the synchronized orchestration of cytoskeletal filaments and transport machinery (1-3). Cytoskeletal filaments in the cell serve as tracks to which different motor proteins performing specific functions are recruited. Some motor proteins function as freight carriers while others are engaged in maintenance of the tracks (4). It has been previously shown *in vivo* that cells are able to preferentially localize cargo specifically to certain regions but not others (5-9). From this point of view, polarized cells such as neurons or epithelial cells make ideal model systems for the study of targeted transport because their functionality and survival depends on the ability to localize proteins, a process that generates the desired polarity (10-11). For example, in neurons, pre-synaptic vesicles carrying specific neurotransmitters to be released at the synapse, must make their way specifically down the axon but not the dendrites. Mis-localization of these vesicles is hypothesized to be an underlying cause of several neurodegenerative disorders (12-17). From a mechanistic standpoint, cargo mis-

localization could occur from a deficit in any of the following major factors: the motor protein, the cytoskeletal filament, linkages between motor proteins or the interaction between motor proteins and cytoskeletal filaments. I am particularly interested in how the interaction between motor proteins and cytoskeletal filament is regulated to allow for targeted transport. Once we establish a framework for the intra-cellular transport system by identifying known key elements of the transport machinery, we will be directed towards the most likely mechanisms by which targeted transport in cells can be achieved.

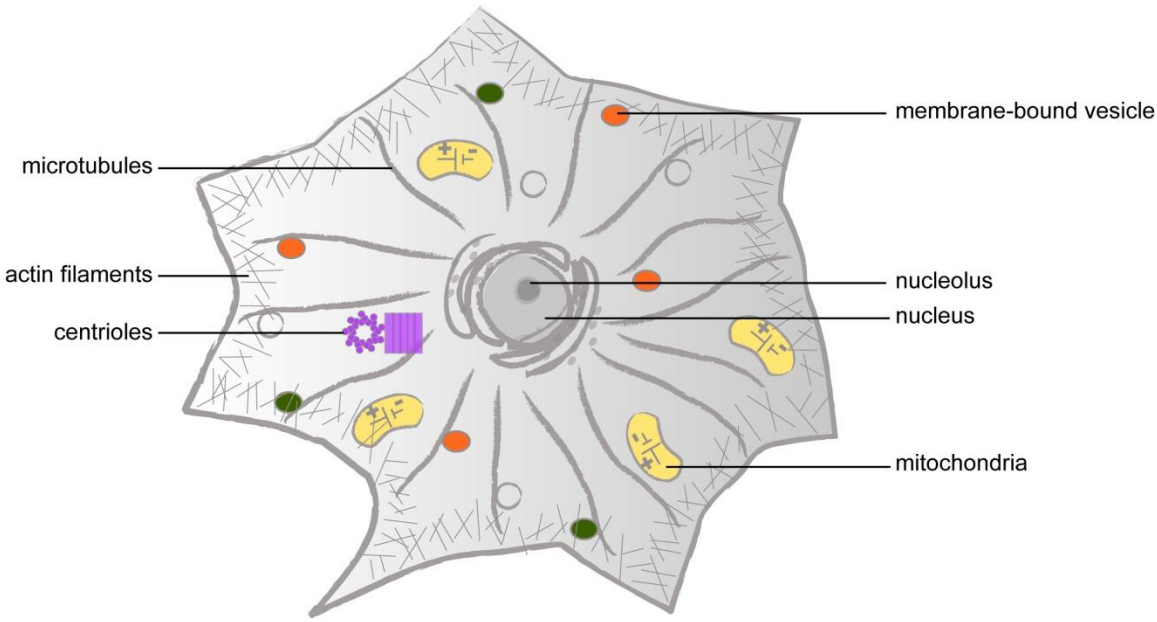

Figure1: Cartoon of a cell. The figure shows the nucleus in the center, membrane-bound vesicles, centrioles, mitochondria, actin filaments and microtubules

There are three types of cytoskeletal filaments that form the structural framework of a cell - actin filaments, microtubules and intermediate filaments. Actin filaments play an important role in cellular processes such as muscle contraction, cell division, cell motility, vesicle and organelle movement, cell signaling, etc. (18). Microtubules are integral to cell division, maintaining cell structure and in the long-range intracellular transport of cargo (2, 19-20). Intermediate filaments are a broad class of fibrous proteins that play a key role in the functional organization of structural elements and are believed to be a mechanical stress absorber (21-22).

Different families of cytoskeletal motor proteins that utilize actin filaments or microtubules as their tracks for cargo transport have been identified (see Figure 2). The

myosin family of motors has been shown to traverse actin filaments while kinesin and dynein families utilize microtubules. Some transport events have been clearly associated with specific filament-motor systems, for example, long-distance transport of mitochondria requires microtubules with the activity of kinesin-1 and dynein motor proteins while short-range transport occurs along actin filaments using myosin as the motor (23-24). While we do not have the complete picture on transport-related activities, research has unraveled the workings of many a motor protein and provided much insight into the mechanics of how these fascinating molecules function (25).

a. b.

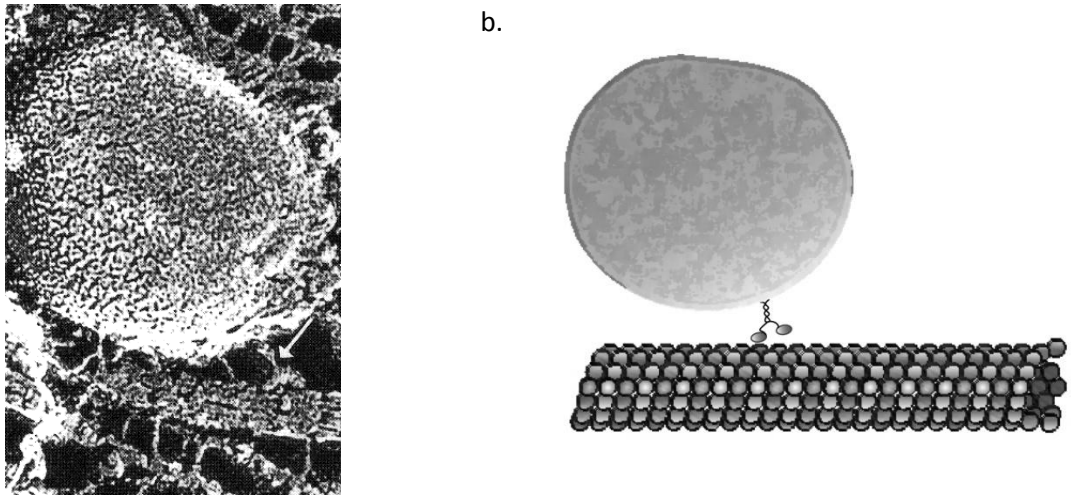

Figure 2. Transport machinery. a. Image of a membranous vesicle attached to a microtubule by a kinesin (indicated by arrow) from a quick frozen, deep-etched axon (26). b. Cartoon of a membrane-bound vesicle on a motor moving along a microtubule.

What Do We Know About Cargo-Carrying Motor Proteins?

Motor proteins are force-generating nucleotide-dependent proteins that can operate on either actin filaments or microtubules in the cell to enable active cargo-transport (27). Myosins are actin-based motors involved in short-range transport whereas certain dyneins and kinesins are the major types of motor proteins responsible for long-range minus-end and plus-end directed cargo transport along microtubules, respectively (see Figure 3). Because I am particularly interested in targeted transport which is likely to be determined by the choice of the long-range carrier, I will hereon focus my discussion on kinesin motors. Kinesin was first identified kinesin in 1985 based on its motility in cytoplasm extruded from squid giant axon and then further characterized upon purification from

bovine brain (28-29). Based on consensus monophyletic groups conserved among past phylogenetic analyses, kinesin have been divided into 14 families as described in Lawrence et al. (30). They play important roles in both cargo-transport and microtubule dynamics by acting as either transporters or microtubule depolymerizing (and possibly polymerizing) agents. Of these, kinesin-1, kinesin-2 and kinesin-3 are the most widely studied kinesins (see Table 1); they are all responsible for cargo transport. Although there are some hints on how kinesin can be regulated *in vivo*, it is not clear how different cargos are linked to the same motors to ensure that they are transported to the correct destinations (31). In considering how kinesin may take biochemical cues from its microtubule tracks in order to correctly select its path, it seems ideal to begin the investigation with the most widely studied kinesin motor, kinesin-1.

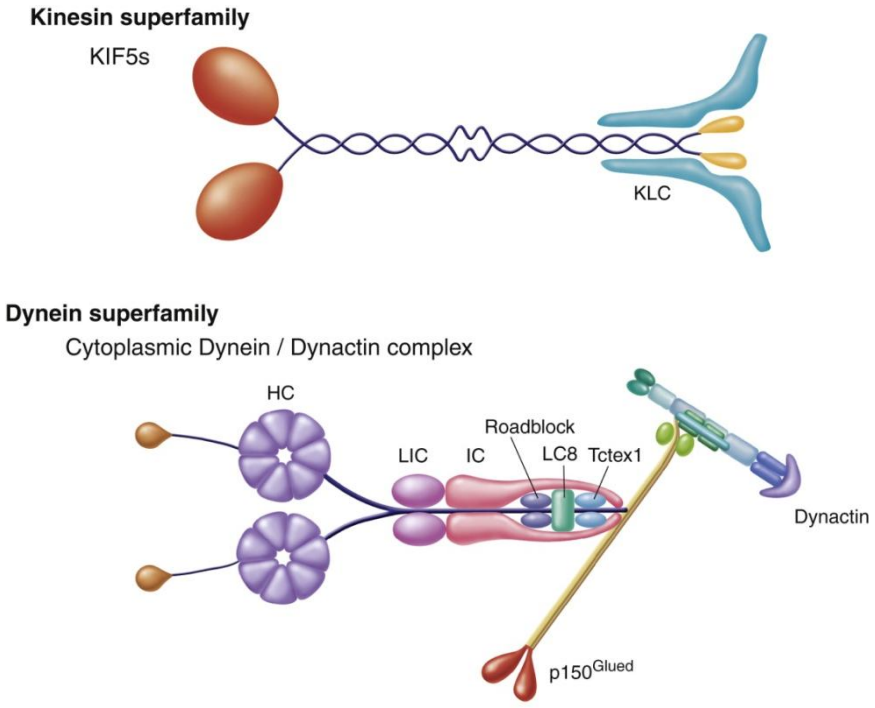

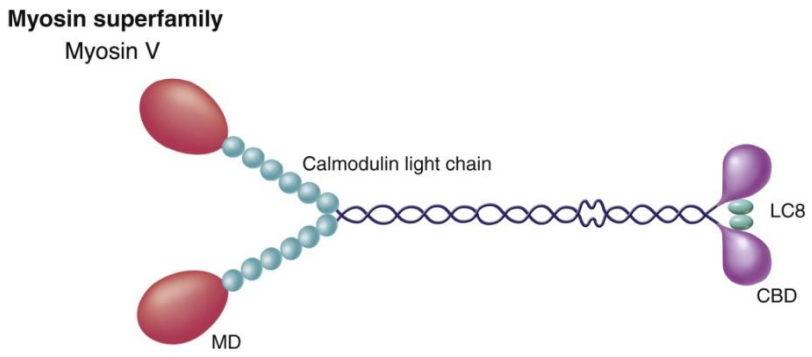

Figure3: Cartoon for kinesin, dynein and myosin (32)

Table1: Kinesin super-families.
Three of the fourteen kinesin super-families (adapted from Lawrence et al. (30))

Standardized Name	Example sequences	Other names for this group of sequences
Kinesin-1	KHC (J05258) KIF5A (AF067179) KHC (L47106) K7 (U41289)	KHC, N-I, Kinesin-I, conventional
Kinesin-2	KRP85 (L16993) KRP95 (U00996) KIF3A (D12645) KIF3B (D26077) FLA10 (L33697)	KRP85/95, N-IV, Kinesin-II, Hetero-trimeric
Kinesin-3	KIF1A (D29951) UNC104 (M58582) KIN (L07879) Unc104 (AF245277)	Unc-104/Kif1, N-III, monomeric

Kinesin-1

Kinesin-1 is a hetero-tetramer composed of two identical heavy chains and two identical light chains. The heavy chains together form a homo-dimer, each consisting of a motor domain, neck-linker, neck, coiled-coil stalk and tail domain (33-34). In the past 20 years, much progress has been made in demystifying the binding, stepping and regulatory

mechanisms for this particular member of the kinesin super-family. The two motor domains sequentially undergo conformational changes to alternate their steps along the microtubule with a corresponding alternating hydrolysis of ATP to release energy (35). ATP hydrolysis is 100-fold enhanced in the presence of tubulin or microtubules (36). Because the chemo-mechanical cycle of kinesin-1 has been studied in much detail, we know that as part of its stepping mechanism, every 8 nm step that kinesin-1 takes is coupled with the hydrolysis of a single ATP (adenosine triphosphate) (37). Kinesin-1 moves processively, which means that it takes several consecutive steps along a microtubule before detaching (38). There is evidence for a front-head gating mechanism to explain the tight chemo-mechanical coordination between the two motor domains but the model is still under debate (39-40). As regards the structure-function relationship, the ATP-binding and microtubule-binding regions of the motor domain have been previously identified (41-42). For cargo-binding, it is believed that the light chains are instrumental in connecting the motor to its cargo and they have been shown to associate with scaffolding proteins to do so (43).. Structural studies documenting the binding of kinesin-1 to microtubules are in support of the generally proposed walking mechanism (42, 44-46). Broadly accepted motility characteristics measured *in vitro* for mammalian kinesin-1 on bovine brain microtubules are a velocity of 0.6 μm/s, processive run length of 1 μm and maximum stall force of 5 pN (47). Binding of kinesin-1 to microtubules is believed to cause a conformational change in tubulin (48) and hence it is plausible to hypothesize that a regulation of this conformational change might regulate motor binding and/or motility. The binding event between kinesin-1 and the microtubule is based on an electrostatic interaction as has been demonstrated by adding positive charges to the neck coiled-coil region and modulating the ionic strength (49). Following this, the processivity of kinesin-1 was shown to change with removal of tubulin C-terminal tails (CTTs) (50). From these observations, it is clear that the motor-microtubule binding interaction can be regulated to affect motor motility. Specific regions of the kinesin-1 motor domain are responsible for ATP-binding and hydrolysis, self-inhibition or microtubule binding (51). While mechanistic details of the kinesin-microtubule interaction have been elucidated, it is still unclear how targeted transport can be achieved. To answer this question, we must

consider the possibility of how kinesin is able to specifically identify one microtubule from others and thus select the correct path for cargo-transport.

a.

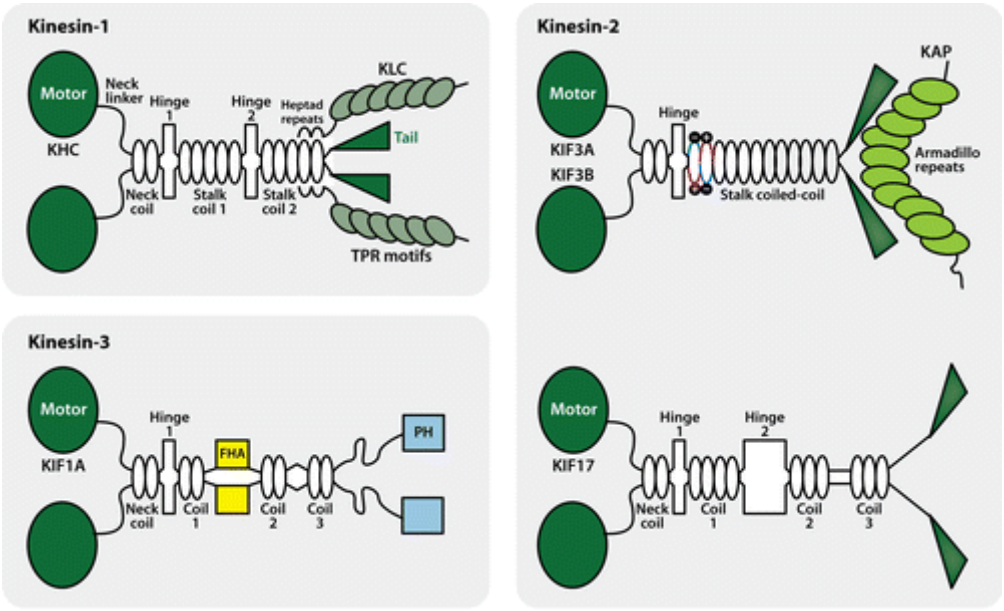

b.

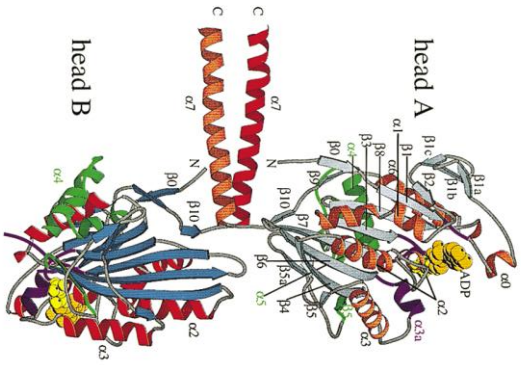

Figure 4. Kinesin and its crystal structure. a. Schematic representations for kinesin-1, 2 and 3 structure highlighting the highly conserved region of kinesin (up to the first hinge) including the motor domain and in contrast, the variation in structure between different super-families upon moving further towards the C-terminal (4). b. Crystal structure for truncated kinesin (42)

What Do We Know About Microtubules, the Cytoskeletal Highways?

Microtubules are 25nm-diameter, long hollow tubular assemblies of protofilaments composed of alpha and beta tubulin heterodimers that self-assemble in the presence of GTP (guanosine tri-phosphate) (52-53). Tubulin assembly is dynamic and microtubules

have been shown to undergo continuous cycles of growth and shrinkage which is achieved by an ongoing polymerization and depolymerization of the constituent dimers (54). The tubulin heterodimers are assembled such that the microtubule is polarized, with the plus end being the one that has a higher turnover than the minus-end. This polarity is useful in establishing the directionality of motor-based transport. Microtubular motors move either to the plus end or the minus end of a microtubule. Microtubule polarity has also been shown to enable the dynamic accumulation of plus-end-tracking proteins selectively at the plus ends of microtubules (9). In combination with the dynamics, it plays a vital role in kinetochore assembly and activity during cell division. Microtubule dynamics can be arrested by the addition of anti-mitotic drugs such as paclitaxel and this makes them an ideal target for chemotherapy.

a.

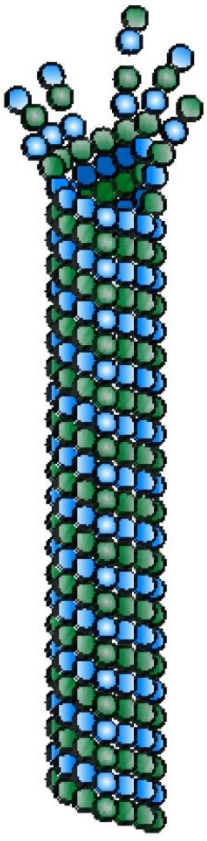

b.

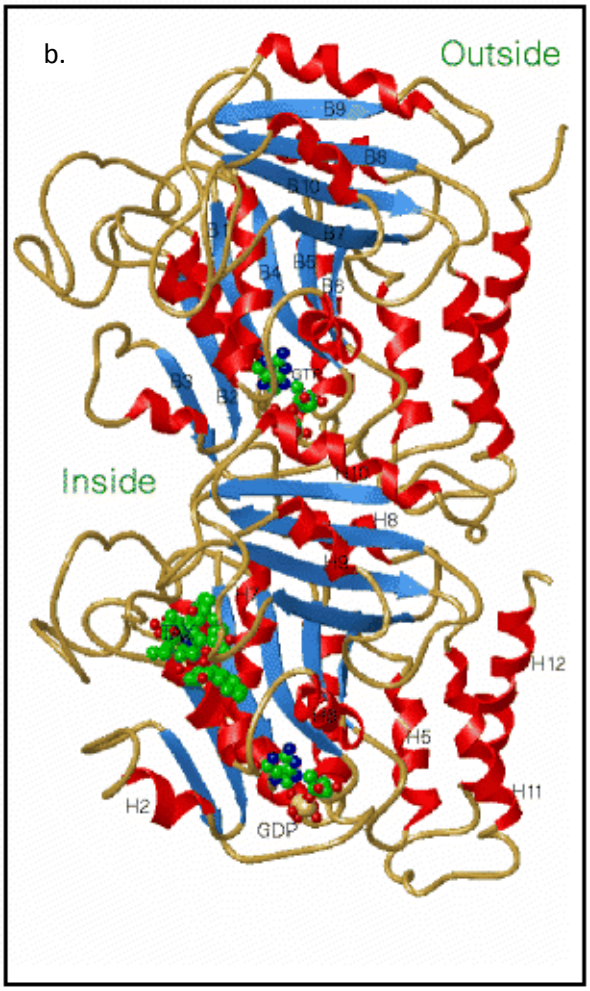

Figure 5. Microtubules and the crystal structure of tubulin. a. Cartoon of a depolymerizing microtubule. b. Tubulin dimer structure from electron microscopy (55)

We know from crystal structure studies that tubulin monomers share 40% amino acid sequence identity with each α and β-tubulin having a GTP-binding site (see Figure 5). While the intra-dimer interface was shown to contain a non-exchangeable GTP, the inter-dimer interface was shown to contain GDP at the E-site (55). Polarity determined by fitting the atomic structure into a 3-D reconstruction also obtained from cryo-EM on intact microtubules, showed that the nucleotide in β is on the surface of the plus end of a microtubule, accounting for the exchangeability of the nucleotide at the microtubule plus end (56). The nucleotide-binding state of tubulin was shown to contribute to the curvature of intra-dimer and inter-dimer contacts in microtubules (57). Thus, a growing microtubule is believed to have a GTP-cap which keeps the tubulin in a conformation stable for incorporation into the microtubule. Once the GTP-cap is lost, the microtubule tip starts to depolymerize through an event known as 'catastrophe'. If a GTP-cap is once again generated at the tip, the microtubule starts to grow again and this event is called 'rescue' (54). In vivo, there are several microtubule-associated proteins (MAPs) that serve in stabilizing microtubules and regulating their interactions with other proteins (58-59). One such example is the MAP tau, which has been shown to stabilize microtubules in a sub-stoichiometric manner, bundle them and even regulate their interactions with motor proteins (60-62). There are although, conflicting studies that indicate tau does not directly affect microtubule-based vesicle motility (63). Thus, it seems that there is much complexity in the many proteins that bind to and interact with microtubules.

Motor proteins bind microtubules and use them as tracks along which cargo is transported but it is unclear what mechanisms the motor uses to select the right track. It has been shown through negative-EM studies that tubulin in microtubules undergoes a conformational change upon the binding of motors (48) and so this is a promising mode of communication between motors or MAPs and microtubules. Moreover, as we shall see in the following text, tubulin heterogeneity is not limited by the number of genes encoding it because tubulin in cells is found to be post-translationally modified, often

after incorporation into microtubules. This process allows for the dynamic and reversible modification of microtubules by one or many enzymes present in the cytosol.

What Do We Know About Post-Translational Modifications (PTMs) of Tubulin?

In most organisms, multiple genes encode for α- and β-tubulins, resulting in a variety of isotypes that are highly conserved (64). For example, in humans, eight genes encode for α-tubulin and seven genes for β-tubulin; the resulting tubulin isotypes are differentially distributed in tissues (65-67). On the other hand, in *Tetrahymena thermophila*, there is only a single gene for α-tubulin (68-69) and two genes encode identical β-tubulins (70). Yet, there are at least 17 different microtubule systems in *Tetrahymena* (71), suggesting that many of these are the result of PTMs. Thus, the small number of genetic tubulin isoforms in *Tetrahymena* presents a clear opportunity for the role of PTMs in microtubule function. Tubulin PTMs have been implicated in the regulation of various cellular functions of microtubules (reviewed by (72-74)). Most PTMs are found on the CTTs of tubulins (75), except for a frequently acetylated lysine residue (K40) that is located close to the amino-terminus of α-tubulin in the lumen of the microtubule (76). Interestingly, both the CTTs and the loops in the microtubule lumen, show the greatest divergence among tubulin isotypes. The most widely-studied PTMs are acetylation, detyrosination, polyglutamylation and polglycylation. The locations of these modifications on the tubulin subunits are shown in Figure 6 and their proposed cellular functions are described in Table 2.

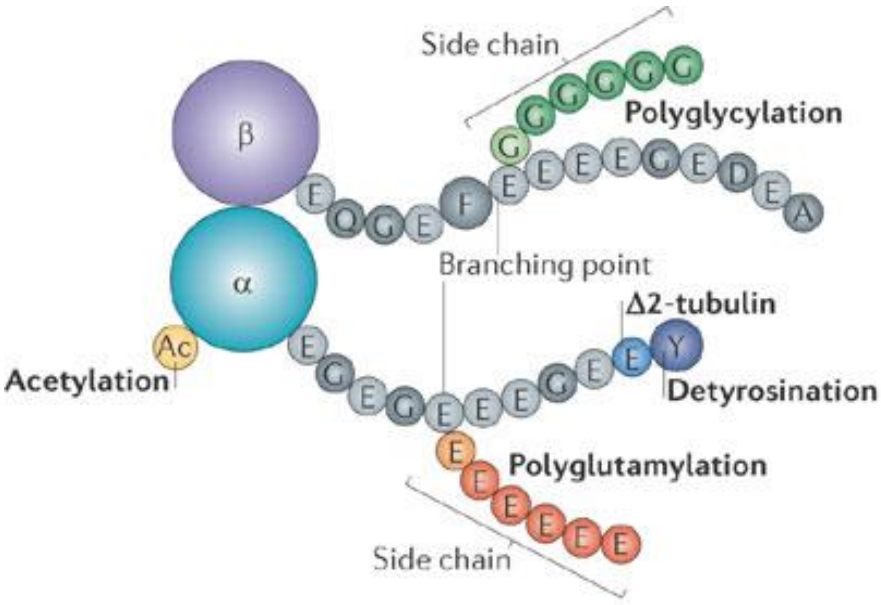

Figure 6: PTM locations on α- and β- tubulin. Adapted from (77). Residues of the C-terminal tails (as translated) are shown in gray while residues added or removed through PTMs are shown in color.

Acetylation

Acetylation of Lysine-40 on α-tubulin is a unique modification in terms of its location being near the N-terminal region of tubulin. The lysine is on a loop between H1 and S2 in the α-tubulin structure that extends into the lumen of the microtubule, presumably inaccessible by proteins that bind to the surface of the microtubule (78). While this residue and those immediately surrounding it are highly conserved (79) in α-tubulin, other residues in the region show large differences in variability between α and β-tubulins (80). Proposed roles for K-40 acetylation on α-tubulin include microtubule stability, regulation of cargo transport, control of MAP-binding to microtubules and involvement in the process of cell-division.

It was shown in 1985 that the 40th residue on α-tubulin, a lysine, is acetylated on its γ-carbon molecule when the tubulin has already been incorporated into microtubules (76, 81). The acetyl group can be removed from the tubulin once it is depolymerized and present in its soluble form in the cytoplasm. The enzyme responsible for acetylation, MEC17, was recently identified by Akella *et al.* and Shida et al. (82-83). The

deacetylases HDAC6 and SIRT2 from the enzyme family of histone deacetylases (HDACs) were both shown to deacetylate α-tubulin and other cytoplasmic substrates (84-86). Purified as recombinant proteins, both the acetyl transferase and deacetylase can catalyze their respective reactions on K-40 on α-tubulin in microtubules *in vitro*. Recently, a novel acetylation site on β–tubulin at lysine 252 was reported (87). There are no corresponding cell biological observations yet.

Detyrosination

Detyrosination involves the removal of a tyrosine exposing an underlying glutamate residue at the α-tubulin CTTs. It is believed that *in vivo*, tyrosinated tubulin is the nascent form of tubulin. Tubulin is detyrosinated while in the polymerized form and then re-tyrosinated once it is in its soluble form in the cytosol. The enzyme for tyrosination was identified as the tubulin tyrosine ligase (TTL) and was first purified from porcine brain (88-90). The ligase adds a tyrosine residue to the CTT of a detyrosinated α-tubulin. Szyk et al. recently showed through small angle x-ray scattering studies that TTL binds α-tubulin on the surface that would form an interface with beta tubulin when incorporated into a microtubule (91). Following this, they showed that TTL inhibits tubulin polymerization *in vivo* and *in vitro*. The enzyme for removal of the tyrosine residue is an unknown carboxypeptidase remaining to be identified.

Polyglutamylation and Polyglycylation

Polyglutamylation and polyglycylation are both poly-modifications that occur on α and β-tubulin CTTs, giving rise to a more variable form of modifications unlike the binary acetylation and detyrosination. Polyglutamylation refers to the addition of more than one glutamate residue on to the γ-carboxyl group of one of the several Glu residues on the tubulin CTTs (92-94). Polyglycylation involves the addition of one or more glycine residues on similar CTT sites (95-96). There is even some evidence that this modification may compete with polyglutamylation for modification sites on the tubulin CTTs (97). While polyglutamylation is observed on microtubules from different cell types, polyglycylation is primarily found on flagellar and ciliary tubulin, thus mostly confining it to cells that contain cilia and flagella (95).

In cells, polyglutamylation and polyglycylation are both catalyzed by the family of enzymes known as the tubulin tyrosine ligase like (TTLL) family. Regnard et al. were the first to show the existence of different types of polyglutamylases followed by the identification of TTLL1 by Janke et al. (98-100). Since then, different TTLLs have been identified to show varying substrate specificity for α or β-tubulin and in the length of the side chains they can generate. Six autonomously active polyglutamylases were identified that all share the extended TTLL domain with TTLL1 (101). Less was known about the deglutamylases for a long time but recently, cytosolic carboxypeptidases CCP6 and CCP1 have been identified as deglutamylating enzymes (102-103). It is not yet understood how the activity of these different enzymes is coordinated in the cell so as to generate and maintain specific patterns and levels of polyglutamylation. Rogowksi et al. identified TTLL3 and TTLL8 proteins as initiating glycylases in Drosophila, with different substrate preferences whereas TTLL10 was identified as an elongating polyglycylase responsible for subsequent glycine additions leading to the poly-modification (104). Wloga et al. independently identified TTLL3 as a tubulin polyglycylase in *Tetrahymena* (105). Both poly-modifications are believed to cycle between their modified and de-modified states through the continuous intra-cellular activity of modification and de-modification enzymes (96, 101).

The broad effects of PTMs on cellular functions have been outlined nicely in previous review papers (74-75, 106-108). A figure from one of these papers showing the sub-cellular distribution of modifications in cells is shown in Figure 7. In the next section, I will focus on discussing relevant experiments from literature that have enabled a better understanding of the role of PTMs in intra-cellular targeted transport.

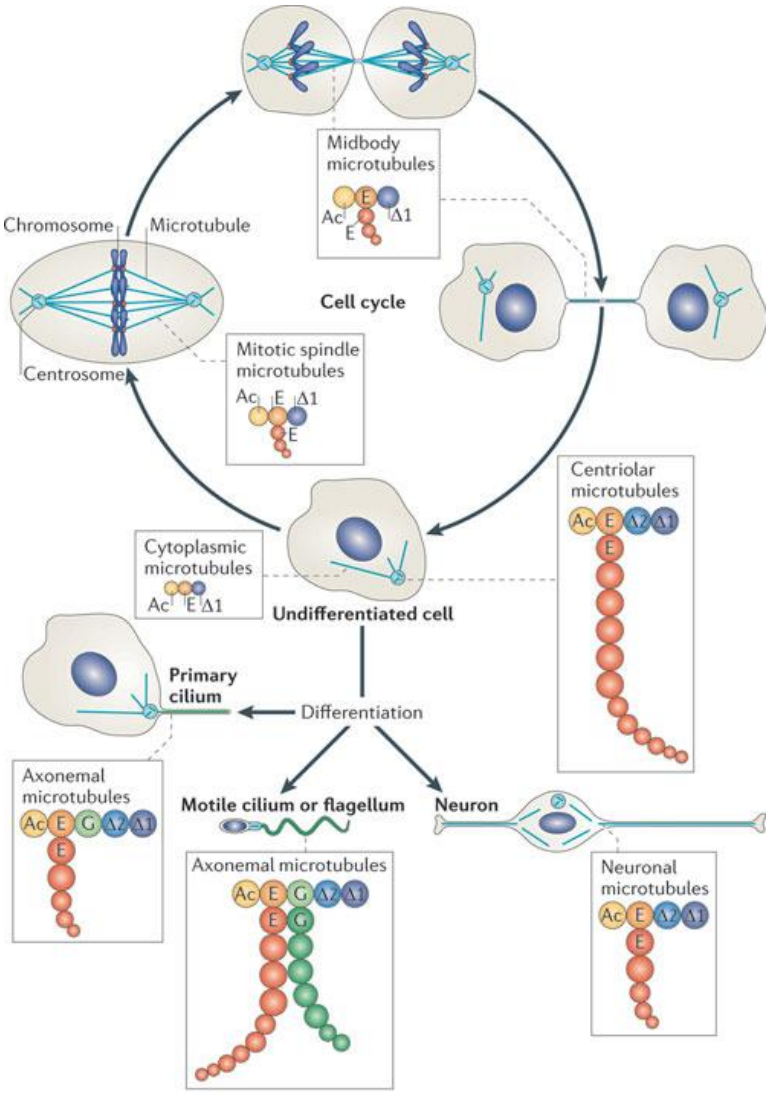

Figure 7: PTM distribution in cells. Adapted from (77). The dynamic nature of PTMs allows cells to tailor their PTM distributions as per requirement enabling the spatial and temporal distribution of microtubule PTMs in cells. Differentiation also leads to cells adopting specific PTM patterns

Do Microtubule PTMs Affect Kinesin-Based Transport?

The functional diversity of microtubules in a cell is not accounted for by the limited number of genetic isotypes of tubulin available to the cell. Yet, motors and MAPs must recognize specific microtubules to interact with them and thus enable a multitude of well-regulated cellular processes. *In vivo* single molecule experiments performed by Cai et al.

showed that a 560 amino-acid heavy chain truncation of kinesin-1 is sufficient for the motor to selectively translocate along a subset of microtubules in a COS cell (109). This observation raises the fundamental question of how microtubule identity can be selectively recognized by the kinesin-1 heavy chain. Maximum heterogeneity in tubulin is seen either on the CTTs or on the loops in the lumen of the microtubule (56). These also happen to be sites for tubulin PTMs, the modulation of which could provide a powerful and dynamic means for designating microtubule identity. Interestingly, while motor and MAP binding sites are on the external surface of the microtubule, sites for paclitaxel and colchicine binding are on the inside (56). In addition, conformational changes in tubulin upon kinesin binding, observed through negative stain electron microscopy using tubulin sheets, were visible only when looking at tubulin monomers on the interior surface of the microtubule (48). This is a reminder that the interior surface of microtubules may be just as important as the exterior, in events of binding and conformational-change.

Kinesins appear to selectively bind a subset of microtubules and in polarized cells, microtubules are shown to compartmentalize into sections of the cell based on their PTMs. Thus targeted transport of cargoes in cells has recently been correlated with microtubule PTMs (for recent reviews see (72-74, 77, 110-111)). According to this hypothesis, different kinesin motors interact selectively with microtubules that are marked by different PTMs such that they, along with associated cargo, can be preferentially transported along certain subsets of modified microtubules. In this way, PTMs on microtubules could de facto serve as "road-signs" to direct polarized trafficking such as axonal and dendritic transport in neuronal cells.

PTMs of tubulin were first discovered in 1973 when Arce et al. found that α-tubulin in rat brain homogenate could be tyrosinated in an ATP-dependent, RNA-independent manner (112). Tubulin is particularly abundant in brain tissue and its role in neurons has therefore been studied extensively. A majority of *in vitro* studies also use brain tissue as their source for tubulin purification. Another characteristic property of neurons is that their structural polarization is essential to their function and not surprisingly, the first clues for selective, targeted transport came from observations in neurons (113-115). To show motor-based selectivity for cargo transport, Nakata et al. used confocal laser scanning

microscopy in neurons to show that post-golgi transport of the VSV-G protein (carried by KIF-5B) was biased towards axons, indicating polarized transport. When tailless KIF5-GFP (shown to transport VSV-G) was expressed, they accumulated at the tips of axons. Chimeric studies with switched KIF17 and KIF5 domains further suggested that the motor domain is the key in determining KIF5 preference for axons. Other studies have shown similar results for the selective localization of kinesin-1 or its cargo specifically to axons (116-118). Recently, Huang et al. compared the translocation selectivity of kinesin from four different super-families to find that different kinesin showed differential preferential selectivity in their translocation to axons, but not dendrites (119).

Early on, it was shown that acetylated α-tubulin is preferentially enriched in axons and that these acetylated axonal microtubules are also detyrosinated (120-121). In 2007, Dunn et al. observed in both neuronal and non-neuronal (COS) cells that fluorescently labeled full length kinesin-1 localized to a subset of stable microtubules. In COS cells, it was shown that only 0.5% of the total microtubules are marked by α-tubulin detyrosination. Yet, upon immunofluorescence labeling for acetylated, tyrosinated and detyrosinated microtubules, it appeared that kinesin-1 specifically localized to this small subset of microtubules that were predominantly detyrosinated (122). They also confirmed by using FRAP (fluorescent recovery after photo-bleaching) that the observed distribution of fluorescently labeled kinesin was not from static aggregation but instead a result of the motor's dynamic behavior. Further, Cai et al. showed through single molecule *in vivo* TIRF imaging followed by immunofluorescence, that in COS cells the kinesin-1 motor domain is sufficient for preferential translocation of the motor along a subset of microtubules that is marked by α-tubulin acetylation and detyrosination (109). These experiments clearly demonstrate a correlation between specific PTMs, either independently, or in combination, and the microtubule- selectivity of kinesin-1-based transport. On the other hand, there have been few observations to indicate the effects of polyglutamylation and polyglycylation on kinesin-1 motility.

Multiple studies have observed the preferential selectivity of kinesin for specific subsets of microtubules and some have even shown a correlation with specific PTMs. Yet, our knowledge of what factors are required for the motor to differentiate between one PTM and another is very limited. The direct effects of PTMs on kinesin motility and their

mechanisms are yet to be studied. I have attempted to summarize the specific motor/MAP- PTM correlations in Table 2. The next section will list out in more detail the experiments that lead to our current understanding of the correlation that has been established between targeted transport and tubulin PTMs.

Table 2: Cellular functions of PTMs (75, 106)

Modification	Function
Acetylation	Regulation of cell motility; exists in stable long-lived microtubules; guidance cue for selected motors (109, 117); regulation of katanin activity (123)
Detyrosination	Role in cell differentiation; exists on stable long-lived microtubules; contributes to microtubule stabilization; regulation of +TIPs binding (124-125) and motor binding (109, 122, 126)
Polyglutamylation/ polyglycylation	Centriole maturation and stability; Flagellar and ciliary motility; cytokinesis; axonemal organization; regulation of interactions between microtubules and MAPs ; regulation of spastin (127)

The Role of Acetylation in Kinesin-1 Motility

Tubulin acetylation of the lysine-40 site on α–tubulin has been postulated to play different roles in microtubule-based activities including dynamics, motor-binding and MAP-binding. Many of these hypotheses are still being debated and the exact role of the modification remains unclear. After it had been demonstrated that α–tubulin acetylation and detyrosination are preferentially distributed in the axons of neurons, Verhey et al. showed that the concentration of JIPs at nerve terminals requires kinesin (116). This was followed by observations of kinesin-1 and JIP-1 localization in neurites by Jacobson et al. and Reed et al., respectively (117-118). In fact, Jacobson et al. observed that kinesin-1 could dynamically be localized to different neurite-tips before the future axon was established, indicating that the kinesin-1 were being recruited to different neurites by a dynamic process. Evidence was presented in support of acetylation-enhanced motility of kinesin-1 *in vitro* by using tubulin from genetic mutants of the *Tetrahymena thermophila*

species (117). Further evidence for the up-regulation of kinesin-1 activity due to hyper-acetylation came from Dompierre et al. who showed that in cells afflicted with Huntington's disease, inhibition of the deacetylase HDAC6 could rescue the transport deficit typical in the diseased cells (128). But this result has found itself in conflict with recent findings by Bobrowska et al. who in turn proved that while HDAC6 modification causes hyper-acetylation, it does not rescue the transport deficit occurring in Huntington's disease and also does not modify disease progression (129). The interpretation of these results was not altogether straightforward owing to the use of the deacetylase inhibitor, which has been shown to affect cells in a way that would create interference in these experiments (130-133).

The studies discussed above provide valuable correlations specifically between α–tubulin acetylation and kinesin-1-based transport. To understand the role of acetylation, we must look at the mechanism by which acetylation is recognized by the motor. Since this is a modification that resides in the lumen of the microtubule, it is difficult to imagine how the motor would be able to directly interact with the modified region. On the other hand, there is much tubulin heterogeneity in the intra-lumenal loops of tubulin in microtubules and the action of stabilizing drugs that bind in the lumen is also well-established (56). Keeping in mind the current literature for the effect of α–tubulin acetylation on kinesin-1 motility, it would be ideal to perform an *in vitro* experiment with completely acetylated or completely deacetylated microtubules, homogenous in every other way, to test the motility of kinesin-1 *in vitro* and measure changes in motility parameters, presumably resulting from only a change in the acetylation state. Performed with purified components, such an experiment would test the direct effect of α–tubulin acetylation on kinesin-1 motility.

The Role of Detyrosination in Kinesin-1 Motility

Detyrosination of α-tubulin CTTs has also been implicated in recruiting kinesin-1 motors and promoting higher velocity for the motor. Dunn et al. showed that the distribution of full length kinesin-1 *in vivo* is preferentially localized to a narrow subset of microtubules in which the α–tubulin is both acetylated and detyrosinated (122). In contrast when they compared velocities in an *in vitro* gliding assay for tyrosinated and detyrosinated

microtubules with kinesin-1, they found a higher gliding velocity for tyrosinated microtubules then for detyrosinated microtubules. Following this, Cai et al. used *in vivo* single-molecule imaging to reveal that truncated kinesin-1 translocate preferentially along microtubules that are marked by α–tubulin acetylation and detyrosination (109). More recently, Konishi et al. showed that kinesin-1 is preferentially recruited to detyrosinated microtubules in neuronal cells and that, in an *in vitro* AMPPNP-binding assay, more kinesin-1 binds to detyrosinated microtubules (126). While these findings confer a second layer of complexity to the question of how PTMs affect kinesin-1, it is interesting to note that an overlap between α–tubulin acetylation and detyrosination of microtubules has been consistently observed in experiments wherein the *in vivo* motility of kinesin-1 was shown to localize preferentially to a particular subset of microtubules. This observation raises the question of interplay between microtubule PTMs. Controlling the extent of more than a single PTM at a time would allow us to not only isolate the independent roles of PTMs, but also understand if and how they might act in combination.

The Role of Poly-modifications in Kinesin-1 Motility

The two poly-modifications, polyglutamylation and polyglycylation, form heterogeneous branches extending out from the flexible tubulin CTTs. Their location and complexity makes them the most likely modifications to interact with motor proteins binding the outside surface of the microtubule. Yet, there is little data to indicate what their effect on kinesin motility might be. Ikegami et al. showed that the distribution of Kif1A (kinesin-3) motors was altered upon mutating a functional subunit of the tubulin polyglutamylase whereas Kif5 (kinesin-1) or Kif3A (kinesin-2) distributions remain unchanged (134). Cai et al. showed through single molecule *in vivo* motility assays that the path for kinesin motility in COS cells reproduced by measuring and plotting the standard deviation in fluorescence intensity from one frame to the next, when overlaid on immunofluorescence images from an anti-polyglutamylated tubulin antibody staining the same cell, indicated that kinesin-1 motility does not correlate with polyglutamylated microtubules (109). For polyglycylation, there is no identified role in the motor-microtubule interaction yet. This

is likely because the modification is abundant primarily in ciliary tubulin. Consequently, polylgycylation has been proposed to play a role specifically in ciliary functions (95-96).

Summary of the Problem

Taken together, there exists significant evidence for subsets of cellular microtubules to be marked with specific PTMs that serve as traffic signals to regulate kinesin-based transport in cells. It seems that *in vivo*, a subset of microtubules is modified and within this subset, acetylated and detyrosinated microtubules are distinctly concurrent with one another. It is not clear what independent effects tubulin PTMs have on kinesin motility, what the combined effects of multiple PTMs might be and finally, what could be the mechanism for regulation of kinesin motility by PTMs, independently or in combination. The best approach to this problem, therefore, would be to create a system wherein the levels of PTMs can be independently controlled, to test their independent and combined effects on kinesin motility. Results from current literature suggest a role for acetylation and detyrosination of tubulin in modulating kinesin-1 motility. However, all of the previous experiments were either performed *in vivo* or with the introduction of genetic mutations. A first step, therefore, would be to look at the overlapping modifications, i.e., acetylation and detyrosination, in isolation and in concurrence. To understand the mechanism by which these modifications act, we must seek to make a direct observation of their effects using a reductionistic approach. In trying to do so, this thesis will address the question of the direct effects of these α-tubulin acetylation and detyrosination on kinesin-1 motility by performing *in vitro* experiments to observe the same.

THESIS STATEMENT

This thesis aims to answer the question of how post-translational modifications (PTMs) of tubulin regulate kinesin-1 motility. The hypothesis being tested is that PTMs of tubulin in microtubules directly act as traffic signals for the regulation of kinesin motility. This means that a change in tubulin PTMs would result in a change in kinesin-1 motility. To begin, kinesin-1 was selected as the motor and α-tubulin K-40 acetylation as the modification of interest. Microtubules polymerized from either acetylated or deacetylated tubulin were used in single molecule *in vitro* TIRF assays to observe changes in the motility of kinesin-1 on the differentially modified microtubules. The scope of the thesis was further expanded to consider the additional effect of α-tubulin CTT detyrosination on kinesin-1 motility. The combination of α-tubulin acetylation and detyrosination is commonly found on microtubules frequented by kinesin-1 *in vivo* and so experiments were performed to observe changes in kinesin-1 motility due to detyrosination with and without the presence of acetylation.

The motivation for this study is seeded by findings that changes in tubulin PTMs show a marked correlation with cell pathogenesis such as in the case of neurodegenerative disorders and tumor progression. The results from our experiments provide the first single-molecule observations for the direct effect of tubulin PTMs on kinesin-1 motility. Moreover, the quantitative and reductionistic theme of these experiments presents a new approach to the traffic-regulation problem and thus offers a new platform for future studies on this subject.

The work undertaken in this thesis was performed in collaboration with Kristen Verhey of the Cell and Developmental Biology Program at the University of Michigan, Ann Arbor.

CHAPTER 2

The Effect of Tubulin Acetylation on the *in vitro* Motility of Kinesin-1

Targeted delivery of a large range of materials, including lipids, proteins and RNA, to specific domains within cells through intracellular trafficking networks is essential to cellular function (23, 135-136). Neurons with their selective, long-range transport into dendrites and axons serve as particularly illustrative and well-studied examples of these mechanisms, but every eukaryotic cell requires highly targeted transport mechanisms. Fundamentally, these transport mechanisms are widely believed to be based on a network of microtubules (137) that assemble and disassemble from α-β-tubulin heterodimers to form a dynamic network of polarized tracks along which long-range transport by molecular motors from the kinesin and dynein families takes place (138). In recent years, much has been learned about the general mechanisms by which motors and microtubules interact and hydrolyze ATP to generate force and movement (39-40, 47, 138-141). While this work provides critical insights into the chemomechanical energy transduction mechanism and mechanistic details of how the movement of motors and cargoes along microtubules is generated, the mechanism by which molecular motors and specific cargo select microtubules to reach a desired destination remains fundamentally unexplained (31).

In cells, microtubules are characterized by a number of dynamic PTMs such that temporal and spatial variations in the degree of each modification generate sub-populations of microtubules (73, 142-143). A number of studies, mostly based on cell biological observations, have led to first lines of evidence suggesting that tubulin PTMs are involved in regulating microtubule function and modulating the interactions of microtubules with molecular motors, MAPS and various proteins and complexes (75, 77, 107-108, 144-145). Of particular interest for this work are the interactions with kinesin motors, which are responsible for the anterograde transport along microtubules and ability to selectively localize cargo to specifiic destination in cells (13, 23, 30, 116).

Based on the variety of proposed functions for PTMs and the broad requirements for complex, targeted transport mechanisms in cells, one hypothesis that has recently been gaining popularity is that different members of the kinesin super-family selectively interact with specific combinations of microtubule PTMs such that intra-cellular transport along the microtubular network is temporally and spatially regulated through this PTM-code.

A number of investigations, in support of the PTM-code hypothesis, have established correlations between PTMs of microtubules and specific kinesin-based transport processes. For example, in neurons the distribution patterns of microtubule PTMs are different in axons than in dendrites, possibly to maintain neuronal polarity (106). Kinesin-1 locates to axons and not dendrites, whereas the motors KIF1A (kinesin-3) and KIF17 (kinesin-2) are bidestination transporters (5, 126). Acetylation of the α-tubulin residue K40 in microtubules is believed to enhance kinesin-1 motility in regard to binding, velocity or both. Specifically, Reed *et al.* presented detailed evidence that kinesin-1 binding and velocity is enhanced on α-tubulin K40 acetylated microtubules (117), and Dompierre *et al.* demonstrated that α-tubulin K40 acetylation enhances *in vivo* cargo-transport to compensate for effects associated with the neurodegenerative Huntington's disease (128). In addition to acetylation, other modifications such as polyglutamylation and detyrosination have been shown to influence transport by different members of the kinesin super-family *in vivo* and *in vitro* (122, 126, 146-147). The possible interplay between PTMs was clearly demonstrated by Cai *et al.* through single-molecule *in vivo* observations showing that kinesin-1 selectively binds to and translocates along a subset of microtubules that are found to be marked by acetylation of the residue K40 of α-tubulin and detyrosination (109). Nonetheless, it remains unclear whether the PTMs directly regulate motor molecules or if they exert their effect through other proteins, like MAPS, or if the PTMs work in combinatorial fashion, and there is little known as to which PTMs are actually guiding kinesin-based transport, and which molecular mechanisms are responsible for the observed targeted transport.

2.1 Preliminary Studies with Doublet Microtubules

Tetrahymena is a unicellular protozoan ciliates (see Figure 8) possessing hundreds of motile cilia and a variety of microtubular systems. The cilia are constructed from doublet microtubules in a 9+2 arrangement as shown in Figure 8. Doublet microtubules from wild-type (WT) *Tetrahymena* are mostly acetylated on K40 of α-tubulin. This acetylation can be prevented in a viable mutant where the K40 residue is substituted by an arginine, which cannot be acetylated (71, 117). Before the acetyl transferase for K40 α-tubulin acetylation was identified, we decided to extract doublet microtubules from *Tetrahymena thermophila*, taking advantage of the difference in acetylation levels between doublets extracted from WT and K40R mutant cells. The benefit of using doublets from *Tetrahymena* is that there is only a single type of α-tubulin gene (68, 148) which eliminates any variation in tubulin arising from its genetic isoforms.

a. b.

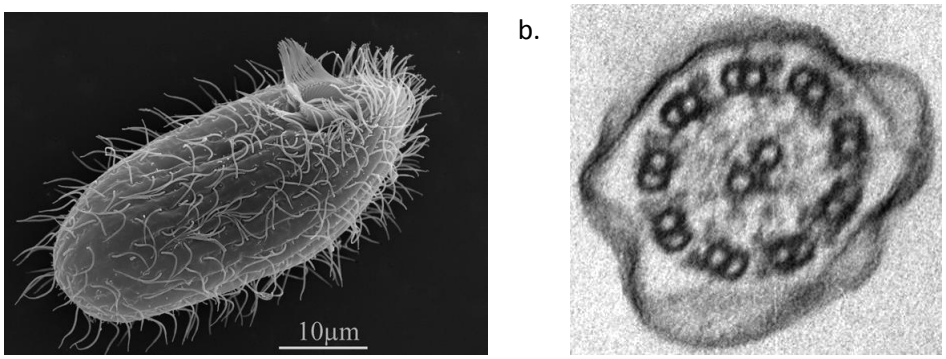

Figure 8. Tetrahymena and their cilia. a. Image of Tetrahymena thermophila (by Aswati Subramanian, Miami University) and b. electron micrograph of Tetrahymena cilium in cross-section (from cell image library)

The goal of this preliminary study was to observe any changes in motility for kinesin-1 between normally acetylated doublets from WT cells and un-acetylated doublets from K40R mutant cells. To do this we first performed multi-motor gliding assays to compare the velocity of WT doublets with K40R doublets. This was followed by single-molecule *in vitro* TIRF (Total internal reflection fluorescence) motility assays for kinesin-1 on WT and K40R doublets. All data was analyzed manually yielding measurements for velocity, run length and binding.

Materials and Methods

Cloning and Preparation of Proteins

Bacterially Purified Motor: Constructs consisting only of the N-terminal 560 amino acids of the kinesin-1 heavy chain containing the neck and the neck linker were used in our assays. NKHK560 was expressed and purified from BL21DE3 cells as described in Lakamper et al. (50).

Mammalian Lysates: An RnKHC560 kinesin construct was C-terminally tagged with a 3x-mcit sequence to produce RnKHC560-3xmcit and transfected into mammalian COS cells as described in Cai et al. (149). Transfected cells were allowed to over-express the recombinant kinesin for 4-10 hours. Cells were detached using trypsin-EDTA and excess trypsin was quenched with fetal calf serum. The cells were washed and then lysed using lysis buffer (40 mM HEPES/KOH, 120 mM NaCl, 1 mM EDTA, 10 mM pyrophosphate, 10 mM β- glycerophosphate, 50 mM NaF, pH 7.5) supplemented with 0.5% Triton X-100, protease inhibitors (PMSF and CLEP) and 1 mM ATP. The lysate was separated from cell bodies by centrifugation, aliquoted and flash-frozen for storage at -80 ºC.

***Tetrahymena* Doublet Purification:** 4L cultures of *Tetrahymena* cells were grown over 16 hours at 170 rpm. At a cell density of 2 x 10^5 – 3 x 10^5 cells/mL, the cells were pelleted to separate them from the media. After discarding the supernatant, the cells were washed in 10 mM tris buffer three times. Following this, they were resuspended in 100 mL deciliation buffer (10 mM Tris, 50 mM sucrose, 10 mM CaCl2), pH 8.0 with added protease inhibitors (PMSF and CLEP). The solution was chilled to prepare for a pH drop from 7.8 to 5.0 and then back to 7.3. Cells were checked under the microscope to ensure they were not swimming. Cell bodies were centrifuged and discarded. The supernatant with the cilia was centrifuged so that the cilia were pelleted. Cilia were resuspended in demembranation buffer (0.5% Triton X-100, 30 mM Tris, 3 mM $MgCl_2$, 1 mM EGTA, 0.1 mM DTT, pH 8.0 with HCl) + 0.2 mM DTT and incubated on ice for 10'. Axonemes were pelleted and resuspended in deciliation buffer. The axonemes were dialyzed overnight against 1 mM Tris, 0.1 mM EGTA, 20 μL BME, pH 8.0. The resulting doublets were pelleted and resuspended in PMG (10 mM K-phosphate, 10 mM $MgCl_2$, 0.1 mM GTP, pH 7.0 with KOH).

Labeling of Doublets

Doublets were labeled by incubating them with a 5-fold excess of Cy5 succinimidyl ester (GE Lifesciences, Piscataway, NJ) in the presence of 10% DMSO. The excess dye was quenched with 20 mM glycine. The doublets were airfuged through a 60% glycerol cushion and resuspended in 20 μM taxol in PMG.

Gliding Assays

Gliding asays were performed with TMR-labeled doublets that were labeled with the same procedure as outlined above using TAMRA, SE (Invitrogen, Grand Island, NY). The assay chamber was pre-coated with 94 μg/mL casein and then coated with 50 μg/mL NKHK560 in BRB80. Microtubules were flowed through in a solution of 0.2 mg/mL catalase, 1.7 mg/mL glucose oxidase, 22 mM glucose, 10mM DTT in BRB80 supplemented with 1mM ATP. Gliding microtubules were visualized after a 20 min incubation period. BP450-490, FT510, BP515-565 filters were used for visualizing TMR-labeled microtubules

Single-molecule TIRF Motility Assays

Motility assays were performed on a Zeiss Axiovert microscope modified to allow TIRF microscopy using a 488nm Ar-ion laser for excitation (50). The resulting images were chromatically separated using a commercial dual view device (Photometrics, Tucson, AZ,) with a T585lpxr dichroic and HQ510, ET525/50m filters (Chroma Technology Corp., Bellows Falls, VT, USA) such that kinesin-1 events and the doublets could be visualized side-by-side using a single CCD camera chip. Flow chambers were made using cover slips (Corning, Lowell, MA) that were cleaned with deionized distilled water. Doublets were allowed to adsorb to the cover-slip for 5 min, following which, 1 mg/mL BSA was introduced into the chamber so as to reduce nonspecific binding of kinesin to the glass surface. The final flow-through for the assay was ~10 nM kinesin in P12 buffer (12 mM PIPES, 2 mM $MgCl_2$, 1 mM EGTA, pH 6.8) containing 1 mM $MgCl_2$, 2 mM ATP, 1 mg/mL BSA, 10 mM glucose, 1.65 mg/mL glucose oxidase, 0.27 mg/mL catalase, 143 mM BME.

Data Collection and Analysis

Movies were recorded at a rate of 1frame/s for gliding assays and 10 frames/s for single-molecule TIRF motility assays. Data was manually analyzed in ImageJ by selecting microtubule ends and tracking them in gliding assays or selecting fluorescent kinesin and tracking them through multiple frames in single-molecule assays. Velocity for data from the gliding assays and additionally run length for data from the single-molecule TIRF assays was calculated from the displacements measured manually. A test version of the program described in chapter 4 was used to analyze data from the control assays. Velocity data generated from single-molecule assays was tested for normality using the k-s test (Kolmogorov-Smirnov test) at the 0.05 level in OriginLab (Northampton, MA, USA). Data that was significantly drawn from a normal distribution was then compared for statistical significance using a paired t-test. For data that did not fit a normal distribution, a two-sample k-s test was used to determine the statistical significance of any changes observed in the measured parameters between WT and K40R doublets. All statistical analysis was performed in OriginLab (Northampton, MA, USA).

Results

Samples from the *Tetrahymena* doublet purification procedure were run on a 7.5% SDS-PAGE gel. The results are shown in Figure 9. Lanes 2-5 contain WT ciliary proteins at different stages of the purification and lanes 6-9 contain K40R ciliary proteins. Lane 5 contains the purified WT doublets while lane 9 contains the purified K40R mutant doublets. Lane 10 contains 1mg/mL BSA for comparison of protein mass. The final product is enriched in doublets but contains other proteins as well.

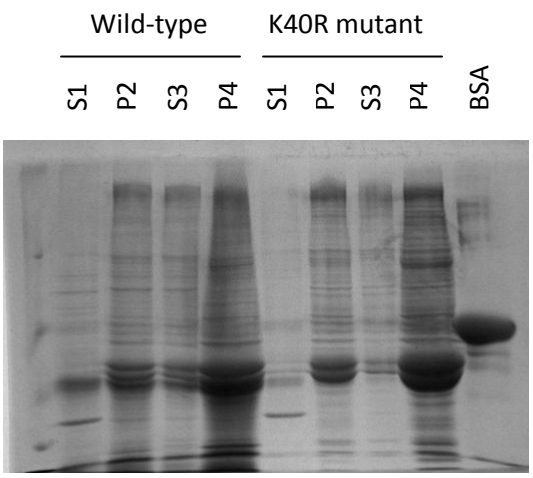

Figure 9: SDS-PAGE for doublet purification. S1 = cilia, P2 = axonemes, S3 = soluble axonemal protein after dialysis, P4 = microtubule doublets, 1 mg/mL BSA standard

Gliding Assays

To begin our analysis, we performed multiple-motor gliding assays on NKHK560cys with WT (N = 26) and K40R (N = 9) doublet microtubules labeled with TMR dye. Velocity for WT (acetylated) doublets was found to be 1.11 μm/s, almost twice the velocity for K40R (unacetylated) doublets which was found to be 0.69 μm/s as shown in Figure 10. A k-s normality test showed that the data was significantly drawn from a normally distributed population ($p>0.05$). Based on this, a paired-sample t-test was performed to show that the 0.42 μm/s difference in velocities is statistically significant ($p<0.05$) with a 95% confidence interval for a difference of 0.28- 0.59 μm/s. To further investigate this difference in motility between the WT and K40R doublets, we went ahead to perform in vitro single-molecule motility assays for the doublets with kinesin-1. In these assays, we hoped to capture changes in other motility parameters, such as run length and binding that might be altered due to a change in the acetylation state of α-tubulin.

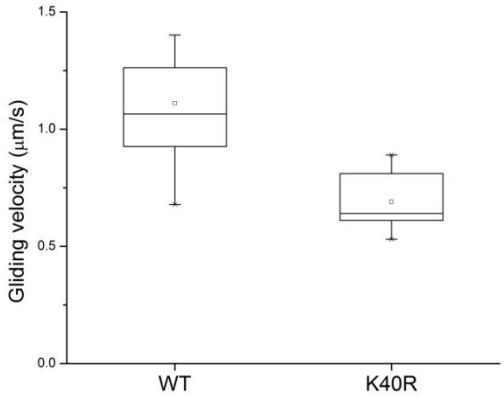

Figure 10: Velocity of WT and K40R doublets in gliding assays with NKHK560 kinesin. Wild-type doublet microtubules moved at 1.11 ± 0.31 μm/s and K40R doublet microtubules moved at 0.69 μm/s ± 0.13

Single-molecule TIRF Motility Assays

Single-molecule motility of RnKHC560-3xmcit was observed on labeled WT or K40R mutant doublets. Individual events were tracked and the data was manually analyzed to compute the velocity and run length for the motor on (WT) acetylated and (K40R) unacetylated doublet microtubules, as summarized in Figure 11. We found that RnKHC560 moves at the same velocity of 0.63 μm/s with standard deviations of ± 0.16 μm/s on WT and ± 0.13 μm/s K40R mutant doublets. The run length on WT doublets is 0.17 ± 0.06 μm (mean ± s.e.) and on K40R doublets, it is 0.18 ± 0.08 μm. These measurements were made from 172 data points for WT doublets and 105 data points for K40R doublets in ten assays for each type of doublet. It was clearly observed in the single-molecule motility assays that over time, kinesin-1 tends to accumulate on and decorate *Tetrahymena* doublet microtubules by sticking to them. The high number of non-moving kinesin observed in these assays could explain the lower velocities recorded here as compared to velocities from our gliding assay results. It is unclear what the cause for kinesin decoration of doublet microtubules might be. We cannot rule out other PTMs or doublet-associated proteins.

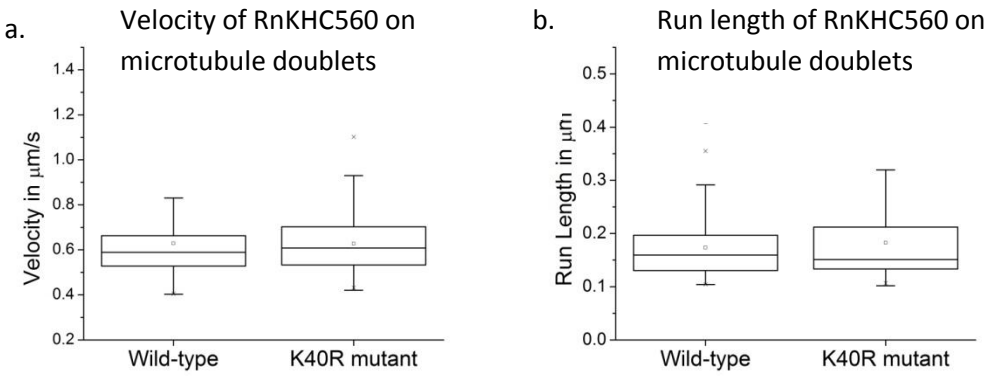

Figure 11: Velocity and run length of RnKHC560 on WT and K40R doublets.
a. Velocity: WT doublets = 0.63 ± 0.16 µm/s, K40R doublets = 0.63 ± 0.13 µm/s;
b. Run length: WT doublets = 0.17 ± 0.06 µm, K40R doublets = 0.18 ± 0.08 µm

Control Experiment

To avoid assay-specific differences in kinesin-concentration, we performed single-molecule TIRF motility assays with simultaneous observations on WT and K40R doublets by flowing them through the same assay chamber. To do this, the doublets had to be differentially labeled. WT doublets were labeled with a 15-fold molar excess of Atto590 (Attotech, Amherst, NY) and K40R mutant doublets were labeled with a 3-fold molar excess of Alexa488 (Invitrogen, Grand Island, NY) following the procedure outlined in the methods section. An image of the Alexa-labeled doublets was captured within the first few seconds of exposure, after which the signal rapidly photo-bleached away, allowing the visualization of single fluorescent kinesin in the same imaging channel. Data was analyzed using a preliminary version of the image processing program described in Chapter 4. Results from 136 events were identified on WT doublets and 206 on K40R doublets are summarized in Figure 12. We found that RnKHC560 runs at a velocity of 0.67 ± 0.22 µm/s on WT doublets and 0.69 ± 0.26 µm/s on K40R mutant doublets (mean ± s.d.). A k-s normality test showed that, at the 0.05 level, the velocity data was not significantly drawn from a normal distribution ($p = 0.002$). A two-sample k-s test showed that the velocity data for RnKHC560 on WT and K40R doublets are not significantly different at the 0.05 level ($p = 0.20$). The run length on WT doublets is 0.36 ± 0.06 µm and on K40R doublets, it is 0.37 ± 0.09 µm (mean ± s.e.). A two-sample k-s

test showed that the run lengths are not significantly different on WT and K40R doublets ($p = 0.15$). Binding was inferred from the landing rate, calculated as the number of events per µm microtubule length per minute. The landing rate was found to be 1.59 events/µm/min on WT doublets and 1.38 events/µm/min on K40R doublets.

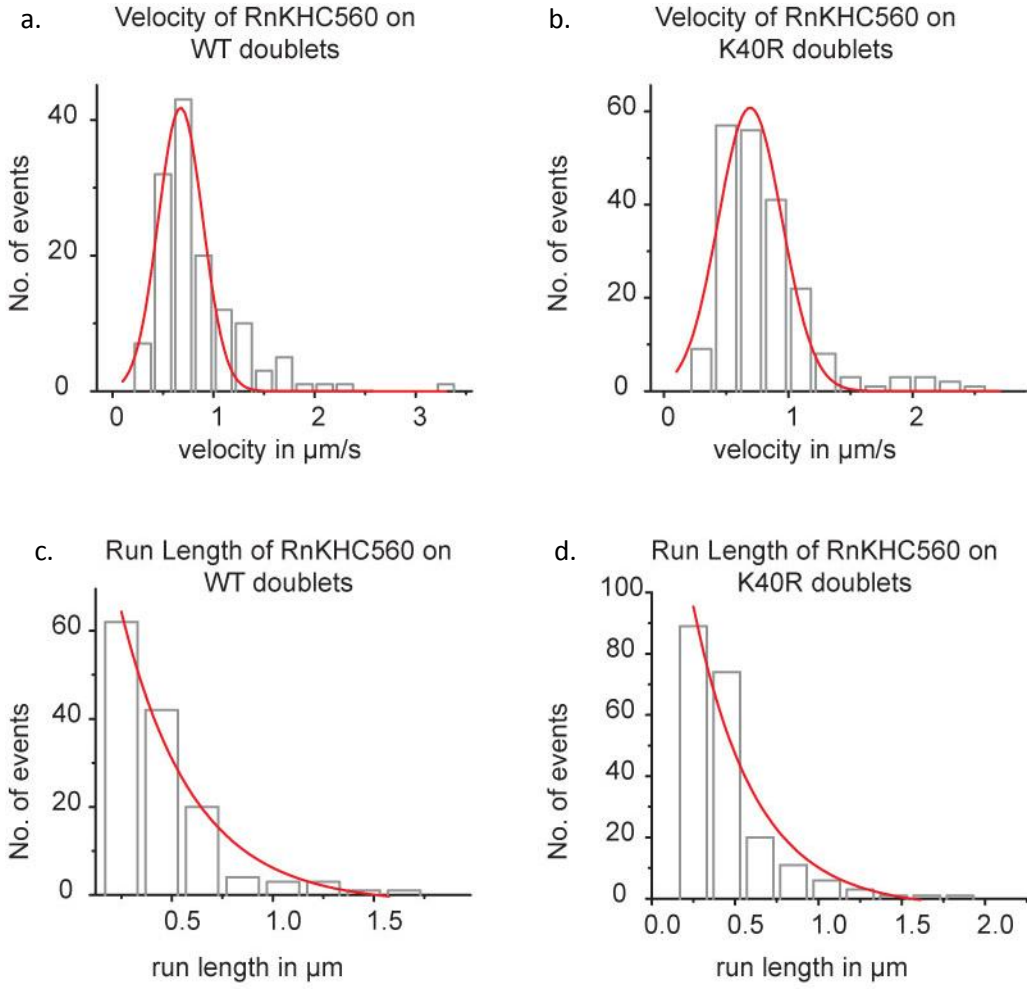

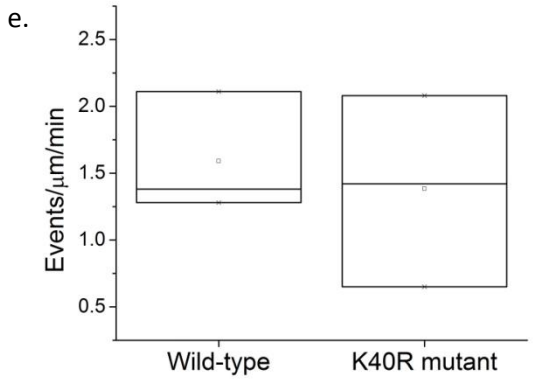

Figure 12: Motility parameters for RnKHC560 on WT and K40R doublets in the same assay. Motility on WT doublets: a. velocity = 0.67 ± 0.22 μm/s, c. run length = 0.36 ± 0.06 μm; Motility on K40R doublets: b. velocity 0.69 ± 0.26 μm/s, d. run length = 0.37 ± 0.09 μm. e. Landing rate on WT doublets = 1.59 events/μm/min; K40R doublets = 1.38 events/μm/min

Discussion of Preliminary Studies

We performed multiple-motor gliding assays and single-molecule TIRF motility assays for kinesin-1 with doublet microtubules extracted from the cilia of WT or K40R mutant Tetrahymena thermophila. While our results from the multiple-motor gliding assay showed that kinesin-1 moves with at 1.11 μm/s on (WT) acetylated doublets but only 0.69 μm/s on K40R doublets, results from the single-molecule assay did not follow the same trend. In single-molecule assays, there was no significant difference between motility on wild-type and mutant doublet microtubules. Identical mean velocities of 0.63 μm/s were recorded for kinesin-1 on wild-type and mutant doublets with slightly different standard deviations of ± 0.16 μm/s and ± 0.13 respectively. Run lengths of 0.17 ± 0.06 μm and 0.18 ± 0.08 μm were recorded on wild-type and mutant doublet microtubules respectively. In assays performed with differentially labeled doublets in the same flow chamber, landing rate of kinesin-1 on mutant microtubules was found to be reduced by a moderate 13%. In my observations of kinesin-1 motility in the single molecule assays performed with doublets, mammalian kinesin did not unbind from doublet microtubules readily. Instead, it showed a tendency to remain bound, eventually decorating the microtubules. This persistent delay in unbinding, which seems to be characteristic of doublet microtubules but not bovine brain microtubules, could create a hidnerance in

motility and lower the mean values of the measured parameters. Despite this consistent underlying observation, the data should still highlight any major differences in binding or motility of kinesin-1 that arise from the absence of acetylation in the K40R mutant doublets. Instead, based on the preliminary results presented here, it appears that kinesin-1 motility does not depend on the presence of the K40 group on α-tubulin. Aside from the observed difference in the interaction of kinesin-1 with doublet microtubules, it is known that axonemal tubulin differs from mammalian neuronal tubulin in many ways. It is rich in poly-modifications charactersitic of axonemal tubulin; for example, microtubules extracted from doublets carry a special axonemal motif (150). Another important difference is that ciliary tubulin has been shown to bind microtubule-inner proteins (MIPs) that play a role in ciliary motility (151-152). Keeping in mind all of the known and observed species- specific differences, it is not completely surprising that our observations do not correlate particularly well with previous *in vivo* observations from literature citing the effect of tubulin acetlyation on kinesin-1 motility in mammalian cells. In my opinion, due to the observed hinderance in motility characteristics for mammalian kinesin, *Tetrahymena* tubulin does not offer a robust substrate to test for the effect of acetylation on kinesin-1 motility. As a result, we revised our strategy and proceeded to work with purified mammalian tubulin which could then be modified with recombinant, purified enzymes. While we began the study by generating deacetylated tubulin through the *in vitro* treatment of bovine brain tubulin with the deacetylase SIRT2, we were fortunate that the acetyl transferase MEC-17, was identified (82). With this new finding, tubulin from a single pool of bovine tubulin could be treated with a deacetylase (SIRT2) or an acetyl transferase (MEC-17) and used to generate two distinct populations of tubulin that were identical in every other way except for their state of acetylation. Microtubules could be polymerized from these populations of tubulins allowing for complete control over the extent of acetylation. We took this opportunity in transitioning over exclusively to observations on mammalian proteins.

2.2 Acetylated and Deacetylated Microtubules

In our preliminary studies, we were faced with the limitation of using doublet microtubules from *Tetrahymena* in our assays. While this provided a stepping stone to

begin the project with, in our observations, we could not rule out effects from doublet-associated MAPs or MIPs and a species-dependent difference in the PTMs. To address our hypothesis that acetylation of α-tubulin K40 alone enhances or upregulates the motility of kinesin-1, we believe that a reductionistic and direct approach is required. While we began working on this approach by using *in vitro* treatment of bovine brain tubulin with the deacetylase SIRT2 to generate deacetylated tubulin (85), we were fortunate that the acetyl transferase MEC-17, was identified (82). With this new finding, tubulin from a single pool of bovine tubulin could be treated either with a deacetylase (SIRT2) or an acetyl transferase (MEC-17) and used to generate two distinct populations of completely acetylated or completely deacetylated tubulin that were homogenized in terms of other modifications or tubulin isotypes. Microtubules could be polymerized from these populations of tubulins allowing for complete control over the state and extent of acetylation. We took this opportunity in transitioning over exclusively to observations on mammalian proteins.

Using microtubules polymerized from the purified and enzyme-treated tubulins, we performed *in vitro* experiments to test our hypothesis. We were able to observe the motility of kinesin-1 on completely acetylated or completely deacetylated microtubules and compare the measured motility parameters. This is the first time that α-tubulin K40 acetylation has been studied in isolation and the direct effect of this modification on kinesin-1 velocity, run length and binding has been recorded.

SIRT2 and MEC17 constructs for the modifying enzymes were gifts from B.J. North and J. Gaertig respectively. Both enzymes were purifed by Virupakshi Soppina. Enzyme-treatment and AMPPNP microtubule-binding experiments were performed by him. Any lysate used in the following experiments was extracted from COS cells by Virupakshi Soppina and Steve Norris.

Materials and Methods

Cloning, Purification and Preparation of Proteins

Mammalian Cell Lysates for Kinesin: The RnKHC560-3xmcit lysate was extracted as described in the previous section.

Bacterial Expression of Kinesin: NKHK560cyshis was purified as described in the previous section. The RnKHC560 sequence was C-terminally tagged with a 6x-histidine tag and transformed into BL21(DE3) cells. Protein expression was induced by addition of 0.4 mM IPTG to a 2L culture in an Erlenmeyer flask. Expression was allowed to proceed for 10 hours at 22 ºC, 225 rpm in a floor incubator. Bacterial lysate was loaded on to a C10 AKTA column packed with Ni-NTA superflow resin (Qiagen, Valencia, CA). The column was washed with 60 mM imidazole and kinesin eluted with 500 mM imidazole on an AKTA FPLC following the purification procedure previously outlined by Hancock and Howard (38).

Enzyme Purification

The MEC17 construct was expressed in a *Rosetta* strain of E. Coli cells and purified as described in Akella et al. (82) using a column packed with GST beads (GE Lifesciences, Piscataway, NJ). Following elution with 10 mM reduced glutathione, the protein was dialyzed in dialysis buffer (20 mM Tris-HCl, pH 8.0, 0.2 mM DTT) overnight at 4 ^{o}C. Recombinant SIRT2 was bacterially expressed in BL21(DE3) cells and purified using the Ni affinity chromatography procedure from North et al. (85). Expression of the SIRT2 enzyme was induced by IPTG over 3 hours at 37C, 250rpm. The bacterial lysate was loaded on a Ni-NTA agarose bead column (Qiagen, Valencia, CA) and the column was washed with 20 mM imidazole. Following elution with 300 mM imidazole, the protein was dialyzed in a Tris-HCl buffer (20 mM Tris-HCl, pH 8.0, 0.2 mM DTT) overnight at 4 ^{o}C.

Tubulin Purification

Tubulin was purified bovine brain through three cycles of polymerization and depolymerization using a modified procedure of the purification protocol from Castoldi and Popov (153).

***In vitro* Enzyme Treatment of Tubulin**

Acetylated tubulin was prepared by incubating purified bovine brain tubulin with purified MEC17 enzyme in the presence of 10 µM Acetyl coenzyme A for 2 hrs at 28^{o}C under constant mixing at 100 rpm on a floor incubator. To obtain deacetylated tubulin, purified bovine brain tubulin was incubated with purified SIRT2 enzyme in the presence of 1 mM NAD (nicotinamide adenine dinucleotide) for 2 hrs at 37^{o}C with constant mixing at 100

rpm on a floor incubator. The resulting modified tubulin was cycled through polymerization and depolymerization to remove any incompetent tubulin generated during enzyme treatment. Acetylation and deacetylation of tubulin was confirmed by using immunoblotting with mouse anti-acetylated tubulin (T6793, Sigma-Aldrich, St. Louis, MO).

Labeling of Tubulin

The two pools of tubulin thus generated were labeled by incubating them with 10-fold excess amine-reactive fluorescent dye at 4C. Excess dye in labeling reactions was quenched with 50 mM K-glutamate after which the tubulins were cycled to remove any incompetent tubulin generated during the labeling procedure. Deacetylated tubulin was labeled with Alexa Fluor 488 carboxylic acid, succinimidyl ester (Invitrogen, Grand Island, NY) with a resulting labeling ratio of 0.90 while acetylated tubulin was labeled with Atto590 carboxylic acid, succinimidyl ester (ATTO-TEC GmbH, Amherst, NY) with a resulting labeling ratio of 0.57.

Kinesin Binding Assay

Increasing concentrations of kinesin lysates were incubated with 0.1mg/mL taxol-stabilized microtubules and 1 mM AMPPNP for 30 minutes at room temperature with constant mixing. The kinesin-microtubule complexes were pelleted at 18^{o}C for 30 min through a 60% glycerol cushion. The pellet and supernatant was dissolved in SDS-PAGE sample buffer and used for immunoblotting as previously described (117). Mouse anti-acetylated tubulin (T6793Sigma), anti-myc antibody and anti-β-tubulin antibody were used for Western-blotting. The blots were scanned and used for quantification in ImageJ (NIH) software.

Gliding Assays

Gliding assays were performed as described in the previous section on *Tetrahymena* doublet microtubules. Motors used for gliding assays were bacterially expressed NKHK560cys his and RnKHC560cyshis. BP450-490, FT510, BP515-565 filters were used for visualizing Alexa488-labeled microtubules and Q555LP, HQ590/50m, HQ525/50x filters were used for visualizing Atto590- labeled microtubules.

Single-molecule TIRF Motility Assays

Motility assays were performed on a Zeiss Axiovert microscope modified to allow TIRF microscopy using a 488nm Ar-ion laser for excitation (50). The resulting images were chromatically separated using a commercial dual view device (DV2, Photometrics, Tucson, AZ) with a T585lpxr dichroic and HQ510, ET525/50m filters (Chroma Technology Corp., Bellows Falls, VT, USA) such that motility events on acetylated and deacetylated microtubules in the same assay could be visualized side-by-side using a single CCD camera chip. Flow chambers were made using cover slips (Corning) that were cleaned with deionized distilled water and then coated with poly-lysine. Microtubules were polymerized in the presence of 1 mM GTP using 4mg/mL tubulin such that labeled: unlabeled tubulin ratios were 1:60 and 1:15 for deacetylated and acetylated microtubules respectively. Polymerized deacetylated and acetylated microtubules were mixed together and then flowed through the same flow chamber. Microtubules were allowed to adsorb to the cover-slip for 5 min before 1mg/mL BSA was introduced into the chamber as to reduce nonspecific binding of kinesin to the cover-glass surface. The final flow-through for the assay was ~10 nM kinesin in P12 buffer (12 mM PIPES, 2 mM $MgCl_2$, 1 mM EGTA, pH 6.8) containing 1 mM $MgCl_2$, 2 mM ATP, 1 mg/mL BSA, 10 mM glucose, 1.65 mg/mL glucose oxidase, 0.27 mg/mL catalase, 143 mM BME, 10 mM phosphocreatine, 0.05 mg/mL creatine phosphokinase. Control experiments were performed with unlabeled microtubules to account for any effects the different dyes may have had or in the presence of 1 mM GMPCPP instead of GTP to avoid the use of taxol for stabilization. We also repeated the assays in the presence of high ionic strength buffer (25 mM HEPES, 115 mM KOAc, 5 mM NaOAc, 5 mM $MgCl_2$, 0.5 mM EGTA, pH 7.4) instead of P12 to mimic physiological environmental conditions.

Data Collection and Analysis

Movies were recorded at a rate of 10 frames/s and analyzed using a custom-written single-molecule tracking Matlab (Mathworks Inc., Natick, MA) program. The program identifies fluorescent peaks within a selected region of interest and then determines the exact location for the centroid of each peak based on its fit to a Gaussian profile. It then tracks these identified points if they are consistently progressing from one frame to the

next and records a series of points for each motility event. Finally, it calculates individual velocities and run lengths for each of the recorded events. All runs above 0.15 µm were included in the analysis. To obtain a distribution for the velocity and run length measurements, histograms were generated by plotting the number of events observed against binned values. The velocity profile was fit to a Gaussian distribution with the centroid of the Gaussian specifying the mean velocity. The run length profile was fit to an exponential distribution with the decay constant of the exponential specifying the mean run length. The R^2 value of the fits indicates the proportion of variability that the fit is able to account for. Histograms for the velocity data were fit to Gaussian distributions with R^2 >95% and histograms for the run length were fit to single exponential distributions with R^2 >80% in Origin Lab. Binding was estimated by measuring the landing rate on microtubules. The number of events on a selected microtubule in a recorded movie was counted and then divided by the length of the microtubule and the length of the movie in order to obtain a landing rate with the units of events/µm/min. Velocity data generated from single-molecule assays was tested for normality using the k-s test at the 0.05 level. A two-sample k-s test was used to determine statistical significance in the comparison of velocities and also that of run lengths.

Results

In vitro assays performed using microtubules polymerized from the generated pools of completely acetylated or completely deacetylated tubulin allowed us to isolate the effect of K40 α-tubulin acetylation on kinesin-1 motility. The distinct populations of acetylated and deacetylated tubulin were generated by *in vitro* enzyme-treatment of tubulin with bacterially purified deacetylase SIRT2 (85) and acetyl-transferase MEC17 (82). While purified bovine brain tubulin used for *in vitro* modifications already contains some amounts of α-tubulin that is acetylated on the ε-amino group of K40, when treated with MEC17 in the presence of Acetyl coenzyme A, an acetyl group is transferred from coenzyme A to those K40 α-tubulins whose ε-amino groups are not already acetylated. The same acetyl group is completely removed upon treatment with SIRT2, an NAD^+-dependent deacetylase. Results obtained from the enzyme treatment are confirmed by blotting with an antibody specific to the K40 acetylation site on α-tubulin (T6793 sigma)

as shown in Figure 13. We expect that a comparison of the binding and motility parameters of the motor on completely acetylated and completely deacetylated microtubules through *in vitro* experiments would unambiguously answer the question of whether the kinesin-1 directly recognizes K40 α-tubulin acetylation.

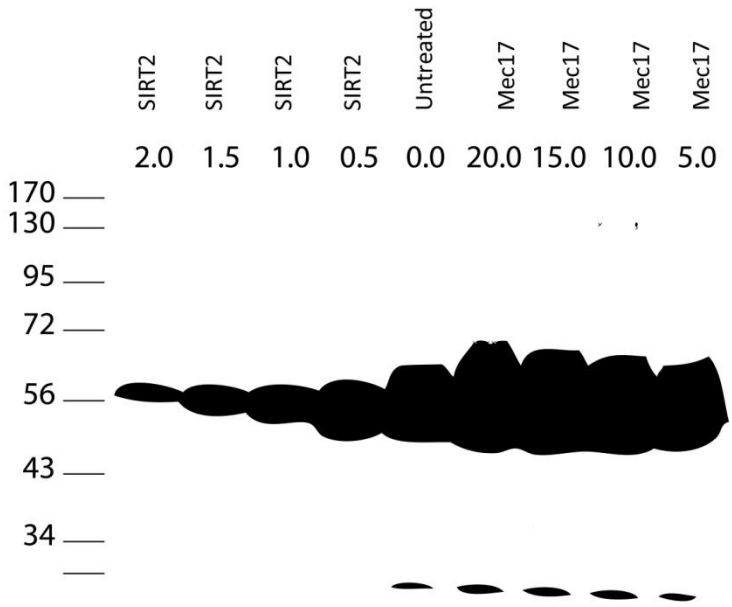

Figure 13: Western blot for acetylation and deacetylation of tubulin. Acetylated tubulin was detected using the 6-11B-1 antibody after enzyme treatment with different concentrations of acetyl transferase or deacetylase enzymes (treatment and Western blot by Virupakshi Soppina). Assuming that untreated bovine tubulin is a reference for 50% acetylated tubulin, completely acetylated tubulin is nearly 100% acetylated while completely deacetylated tubulin is ~5% acetylated

Binding Assays

To confirm that the motor was able to bind to microtubules polymerized from either the pool of acetylated tubulin or deacetylated tubulin, we performed binding experiments in the presence of AMPPNP, a non-hydrolyzable analog of ATP. The kinesin-microtubule complex was pelleted by centrifugation followed by SDS-PAGE analysis of the supernatant and pellet. The extent of binding was then measured by quantifying the kinesin content of the supernatant and pellet on the gel (data not shown). Both mammalian-expressed and bacterially expressed RnKHC560 were tested in these assays. We observed that the fully acetylated and fully deacetylated microtubules were equally competent in binding to kinesin-1 in the presence of AMPPNP. In fact, as expected from

the known kinetic characteristics of kinesin-1, with an excess of microtubules, all the kinesin-1 binds in the AMPPNP state.

Single-molecule TIRF Motility Assays

To determine if acetylation and deacetylation of tubulin directly modulate the motility of single kinesin motors on microtubules, we performed *in vitro* motility assays with fluorescently labeled, acetylated and deacetylated microtubules and rat kinesin (RnKHC560-3xmCit) using TIRF microscopy. In particular, we wanted to determine if K40 α-tubulin acetylation affects the velocity, run length (processivity) and binding of kinesin-1 on microtubules. To avoid any assay-specific differences in motor concentration when comparing the motile properties on acetylated and deacetylated microtubules, events were simultaneously observed on differentially labeled (acetylated and deacetylated) microtubules in the same flow chamber. Initially, for each field of view, a still image of the microtubules made from either acetylated tubulin labeled with Atto590 dye or deacetylated tubulin labeled with Alexa488 dye was captured using dual-color imaging. This initial image was later used for identifying microtubule tracks for each kinesin event traced during data analysis. Motility events for fluorescent kinesin in the same field of view were recorded a few seconds later when the Alexa488 dye marking the microtubules had completely photo-bleached. Fluorescent kinesin could be continuously observed as they were binding, moving along microtubules and unbinding on one half of the image produced by the dual view. To represent the range of velocities and run length, all data were compiled in histograms as shown in Figure 14.

The velocity data fit to Gaussian distributions and the run length data fit to exponential distributions as shown in Figure 14. RnKHC560 moved with a mean velocity of 0.67 ± 0.15 μm/s on acetylated (N = 1151) microtubules and 0.69 ± 0.19 μm/s on deacetylated (N = 1132) microtubules. A k-s normality test showed that the data was not significantly drawn from a normally distributed population ($p<0.05$). Based on this, a two-sample k-s test was performed to show that the 0.02 μm/s difference in mean velocities is statistically significant with $p = 0.001$. However, the 3% decrease in velocity on deacetylated microtubules is not sufficient to explain the exclusive selectivity of kinesin-1 motility along acetylated microtubules observed *in vivo*. Run length was 0.55 ± 0.33 μm on

acetylated microtubules and 0.50 ± 0.43 µm on deacetylated microtubules, also shown in Figure 14. A two-sample k-s test resulted in a p = 0.21, indicating that the difference in run length means is not statistically significant. Landing rate for the motors, calculated as the number of events observed on a given length of microtubules per unit time was found to be 3.84 ± 1.00 events/µm/min on deacetylated microtubules and 3.72 ± 1.48 on acetylated microtubules (see Figure 14). The landing rate data distributions were found not to be significantly different in a two-sample k-s test with a p = 0.19. Data obtained from two separate batches of treated tubulin showed that there was no significant change induced in RnKHC560 motility due to the presence of α-tubulin K40 acetylation.

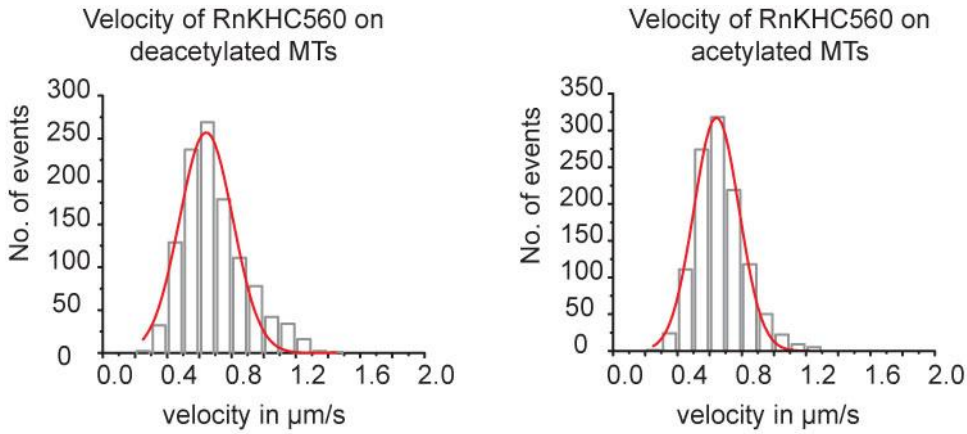

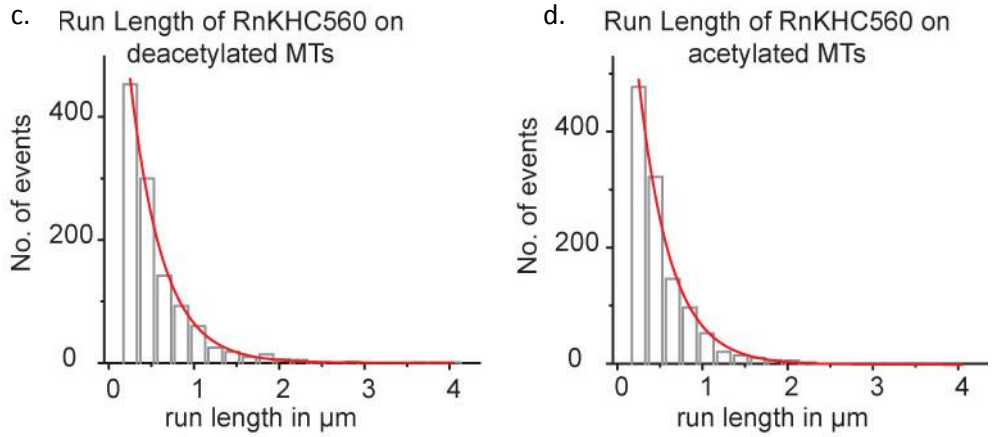

e.

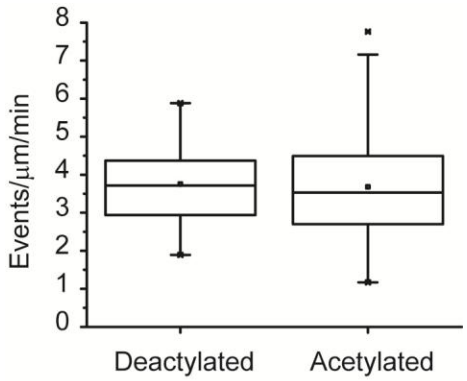

Figure 14: Motility parameters for RnKHC560 on acetylated and deacetylated microtubules in the same assay. A comparison of motility on acetylated and deacetylated microtubules shows no change in motility parameters. Motility on deacetylated microtubules: a. velocity = 0.67 ± 0.15 µm/s, c. run length = 0.50 ± 0.43 µm; Motility on acetylated microtubules: b. velocity = 0.69 ± 0.19 µm/s, d. run length = 0.55 ± 0.33 µm. e. Landing rate on acetylated microtubules = 3.84 ± 1.00 events/µm/min; deacetylated microtubules = 3.72 ± 1.48 events/µm/min

Control Experiments

To be able to visualize events on both acetylated and deacetylated microtubules simultaneously in our assays, the acetylated and deacetylated microtubules were differentially labeled. While deacetylated microtubules were labeled with Alexa488, acetylated microtubules were labeled with the longer Atto590, both using with the same labeling chemistry. Even though the microtubules were minimally labeled with a labeling ratio of 1.5 - 3.8%, different fluorescent dyes may have different properties, including some related to the electrical charge they carry. The concern was that this might interfere with any existing electrostatic or structural interactions between the kinesin and the microtubule. Controls for possible effects of the Alexa488 and Atto590 dyes on the kinesin-microtubule interaction were performed by repeating measurements for velocity, run length and binding in separate assays for unlabeled acetylated or deacetylated microtubules. These assays confirmed that the dyes used in our experiments did not change our results. Figure 15 shows histograms to compare the measured velocities and run lengths, and a bar graph to compare landing rates. Kinesin-1 on unlabeled acetylated and deacetylated microtubules had a velocity of 0.61 ± 0.14 µm/s and 0.67 ± 0.13 µm/s

respectively. While a two-sample k-s test showed that the two distributions are significantly different at the 0.05 level ($p << 0.05$), the 9% difference in mean velocities is not sufficient to explain kinesin-1 selectivity for acetylated microtubules as observed *in vivo*. Run length on unlabeled acetylated and deacetylated microtubules was 0.47 ± 0.29 µm and 0.46 ± 0.33 µm respectively. A two-sample k-s test showed that the run length distributions are not significantly different ($p = 0.54$). Landing rate on unlabeled acetylated and deacetylated microtubules was 4.38 events/µm/min and 6.69 events/µm/min respectively.

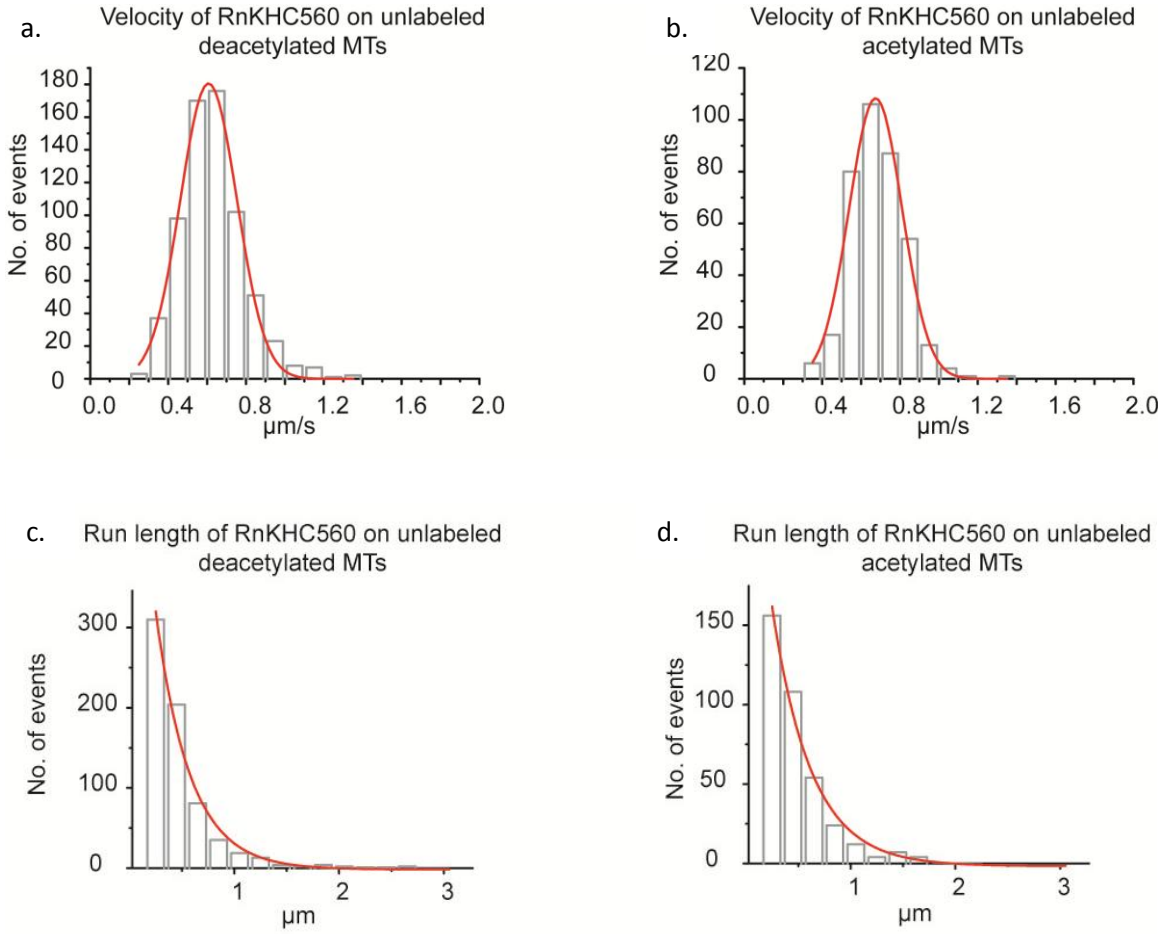

e.

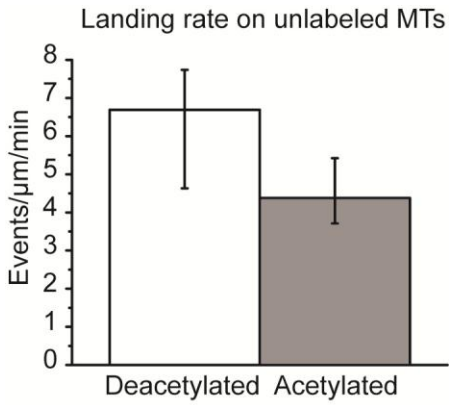

Figure 15: Motility parameters for RnKHC560 on unlabeled acetylated and deacetylated microtubules. The use of different dyes to label acetylated and deacetylated microtubules does not affect motility. Motility on deacetylated microtubules: a. velocity = 0.67 ± 0.13 µm/s, c. run length = 0.46 ± 0.33 µm; Motility on acetylated microtubules: b. velocity 0.61 ± 0.14 µm/s, d. run length = 0.47 ± 0.29 µm. e. Landing rate on deacetylated microtubules = 6.69 events/µm/min; acetylated microtubules = 4.38 events/µm/min

The K40 acetylation site is in the lumen of the microtubule (56), similar to the taxol-binding site and so an associated concern was the possibility of interference from the use of taxol to stabilize microtubules in our motility assays. Because we do not know how acetylation affects microtubules, it is possible that taxol may somehow mask that effect and thus conceal the ability of kinesin to distinguish acetylated and deacetylated microtubules from one another. Controls were performed to exclude this possibility by using taxol-free GMPCPP microtubules. As shown in Figure 16, we found no significant change in the motility properties of kinesin on acetylated or deacetylated microtubules stabilized without taxol. Kinesin-1 on GMPCPP acetylated and deacetylated microtubules had a velocity of 0.74 ± 0.14 µm/s and 0.73 ± 0.16 µm/s respectively. Run length on GMPCPP acetylated and deacetylated microtubules was 0.77 ± 0.14 µm and 0.79 ± 0.10 µm respectively. A two-sample k-s test showed no statistically significant difference in the distributions with $p = 0.91$ for velocity data compared and $p = 0.23$ for run length data compared. Landing rate on GMPCPP acetylated and deacetylated microtubules was 3.23 events/µm/min and 5.00 events/µm/min respectively.

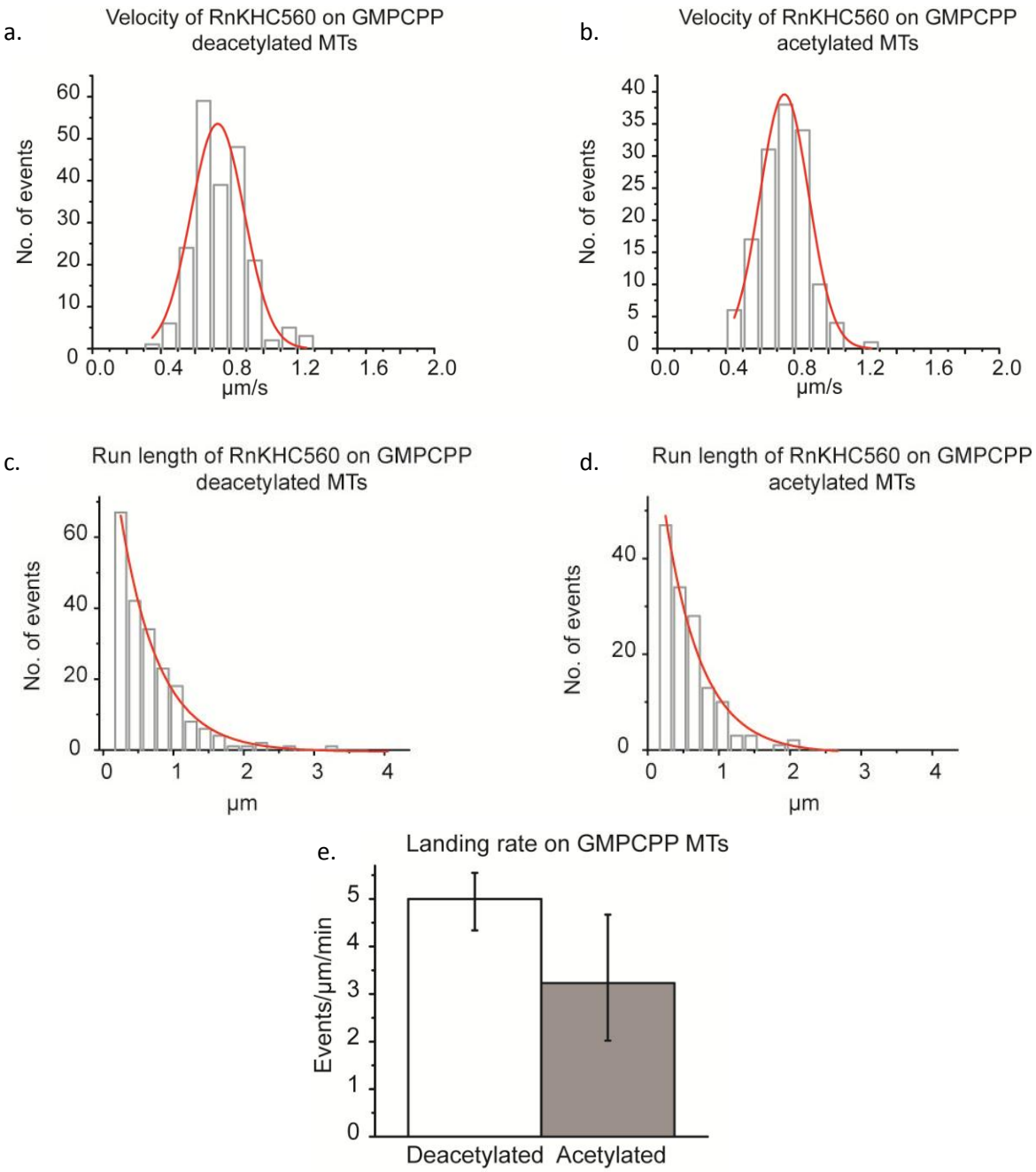

Figure 16: Motility parameters for RnKHC560 on GMPCPP-stabilized acetylated and deacetylated microtubules. The use of taxol to stabilize microtubules does not differentially affect acetylated and deacetylated microtubules. Motility on deacetylated microtubules: a. velocity = 0.73 ± 0.16 μm/s, c. run length = 0.79 ± 0.10 μm; Motility on acetylated microtubules: b. velocity 0.74 ± 0.14 μm/s, d. run length = 0.77 ± 0.14 μm. e. Landing rate on deacetylated microtubules = 5.00 events/μm/min; acetylated microtubules = 3.23 events/μm/min

The kinesin-microtubule interaction has been shown to be dependent on the ionic strength of the motility buffer (154). In order to ensure that our observations were not affected by

assay buffer conditions, we conducted experiments using PERM buffer (25 mM HEPES, 115 mM KOAc, 5 mM NaOAc, 5 mM $MgCl_2$, 0.5 mM EGTA, pH 7.4) to mimic the physiological environment *in vivo*. Figure 17 shows a comparison of the velocity, run length and landing rate measurements. Under these conditions as well, there was no appreciable change in kinesin-1 motility due to a difference in the acetylation state of the microtubules. Kinesin-1 on acetylated and deacetylated microtubules in a high ionic strength buffer had a velocity of 0.78 ± 0.15 µm/s and 0.81 ± 0.18 µm/s respectively. Run length on acetylated and deacetylated microtubules in a high ionic strength buffer was 0.57 ± 0.30 µm and 0.62 ± 0.37 µm respectively. A two-sample k-s test showed that the distributions are not significantly different with p = 0.22 for velocity data compared and p = 0.78 for run length data compared. Landing rate on acetylated and deacetylated microtubules in a high ionic strength buffer was 0.82 events/µm/min and 1.26 events/µm/min respectively.

Our results are not influenced by the use of dyes, microtubule-stabilizing agents or buffer ionic strength. In conclusion, the results show that that enzymatic acetylation of α-tubulin K40 by itself cannot directly account for the highly preferential transport of kinesin-1 on acetylated microtubules observed *in vivo*.

a.

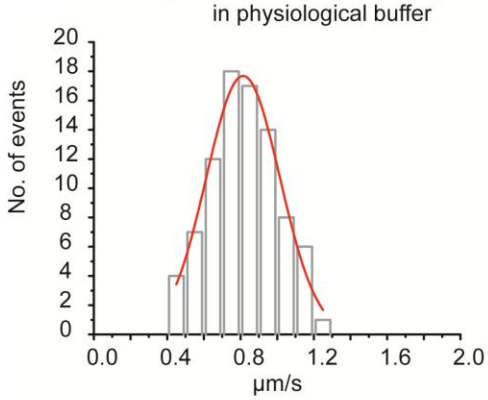

b.

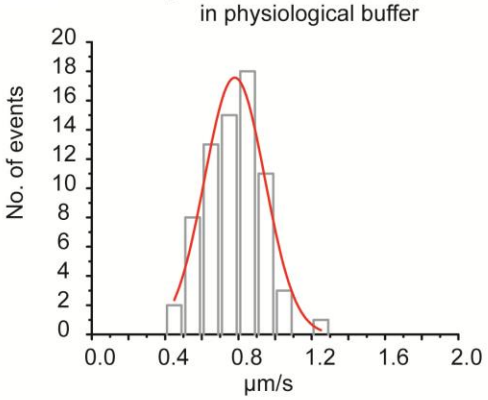

c.

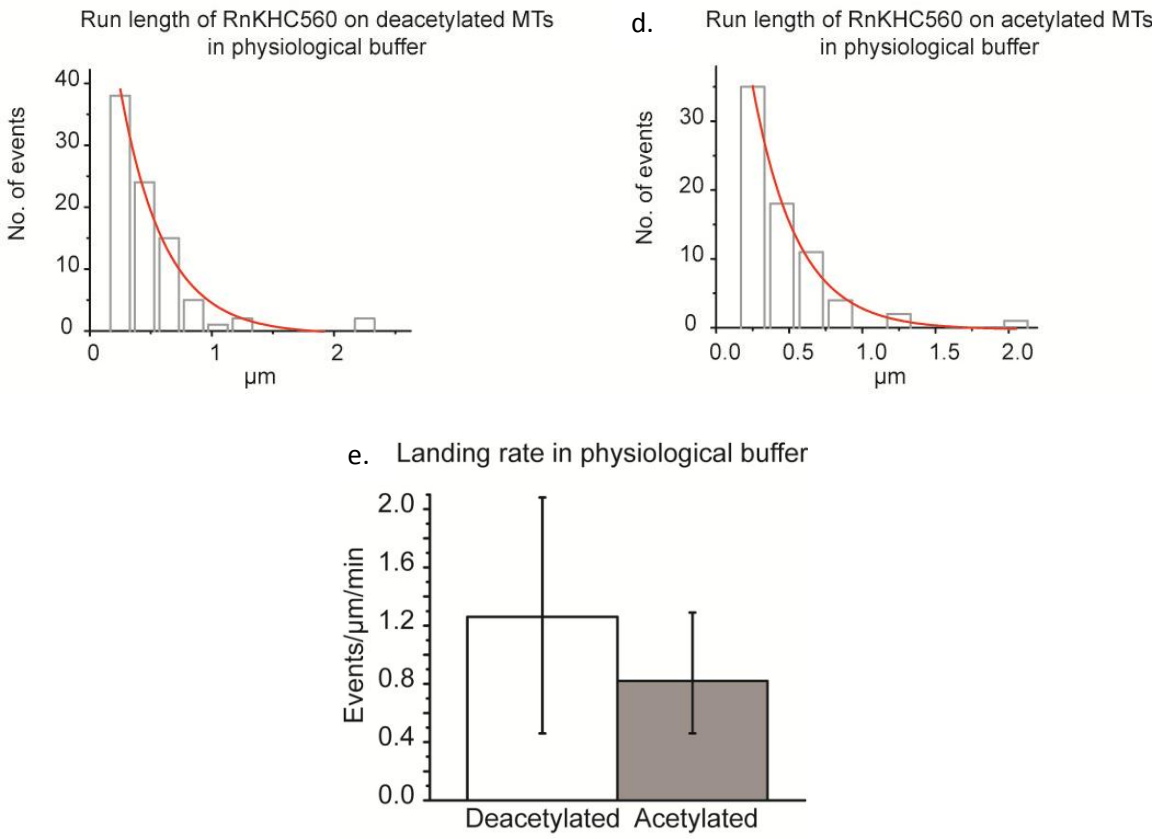

Figure 17: Motility parameters for RnKHC560 on acetylated and deacetylated microtubules in a physiological buffer. Our results are consistent when the assays are repeated in a high ionic strength buffer. Motility on deacetylated microtubules: a. velocity = 0.81 ± 0.20 μm/s, c. run length = 0.62 ± 0.32 μm; Motility on acetylated microtubules: b. velocity 0.78 ± 0.16 μm/s, d. run length = 0.57 ± 0.26 μm. e. Landing rate on deacetylated microtubules = 1.26 events/μm/min; acetylated microtubules = 0.82 events/μm/min

To make a direct comparison to our results from gliding assays performed with the *Tetrahymena* doublet microtubules in the previous section of this chapter, we performed gliding assays with an NKHK560 chimera using our purified, labeled acetylated and deacetylated bovine brain microtubules. Deacetylated microtubules moved at a mean velocity of 1.18 ± 0.06 μm/s while acetylated microtubules moved at a mean velocity of 0.93 ± 0.06 μm/s on NKHK560 kinesin. When this assay was repeated using RnKHC560 kinesin, we found the mean velocity for deacetylated microtubules was 0.50 ± 0.03 μm/s and for acetylated microtubules it was 0.49 ± 0.02 μm/s. N = 24 for all measurements shown in Figure 18. The values are in agreement with previously published data for these

two motors. While, a two-sample k-s test indicates statistically significant differences in velocity data distribution for NKHK560 ($p << 0.05$), the increase in velocity observed with this chimeric motor does not correspond with the trend seen for *Tetrahymena* doublets. Velocity data distribution was not significantly different for RnKHC560 ($p = 0.90$) and these results indicate that K40 acetylation of α-tubulin does not affect kinesin-1 velocity in a multiple-motor gliding assay.

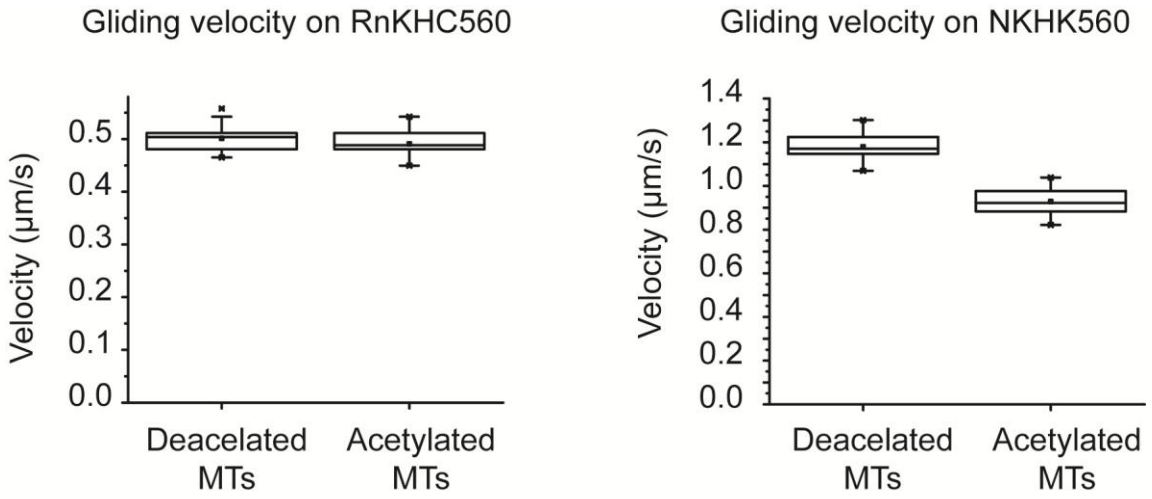

Figure 18: Velocity of acetylated and deacetylated microtubules in gliding assays with NKHK560. There is no significant change in the gliding velocity between acetylated and deacetylated microtubules using either a. RnKHC560 or b. NKHK560 kinesin constructs. The trend for NKHK560 is not consistent with that previously observed for doublets (compare with Fig. 10).

Discussion

PTMs of tubulin are postulated to play many different roles in regulating cellular processes. The goal of our work is to determine if PTMs of tubulin are able to directly modulate the interactions of kinesin with microtubules and thus enable selective, targeted transport in cells. To do this, we compared the binding and motility of kinesin-1 on completely acetylated and completely deacetylated microtubules through *in vitro* experiments. Microtubules were polymerized from purified, enzyme treated tubulin obtained from treating bovine brain tubulin with either the MEC17 or SIRT2 enzymes *in vitro*. Results of enzyme-catalyzed acetylation and deacetylation were confirmed by

using an anti-body specific for acetylation of K-40 on α-tubulin. Based on our hypothesis that acetylation of K40 on α-tubulin directly affects kinesin-1 motility, we expect that any change in the state of acetylation will result in a corresponding change in the motor velocity, run length or binding. We therefore quantified these parameters by observing kinesin-1 motility on acetylated and deacetylated microtubules together in a single-molecule TIRF motility assay. Because the kinesin-1 motility is stochastic in nature, results from the measured motility parameters follow a statistical distribution, from which the means can be estimated. In order to ensure that our results were robust, we made our data sets large enough (n>1000) to comfortably perform stastical analysis such as fitting of Gaussian or exponential profiles to velocity and run length histograms respectively. Our results have shown that the *in vitro* motility of kinesin-1 is indistinguishable on microtubules polymerized from completely acetylated versus completely deacetylated tubulin. A two-sample k-s test performed to show that the 0.02 μm/s difference in mean velocities is statistically significant with $p = 0.001$. However, the 3% decrease in velocity on deacetylated microtubules is not sufficient to explain the exclusive selectivity of kinesin-1 motility along acetylated microtubules observed *in vivo*. A 10% decrease in run length on deacetylated microtubules was shown to be statistically insignificant with a $p = 0.21$ for run length data comparison. Mean landing rate for the motors was found to be nearly 4.0 events/μm/min on both acetylated and deacetylated microtubules. This was also statistically insignificant as per analysis. We also performed control assays to test for the effect of differential labeling, taxol-stabilization and ionic strength on the motility parameters being measured. From our experiments, we conclude that kinesin-1 motility is not directly influenced by acetylation or deacetylation of K40 on α-tubulin of microtubules.

Ours is the first study of its kind because having been conducted in an *in vitro* environment comprising of only the interacting proteins of interest, it eliminates any effects from interactions with the global transport machinery, MAPs or changes in other PTMs. A working example of the effect of such interactions was recently shown by Sudo and Baas through their observation that in cells, the MAP ‘tau’ inhibits acetylation-based enhancement of katanin binding (123). At first glance, our findings may be surprising because simplistically, they appear to be in conflict with previous literature on the same

subject. But a closer investigation reveals that the experimental conditions for these related observations are distinctly different. For the reader's benefit I will briefly discuss the most closely related previously published studies and how the differences between our experiment and theirs lead us a step closer to understanding the mechanism by which tubulin PTMs might function.

The Reed et al. paper was a turning point in establishing a strong correlation between acetylation of K40 on α-tubulin and kinesin-1 motility (117). A majority of the results in this paper were based on cell biological studies using neurons to show that acetylation upregulates the motility of kinesin-1 *in vivo*. In an extension of the results to an *in vitro* assay, microtubules were polymerized from purified WT and mutant *Tetrahymena* axonemal tubulin to show that gliding velocity of K40R microtubules was reduced by 17% on kinesin-1, when compared with the gliding velocity of WT microtubules. A bulk AMPPNP-binding assay showed that significantly less kinesin-1 bound to K40R tubulin than to bovine or WT tubulin. It was concluded that acetylation of α-tubulin K40 promotes anterograde transport of kinesin-1 cargo and that kinesin-1 binding and motility is directly enhanced by acetylation of α-tubulin K40. We have seen a similar increase in velocity for WT (acetylated) microtubules over K40R (unacetylated microtubules) in our gliding assays but subsequent results from motility assays with enzyme-treated acetylated and deacetylated tubulin did not follow the same trend. This apparent conflict could be explained by a number of reasons. It is possible that the difference in kinesin-1 velocity between WT and K40R microtubules is dependent on the multi-motor configuration. Also, WT *Tetrahymena* axonemal tubulin carries vastly different modifications than neuronal (bovine- brain) tubulin and consists of different tubulin isotypes (150). WT axonemal α-tubulin, for example, runs faster on an SDS-PAGE gel than bovine brain α-tubulin (117). For example, axonemal tubulin is known to specifically carry a conserved axonemal motif (EGEFXXX), essential for ciliary beating. Upon genetic mutation, axonemal tubulin in the K40R mutant could have experienced changes in the levels of the other PTMs (155) and so it is possible that mutating the K40 residue could produce different results than the *in vitro* acetylation and deacetylation techniques used in our current work. In our work, we found that the difficulty in working with sticky axonemal tubulin which does not cycle particularly well imposes practical limitations on the

performance of motility assays. While there exist some differences in motility between wild-type and K40R doublet microtubules, the differences are not commensurate with microtubule selectivity observed *in vivo* for kinesin-1. These differences do not repeat in single-molecule motility assays with *Tetrahymena* doublets and most importantly, are not observed in a thorough comparison of kinesin-1 motility on completely acetylated and completely deacetylated microtubules generated by *in vitro* enzyme treatment of bovine tubulin. Our results with purified components conclusively show that acetylation of K40 on α-tubulin does not directly affect the single-molecule motility of kinesin-1.

Another extensive study on the effect of tubulin acetylation on kinesin-1 motility was performed by treating neurons with a deaceatylase inhibitor. Trichostatin A (TSA) is a small molecule that has been shown to inhibit 11 known human histone deacetylases (HDACs) and cause hyper-acetylation in cells (133). Dompierre et al. treated neurons with TSA to show that the kinesin-1 dependent BDNF-vesicle transport deficit resulting from Huntington's disease could be rescued by TSA- treatment (128). An increase in both anterograde and retrograde axonal transport upon TSA-induced hyper-acetylation of microtubules was shown and it was concluded that increased acetylation by HDAC6 inhibitors acts as a general mechanism to regulate microtubule-based transport in cells. Contrary to our experiments, these experiments do not isolate the effect of (K40) α-tubulin acetylation on kinesin-1 motility to focus on the direct interaction between two proteins of interest. In fact, Zilberman et al. showed that specifically the TSA-induced inhibition of HDAC6 (and not siRNA mediated knock-down) in cells affects microtubule dynamics (130). Another recent paper on the effect of HDAC6 on Huntington's disease shows that while HDAC6 knock-out increases tubulin acetylation in neuronal cells throughout the brain, it does not, in fact, modify kinesin-1 dependent BDNF transport or disease progression (129). In co-existence with these conflicting studies, there have been constistent reports of overlapping tubulin PTMs (156), one of which was recently shown to play a more direct role in kinesin-1 motility, as described below.

Konishi et al. showed that in neurons, mutation of a 4-amino-acid sequence in the β5-L8 region of the kinesin-1 motor domain abolished its preferential selectivity towards axonal (detyrosinated) microtubules over dendritic (tyrosinated) ones (126). They further

performed bulk *in vitro* assays to test the binding of kinesin-1 to tyrosinated and detyrosinated microtubules in the presence of AMPPNP. These binding assays were performed in the presence of high tubulin concentrations and with incubation times far exceeding the time for attaining equilibrium in a kinesin-microtubule binding reaction of this nature. For detyrosinated microtubules, they observed increased binding of WT but not mutant kinesin whereas for acetylated microtubules obtained from TSA-treated HeLa cells, they reported an increase in the binding of both WT and mutant kinesin. From this they concluded that tubulin detyrosination in microtubules enables selective binding of kinesin-1 while acetylation may increase overall binding. It is useful here to note that *in vivo* acetylation and detyrosination of microtubules is believed to be concurrent even among different cell types, thus generating a subset of acetylated and detyrosinated microtubules (121, 157-159). Cai et al. and Dunn et al., both observed that kinesin-1 shows preferential motility on this subset of modified microtubules (109, 122), but Dunn et al. observed higher gliding velocities for purely tyrosinated microtubules *in vitro*. Clearly, before the acetyl transferase MEC17 was identified and isolated, it was not easy to isolate the effect(s) of acetylation.

It is for the first time ever that we are presenting results from the direct observation of kinesin-1 motility with specific control over the level of α-tubulin K40 acetylation. We have shown that the motility of kinesin-1 *in vitro* is not directly affected by acetylation of the α-tubulin K-40 residue. From this we conclude that kinesin-1 cannot directly recognize the acetylation state of α-tubulin K40. We have taken the first step in presenting a new approach to understand the functions of PTMs- one that avoids ensemble effects in altering PTMs, global intra-cellular changes occurring from altering one (or more) of the modifications and the influence of MAPs. As is evident from the discussed literature, *in vivo*, PTMs are seldom found in isolation. In this context, acetylation and detyrosination are found to be concurrent modifications. Since we do not yet know why PTMs occur concurrently or how they might influence each other, it would be interesting to investigate the combined effect of α-tubulin acetylation and detyrosination on kinesin-1 motility, such that each modification can be controlled independently. This would help us correctly identify their independent effects and learn how the modifications influence one another to understand their collective effect.

CHAPTER 3

The Combined Effect of Tubulin Acetylation and Detyrosination on the *in vitro* Motility of Kinesin-1

In the previous chapter we have shown through *in vitro* single molecule motility assays, that acetylation of K40 on α-tubulin has no direct effect on the binding and motility of kinesin-1 on microtubules. Our study was robust consisting of a large data set with additional control experiments to test for interference from dyes used to label tubulin, the use of taxol for stabilizing microtubules and the assay buffer conditions used. The result was surprising because it appeared to contradict previous results from literature which suggested an increase in kinesin-1 binding and velocity due to acetylation of K40 on α-tubulin. Upon carefully examining the experimental conditions from previous studies, it became clear that the common denominator for these experiments was the presence of additional tubulin PTMs. In seeking to bridge the gap between their observations and ours, we must take a few steps back to look at the other PTMs that might be involved in the kinesin-microtubule interaction being investigated. It is important to recollect from the introduction to this thesis, that α-tubulin acetylation of microtubules in cells has long been associated with another modification- detyrosination of α-tubulin CTTs. The overlap of these two modifications has been recorded separately in a variety of cell types including neurons, cochlear epithelial cells, chondrocytes and osteoclasts (121, 157-159). In experiments directly related to the PTM hypothesis for kinesin, both Dunn et al. and Cai et al. observed that in COS cells, fluorescently labeled kinesin-1 translocates along microtubules that are marked by anti-bodies for both acetylation and detyrosination of α-tubulin (109, 122). Konishi et al. showed that in neuronal axons, it is α-tubulin detyrosination that leads to the preferential recruitment of kinesin-1 through its motor domain. This led us to speculate that the physiologically relevant state of these two modifications i.e., for them to be concurrent on the same microtubule, could be the related to the observed changes in motility indicated in previous literature. As a result, we

decided to adopt a combinatorial approach by investigating the effect of α-tubulin acetylation plus detyrosination of microtubules on kinesin-1 motility. Since there is no recombinant form of the tyrosine ligase enzyme or the enzyme for detyrosination, we purified tubulin from HeLa cells. This tubulin is >90% tyrosinated (160) and can be acetylated *in vitro* using MEC17 or detyrosinated using a carboxypeptidase (161). An added benefit of using HeLa tubulin is that purified native HeLa tubulin has low levels of polyglutamylation and this alleviates concerns about interference from this PTM in our assays (99). Our new hypothesis is that α-tubulin detyrosination in addition to acetylation affects kinesin-1 motility behavior. To test this hypothesis, we used purified HeLa tubulin and treated it with enzymes to control levels of α-tubulin acetylation and detyrosination. Motility of kinesin-1 was observed on acetylated detyrosinated or acetylated tyrosinated microtubules in single-molecule TIRF motility assays. Changes in the velocity, run length and binding of kinesin-1 on purified populations of acetylated- tyrosinated and acetylated-detyrosinated microtubules were quantified to measure a direct effect of acetylation and detyrosination on kinesin-1 motility.

Materials and Methods

Cloning and Preparation of Proteins

Motors

Mammalian Lysate: RnKHC560-3xmcit in lysate form was extracted from over-expression in mammalian COS cells as described in Chapter 2

Bacterial Expression: RnKHC560 motors were expressed in BL21(DE3) cells and purified as described in Chapter 3 with the only difference being that the RnKHC560 construct was C-terminally tagged with an EGFP sequence inserted before the his-tag. Following Ni-NTA column purification, the RnKHC560-EGFP motor was further purified using microtubule-affinity purification. To do this, GTP- microtubules were polymerized at 4 mg/mL and then stabilized with 100 µL 11 µM taxol in BRB80. The microtubules were centrifuged in the airfuge rotor at 30 psi for 35 s and resuspended in 100 µL 11 µM taxol in BRB80. 20 µL of column-purified kinesin was incubated the microtubules in the presence of 1 mM AMPPNP, 1 mM $MgCl_2$ in BRB80 (80 mM PIPES, 1 mM EGTA, 1 mM $MgCl_2$, pH 6.8) on ice for 40 min. The kinesin-microtubule

complex was centrifuged at 4 ºC, 80,000 rpm in the TLA 120.1 rotor for 5 min and the pellet was resuspended in 25 µL release buffer (BRB80, 10% sucrose, KCl, 5 mM $MgCl_2$, 2 mM EGTA, 12 µM taxol, 5 mM ATP). The microtubule-motor complex was incubated on ice for 20 min and then centrifuged in the TLA 120.1 rotor at 80,000 rpm for 5 min to spin down the microtubules. The kinesin-containing supernatant was aliquoted and flash-frozen for storage at -80ºC.

Enzyme Purification

MEC17 used for acetylation of tubulin was also purified as described in Chapter 3. Carboxypeptidase A (CPA) was purchased from Sigma-Aldrich (St. Louis, MO).

Tubulin Purification

Tubulin was purified from HeLa S3 cells (ATCC, Manassas, VA) using the method of Bulinski et al. (161). Cells were initially plated as adherent cells in F-12K medium (ATCC) supplemented with 10% FBS (Invitrogen, Carlsbad, CA) or Fetalclone III (Thermo Scientific, Waltham, MA) and allowed to grow at 37ºC in a 5% CO_2 incubator. They were then trypsinized and transferred into suspension medium at 37ºC, 5% CO_2, 200 rpm in a floor incubator. Suspension cultures were grown by sequential dilution of cells in minimum essential medium- Joklik modification (Sigma-Aldrich) with 10% FBS. All cells were grown in the presence of 50units/mL pen/strep. 10L of suspension culture yielded 2.5 mg of soluble HeLa tubulin. Tubulin was resuspended in BRB80 before it was aliquoted and flash-frozen for storage at -80ºC. A 7.5% SDS-PAGE gel was run with samples from the purification procedure to demonstrate the purity of the tubulin (see Figure 19).

***In vitro* Enzyme Treatment of Tubulin**

For acetylation of tubulin, purified HeLa tubulin was incubated with purified MEC17 enzyme as described in chapter 2. To detyrosinate the tubulin, it was further incubated with 10ug/mL CPA (Sigma-Aldrich, St. Louis, MO) on ice for 20min. The reaction was quenched with 20 mM DTT and the resulting modified tubulin was processed through two cycles of polymerization and depolymerization to remove any incompetent tubulin generated during enzyme treatment. The effectiveness of the cycling was verified by

running out samples from the cycling procedure on a 7.5% SDS-PAGE gel as shown in Figure 19.

Acetylation and detyrosination of tubulin were confirmed by using immunoblotting with mouse anti-acetylated tubulin (T6793, Sigma-Aldrich, St. Louis, MO) and anti-detyrosinated tubulin AB3201 (Millipore, Billerica, MA) antibodies, respectively.

Single-molecule TIRF Motility Assays

Motility assays were performed on a Zeiss Axiovert microscope modified to allow TIRF microscopy using a 488nm Ar-ion laser for excitation (50). Flow chambers were made using cover slips (Corning) that were cleaned with a small amount of detergent and then with 3 cycles of deionized distilled water in a sonicator. Microtubules polymerized in the presence of 1 mM GTP using 4mg/mL tubulin were stabilized with 10μM taxol in BRB80. The assay chamber was coated with a mono-layer of anti-tubulin antibody (T8328 Sigma-Aldrich) by flowing through a chamber-volume of 0.3 mg/mL anti-body and allowing the chamber to incubate on ice for 3min. Following a wash step at room temperature, microtubules were allowed to bind to the anti-body monolayer for 5 min before 15mg/mL BSA was introduced into the chamber as a blocking agent. The final flow-through for the assay was ~10 nM kinesin in P12 buffer (12 mM PIPES, 2 mM $MgCl_2$, 1 mM EGTA, pH 6.8) supplemented with 1 mM $MgCl_2$, 2 mM ATP, 1 mg/mL BSA, 10 mM glucose, 1.65 mg/mL glucose oxidase, 0.27 mg/mL catalase and 143 mM BME.

Data Collection and Analysis

Movies were recorded at a rate of 10 frames/s and analyzed in the same way as was described in Chapter 2. An additional feature of the program was tested and included that allows the program to concatenate pieces of one single event otherwise separated during analysis due to a photo-blinking event. To obtain a distribution for the velocity and run length measurements, histograms were generated by plotting the number of events observed against binned values. The velocity profile was fit to a Gaussian distribution with the centroid of the Gaussian specifying the mean velocity. The run length profile was fit to an exponential distribution with the decay constant of the exponential specifying the mean run length. The R^2 value of the fits indicates the proportion of

variability that the fit is able to account for. Histograms for the velocity data were fit to Gaussian distributions with R^2 >93% and histograms for the run length were fit to single exponential distributions with R^2 >99% in Origin Lab. Binding was estimated by measuring the landing rate on microtubules. The number of events on a selected microtubule in a recorded movie was counted and then divided by the length of the microtubule and the length of the movie in order to obtain a landing rate with the units of events/µm/min.

Results

Tubulin was purified from HeLa cells using high salt buffer to remove MAPs and competent tubulin was obtained by performing two cycles of polymerization and depolymerization. Purity of the tubulin was estimated using an SDS-PAGE gel as shown in Fig. 19. The cycling and analysis was repeated after treatment with modifying enzymes.

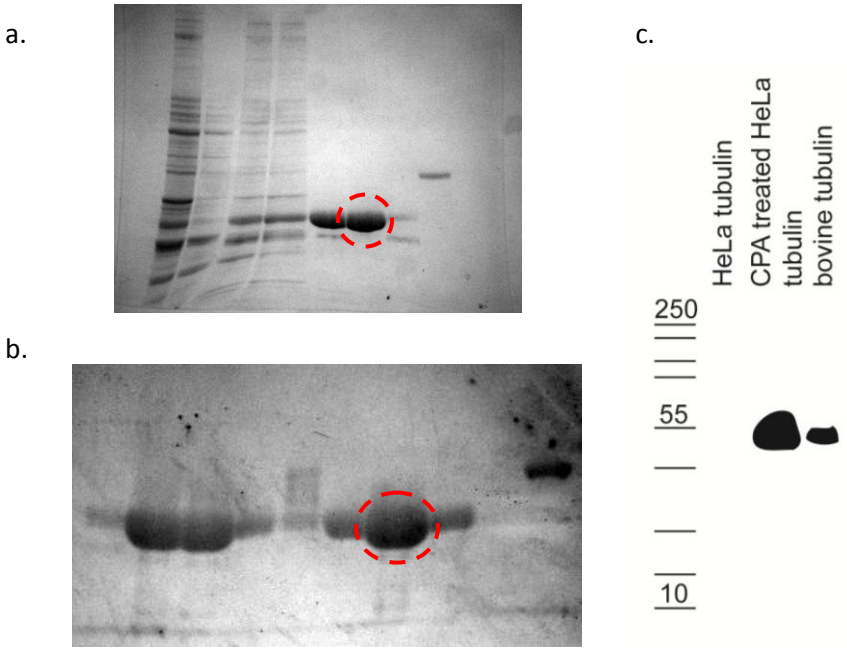

Figure 19. SDS-PAGE and Western Blot for HeLa tubulin purification and CPA treatment. a. purified soluble HeLa tubulin in lane 6 (dashed circle); b. cycled, soluble HeLa tubulin in lane 7 after CPA treatment for detyrosination (dashed circle); c. Western blot results for before and after CPA treatment (lanes 1 and 2) compared with untreated bovine brain tubulin (lane 3) showing no detyrosination of HeLa tubulin before CPA treatment and extensive detyrosination after treatment.

Single- molecule TIRF Motility Assays

We performed single molecule *in vitro* TIRF motility assays to observe the motility of kinesin-1 on acetylated microtubules that are either tyrosinated or detyrosinated. Pools of tyrosinated-acetylated or detyrosinated-acetylated tubulin were generated by sequential *in vitro* enzyme treatment with CPA only or MEC17 and CPA, respectively. Detyrosination was confirmed through immunoblotting as shown in Figure 19. The motility of GFP-labeled purified kinesin-1 was recorded on microtubules polymerized from each pool of differentially modified tubulin. The resulting data was analyzed using a custom-written matlab program for identifying and tracking single-molecule motility events. The analysis was used to compare velocity, run length and binding measurements for the motor were on tyrosinated-acetylated and detyrosinated-acetylated microtubules.

Our results indicate that kinesin-1 does not show any change in velocity, run length or landing rate due to the combination of detyrosination and acetylation of microtubules (see Figure 20). Mean velocity for RnKHC560 on acetylated-tyrosinated microtubules, for n = 1461 events was found to be 0.53 ± 0.19 μm/s. For acetylated-detyrosinated microtubules, velocity of kinesin-1 was found to be 0.46 ± 0.18 μm/s from a total of 854 events. A two-sample k-s test showed that the distributions for velocity are statistically difference with a $p << 0.05$. But a 13% decrease in velocity on tyrosinated microtubules is insufficient to account for the selectivity of kinesin-1 towards a subset of microtubules *in vivo*. The mean run length for kinesin-1 on acetylated-tyrosinated microtubules for the same set of data was found to be 0.54 ± 0.42 μm. For acetylated-detyrosinated microtubules, it was 0.52 ± 0.41 μm. These run length distributions were not found to be significantly different based on a two-sample k-s test with a $p = 0.61$. Landing rate for kinesin-1 on acetylated-tyrosinated microtubules, averaged over multiple microtubules in five different assays was found to be 1.50 ± 0.40 events/ μm/ min. For acetylated-detyrosinated microtubules, the landing rate was 1.70 ± 0.51 event/ μm/ min. The distribution of data for the landing rates was also not found to be significantly different based on a two-sample k-s test with a $p = 0.099$.

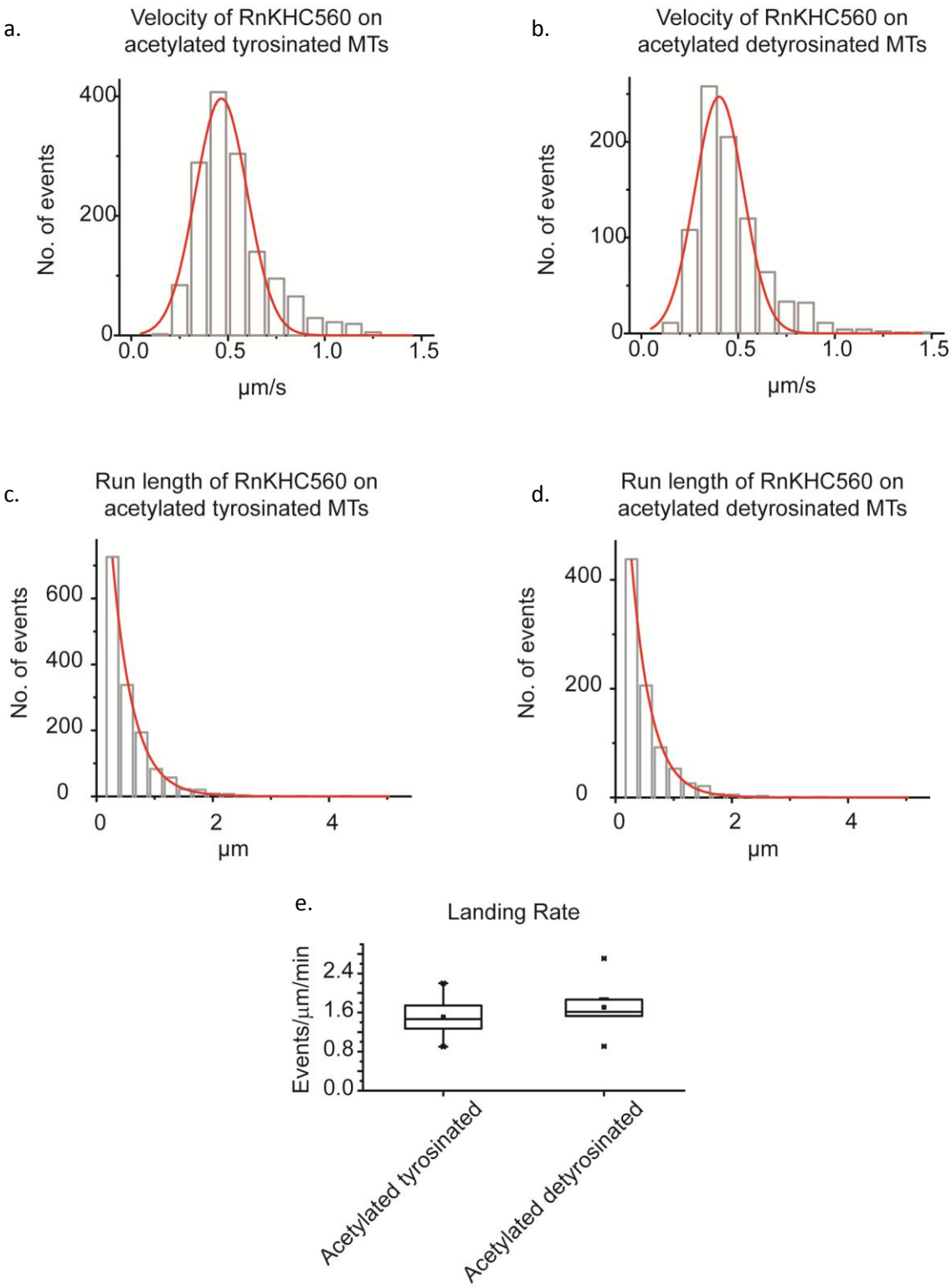

Figure 20: Motility parameters for RnKHC560 on acetylated tyrosinated and acetylated detyrosinated microtubules. Motility is not significantly affected by the state of tyrosination for acetylated microtubules. Motility on acetylated tyrosinated microtubules:

a. velocity = 0.53 ± 0.19 μm/s, c. run length = 0.54 ± 0.42 μm; Motility on acetylated detyrosinated microtubules: b. velocity = 0.46 ± 0.18 μm/s, d. run length = 0.52 ± 0.41 μm. e. Landing rate on acetylated tyrosinated microtubules = 1.50 ± 0.40 events/μm/min; acetylated detyrosinated microtubules = 1.70 ± 0.51 events/μm/min

Control Experiments

A major concern, also voiced in the chapter 2, is the interplay between different tubulin modifications. This was in fact, the motivation for studying the combination of α-tubulin acetylation and detyrosination. Considering this, we could not ascertain the role of α-tubulin detyrosination on kinesin-1 motility by simply discounting a combinatorial effect from α-tubulin acetylation. In order to study the effect of detyrosination independently, we performed *in vitro* enzyme treatment on HeLa tubulin with only CPA and not MEC17. The tubulin treatment and cycling was carried out as before and the resulting detyrosinated microtubules are expected to have acetylation levels of WT HeLa tubulin (<4%). We compared the motility of kinesin-1 on these detyrosinated microtubules with microtubules polymerized from WT HeLa tubulin (99.5% tyrosinated) by repeating the single-molecule TIRF motility assays to characterize motility of RnKHC560-EGFP on the tyrosinated and detyrosinated microtubules. Data analysis revealed no change in velocity, run length and binding, parameters to indicate change in motility behavior. Our data showed that RnKHC560 moved at a velocity of 0.43 ± 0.18 μm/s on tyrosinated microtubules and at a velocity of 0.47 ± 0.19 μm/s on detyrosinated microtubules. The velocity data distributions were found to be significantly different as per a two-way k-s test with a $p << 0.05$. Run length on tyrosinated microtubules was found to be 0.46 ± 0.38 μm and on detyrosinated microtubules it was 0.51 ± 0.53 μm. Run length data distributions were not found to be significantly different with a $p = 0.45$. Landing rates for the kinesin were 1.29 ± 0.16 events/μm/min on tyrosinated microtubules and 1.55 ± 0.08 events/μm/min on detyrosinated microtubules. The landing rate data distributions were not found to be significantly different ($p = 0.1$). Figure 21 shows histograms for distributions of these measurements.

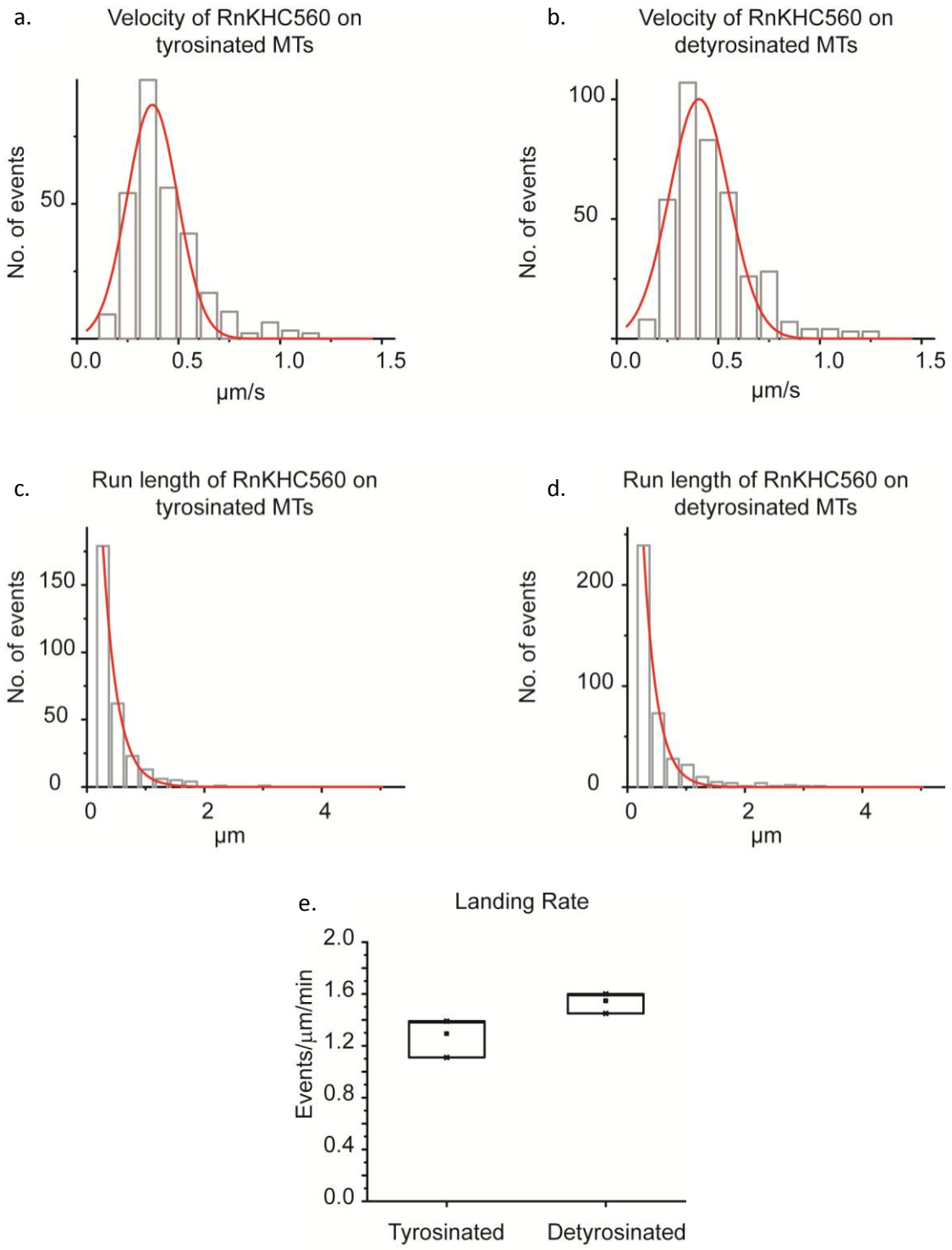

Figure 21: Motility parameters for RnKHC560 on tyrosinated and detyrosinated microtubules. Without modifying the state of acetylation, motility is not significantly affected by changing the state of detyrosination. Motility on tyrosinated microtubules: a. velocity = 0.43 ± 0.18 µm/s, c. run length = 0.46 ± 0.38 µm; Motility on detyrosinated microtubules: b. velocity = 0.47 ± 0.19 µm/s, d. run length = 0.51 ± 0.53 µm. e. Landing

rate on tyrosinated microtubules = 1.29 ± 0.16 events/µm/min; detyrosinated microtubules = 1.55 ± 0.08 events/µm/min

As a test for the kinesin motor purified from bacterial expression, we decided to use the mammalian-expressed RnKHC560-3xmcit COS-cell lysate, as in previous chapters, with microtubules polymerized from tyrosinated and detyrosinated tubulin. To do this, we repeated the above single-molecule TIRF motility assays with 10-fold diluted lysate. While measurements in the velocity and run length again showed little significant change upon α-tubulin detyrosination, the binding of kinesin-1 in lysate form was two-fold reduced upon detyrosination. We found that the velocity of RnKHC560 from lysate on tyrosinated microtubules was 0.46 ± 0.18 µm/s and on detyrosinated microtubules it was 0.42 ± 0.17 µm/s. Run length on tyrosinated microtubules was 0.36 ± 0.23 µm and on detyrosinated microtubules it was 0.29 ± 0.17 µm. Figure 22 shows histograms for distributions of these measurements. For both velocity and run length measurements, a two-sample k-s test indicated that the data distribution is significantly different. To our surprise, the landing rate for RnKHC560 was 1.63 ± 0.13 events/µm/min on tyrosinated microtubules and only 0.71 ± 0.09 events/µm/min on detyrosinated microtubules as shown in Figure 22.

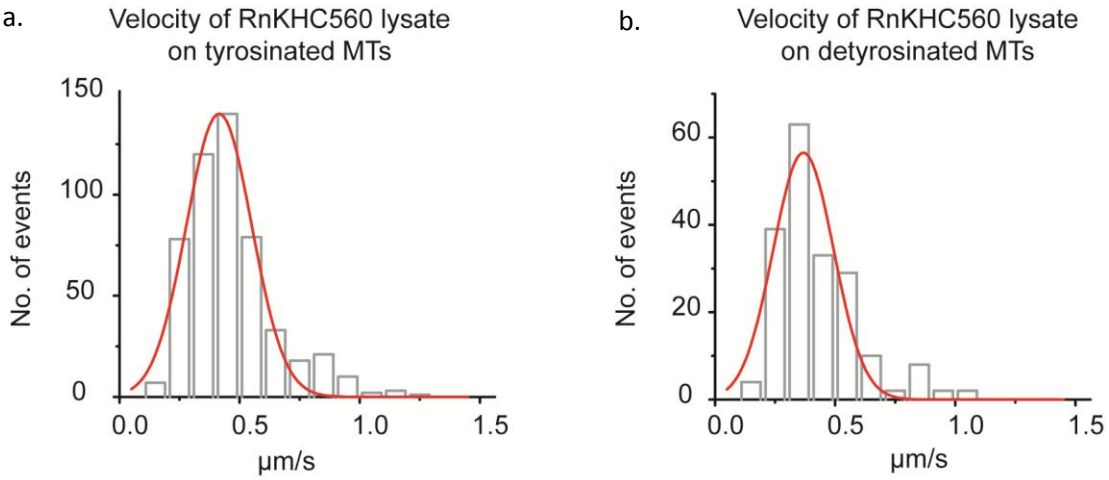

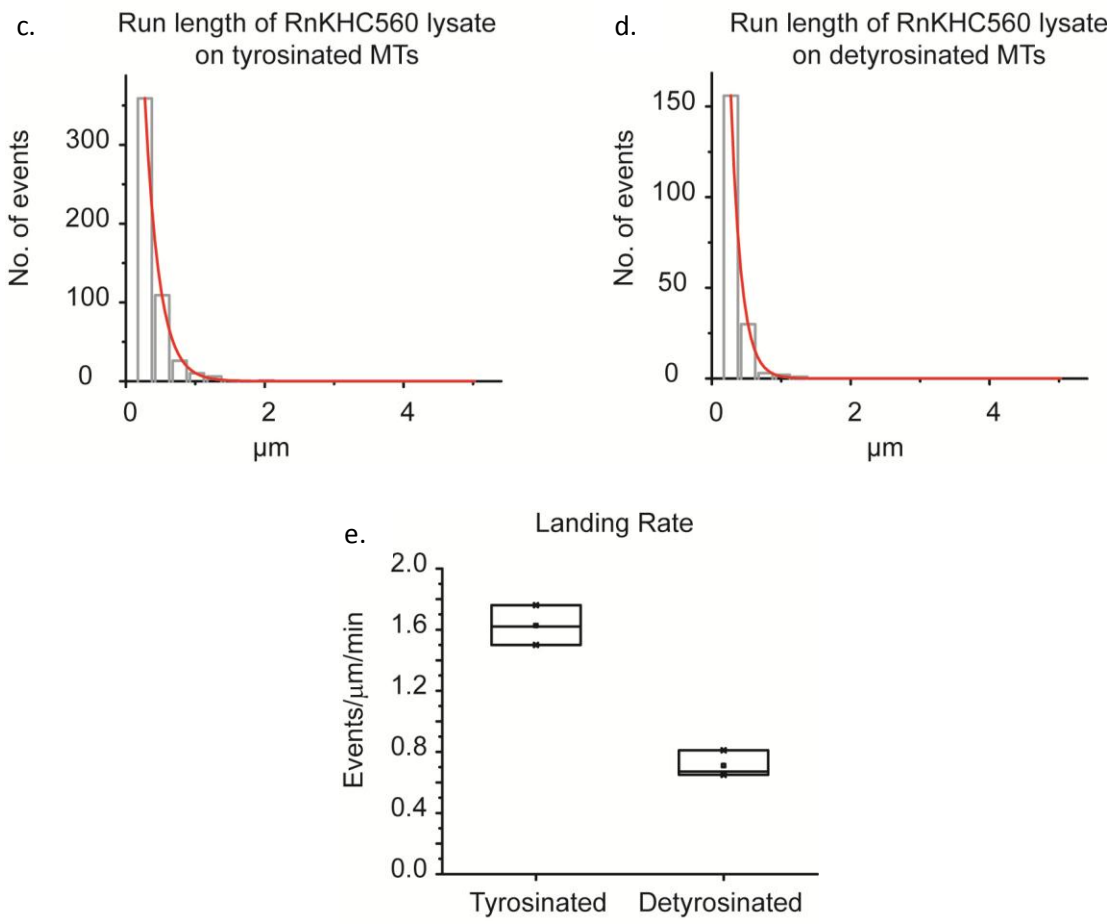

Figure 22: Motility parameters for RnKHC560 lysate on tyrosinated and detyrosinated microtubules. While velocity and run length of kinesin-1 in lysate do not change significantly due to detyrosination, landing rate shows a 2-fold change in favor of tyrosinated microtubules. Motility on tyrosinated microtubules: a. velocity = 0.46 ± 0.18 µm/s, c. run length = 0.36 ± 0.23 µm; Motility on detyrosinated microtubules: b. velocity = 0.42 ± 0.17 µm/s, d. run length = 0.29 ± 0.17 µm. e. Landing rate on tyrosinated microtubules = 1.63 events/µm/min; detyrosinated microtubules = 0.71 events/µm/min

Taken together, our experiments confirm that detyrosination of α-tubulin independently does not cause a change in kinesin-1 motility, with or without the presence of the additional α-tubulin K-40 acetylation. Interestingly, the addition of 10-fold diluted cell lysate in the assay affects the binding of kinesin-1 such that it there is a two-fold increase in kinesin-1 landing rate on tyrosinated microtubules in the presence of lysate. There are several possible explanations for this statistically significant difference in landing rates and therefore interpretation of this result requires careful analysis of the factors in our

experiments that need to be accounted for and addressed, as is discussed in the following section.

Discussion

In the previous chapter, we showed that acetylation of K40 on α-tubulin does not directly affect the motility behavior of kinesin-1. Although this appeared surprising initially, closer investigation revealed differences between previous experimental studies and ours that could well account for the difference in results. *In vivo*, PTMs most often co-exist on the same subset of microtubules. In particular, α-tubulin acetylation and detyrosination are concurrent modifications, frequently occurring on a subset of microtubules which have, in recent years, been shown to preferentially recruit kinesin-1 motors. While acetylation resides in the lumen of the microtubule, detyrosination is a modification on the CTT of α-tubulin, thus presenting itself on the surface. It is believed that removal of the terminal tyrosine residue reveals a glutamate residue beneath (162). In this chapter our goal was to resolve the effects of α-tubulin acetylation, detyrosination and their combination on kinesin-1 motility behavior. To do this, we purified tubulin from HeLa cells and enzyme-treated the tubulin to obtain combinations of detyrosinated and acetylated forms. Kinesin-1 motility on differentially modified microtubules was observed through single-molecule *in vitro* TIRF assays. Velocity, run length and binding measurements for the motors were selected as parameters to characterize changes in the kinesin-1 motility. Upon analysis of our data, we did not see any significant change in kinesin-1 motility due to detyrosination alone or a combination of acetylation and detyrosination together. Velocities and run lengths remained comfortably within a standard deviation of the measurements. We did, however, observe a change in the binding of kinesin-1 upon the addition of COS-cell lysate. Addition of the lysate caused a two-fold decrease in the landing rate of kinesin-1 to detyrosinated microtubules, as compared to tyrosinated microtubules.

We have shown that in the absence of MAPs or other proteins, kinesin-1 cannot identify detyrosination of α-tubulin CTTs, in the presence or absence of α-tubulin acetylation. Based on previous i*n vivo* studies from Dunn et al., Cai et al. and Konishi et al. (109, 122, 126) which provide fundamental clues to the preferential motility of kinesin-1 on

detyrosinated microtubules, our results raise interesting questions about the PTM-recognition mechanism responsible for this observed preferential motility. Interpretations from *in vivo* observations cannot exclude the effect of MAPs. On the other hand, our study focuses on the use of purified components to perform *in vitro* motility assays and evaluate the direct effect of α-tubulin acetylation and detyrosination only.

Dunn et al. showed that the distribution of GFP-labeled full length kinesin-1 in neuronal and non-neuronal (COS) cells was localized to a subset of microtubules in the cells (122). When the microtubules were visualized by immuno-staining with anti-bodies for acetylation, detyrosination and polyglutamylation, it was clear that microtubules in the subset that kinesin-1 preferred for motility were acetylated and detyrosinated. FRAP (fluorescence recovery after photo-bleaching) was used to show that the observed decoration of microtubules with kinesin-1 was due to the dynamic accumulation of kinesin-1 and not simply from aggregation of the motors. Thus, they showed that kinesin-1 motility in the cells is localized to a subset of microtubules that is acetylated and detyrosinated. Further, AMPPNP-binding assay results analyzed by SDS-PAGE suggested that 1.5 times more kinesin-1 binds to detyrosinated microtubules than to tyrosinated microtubules but this difference is not likely to account for the stark contrast in binding preference *in vivo*. On the other hand, they showed in an *in vitro* microtubule gliding assay that the velocity of tyrosinated microtubules was higher than that of detyrosinated microtubules on kinesin-1. Neither result can account for the highly preferential motility of kinesin-1 along acetylated and detyrosinated microtubules *in vivo*.

If we look at the docking studies from 3D reconstruction of cryo-EM images of kinesin on microtubules, it is clear that the α-tubulin surface is out of the way for kinesin-1 motor domains when they bind to the microtubule (163). It is plausible that the CTTs, particularly poly-modified, could contribute to regulating kinesin traffic along a microtubule. The docking results also suggest that a small fraction of the MAP tau, binds with a regular 8nm-periodicity such that it is centered on the α-tubulin subunit. Therefore it is possible that the binding of MAPs but not kinesin-1 motors is regulated by α-tubulin PTMs. The observation from our *in vitro* single-molecule assay showing that kinesin-1 binding shifts in favor of tyrosination upon the addition of lysate, needs to be looked at in

closer detail. There could be several reasons for this observation and we will discuss some of the possibilities here. One explanation is that detyrosination provides a signal for the binding of MAPs or other proteins in the lysate which may bind to or compete with the kinesin-1 motor, demonstrating an effect that we would not see in using the purified kinesin. The purified kinesin, although is obtained by bacterial expression followed by affinity purification using a c-terminal his-tag. The motor is further purified using microtubule-affinity purification but the his-tag remains. It is possible that either point mutations are introduced during bacterial expression due to limitations with codon usage or that the his-tag in our end product interferes with normal electrostatics in the kinesin-microtubule interaction. An experiment to purify kinesin-1 motor directly from the lysate and compare it with bacterially purified motor without a his-tag would provide us answers to these questions. We have already begun cloning to introduce a cleavable thrombin site before the his-tag which will allow the tag to be cleaved off prior to microtubule-affinity purification of the motor.

We have shown that kinesin-1 does not directly recognize tubulin acetylation, detyrosination or a combination, thereof as a cue for a change in its motility along microtubules. While previous studies have used either an *in vivo* approach or one with partially purified proteins, our approach was to extract only the proteins of interest, purify them and then reproduce the kinesin-microtubule interaction *in vitro*, in an effort to identify how kinesin-1 might be able identify differentially modified microtubules. Our results are in good agreement with results from multiple-motor studies performed by Dunn et al. (122). An intermediate step was clearly shown by Konishi et al. wherein microtubules extracted from HeLa cells were detyrosinated to perform *in vitro* binding assays in the presence of 50% AMPPNP and 50% GTP with kinesin but without cycling or purification of the tubulin. They showed that truncated kinesin-1 binds more effectively to microtubules that are detyrosinated. Our assays contain only completely purified proteins of interest and therefore allow us to draw conclusions specifically on the direct interaction of kinesin-1 with tyrosinated or detyrosinated microtubules. We believe that in light of our findings, previous results indicate that the nascent state of the HeLa microtubules, likely from the presence of native MAPs, contributes to the specific microtubule identity that kinesin-1 is able to recognize. In this regard, it would be

interesting to pursue the introduction of specific MAPs in the *in vitro* assays that we have performed.

Microtubules in neuronal axons that have been shown to accumulate kinesin-1 are acetylated, detyrosinated and polyglutamylated. An important difference between brain tubulin and HeLa tubulin is that glutamylated β-tubulin accounts for >50% of tubulin extracted from brains but only <4% of the total tubulin in HeLa cells (99). By controlling α-tubulin modifications of microtubules in our experiments, so far we have found that kinesin-1 does not directly recognize either acetylation or detyrosination or a combination of both. Yet, *in vivo*, kinesin-1 shows preferential motility along a subset of microtubules marked by α-tubulin acetylation and detyrosination. It seems that the mechanism by which preferential motility occurs *in vivo* such that it is concurrent with the α-tubulin modifications, depends on finding the identity of other proteins and PTMs associated with these microtubules. To do this using an *in vitro* approach, we would begin with introducing the most prominent β-tubulin CTT modification, polyglutamylation. With the addition of this modification, we would have covered all the major modifications that axonal microtubules are enriched in.

Previous experiments with subtilisin treatment for complete removal of microtubule CTTs have shown that kinesin-1 motility is affected by the absence of the CTTs (50, 164-165) but results appear to vary under different conditions. While Wang and Sheetz showed a 5-fold decrease in multi-motor run length for full length native kinesin upon subtilisin treatment of microtubules, Thorn et al. observed a modest 30% decrease in the run length of single truncated human kinesin upon subtilisin treatment and Lakamper et al. showed a 50% decrease in run length for Neurospora kinesin. Although there may not be complete agreement on the extent of the observed effect, these studies suggest the role of an electrostatic mechanism in regulating kinesin-1 run length. We do not know anything about the modification states of acetylation or detyrosination for the microtubules used in these experiments. We expect that the addition of polyglutamylation, a charged CTT poly-modification nearer to the binding site of the kinesin-1 motor domain than any other modification, is most likely to yield clues as to the preferential motility of kinesin-1 on a subset of microtubules. Looking at this new

modification in combination with the previous modifications we have looked at will also provide insight on the inter-play between different tubulin modifications which will eventually help us establish cause and effect roles for the effect of each PTM on intra-cellular transport machinery.

CHAPTER 4

Device and/or Software Development

During the course of performing experiments towards my thesis work, I found it extremely useful to leverage my mechanical engineering skills to design new setups or software. This has allowed me to design customized experiments that would not be possible to undertake with commercially available products. Three of the most promising developments will be described in this chapter.

1. Novel Dual- color Imaging Device

Background

A dual color imaging device allows the simultaneous visualization of two different wavelengths emitted from a sample. The fundamental requirement in doing this is for the emitted beam to be chromatically split into two components and the split components to be re-positioned for side-by-side imaging. Thus, the simultaneous imaging of two wavelengths requires some optical manipulation of the beam emitted from the sample. Dual-color imaging is particularly useful in observing two interacting proteins labeled with different fluorophores. For high temporal fidelity in the observation of dynamic processes, it is best to image the two wavelengths on two halves of the same ccd chip. On the other hand, for high spatial fidelity, it is required that the two images can be accurately aligned with each other. Either way, an essential requirement is that the two wavelengths be properly focused with minimal optical aberrations. If the emitted beam suffers optical aberrations before it is split into the desired wavelength components, those aberrations are carried over into the dual view optical system, and depending on the optics mechanism offered by the system, they can either be eliminated or amplified. For example, if the two wavelength components have inherited their chromatic aberration from the optics in the microscope, something that is common for a high numerical

aperture (n.a.) objective lens such as that employed in objective-type TIRF microscopy, then an offset in their focal planes along the optical axis exists from before they enter the dual view device (see Figure 23). Commercial devices such as the one employed in our own laboratory (Photometrics Inc., Tucson, AZ) use a single collimating lens placed in the focal plane of the microscope tube lens in order to collimate the emitted beam before performing any other optical manipulation (see Figure 23). In the case of TIRF microscopy, where a high n.a. objective is required, the pre-existing offset in focal planes of two wavelength components means that there are two focal planes along the optical axis, both of which must somehow lie in the back-focal plane of the first collimating dual view lens, in order for both wavelength components to be collimated simultaneously. Thus, depending on where the lens is positioned, either the shorter wavelength component will be converged or the longer wavelength component will be diverged by the first collimating lens in the dual view device. Other designs for dual-color imaging have been proposed (166).

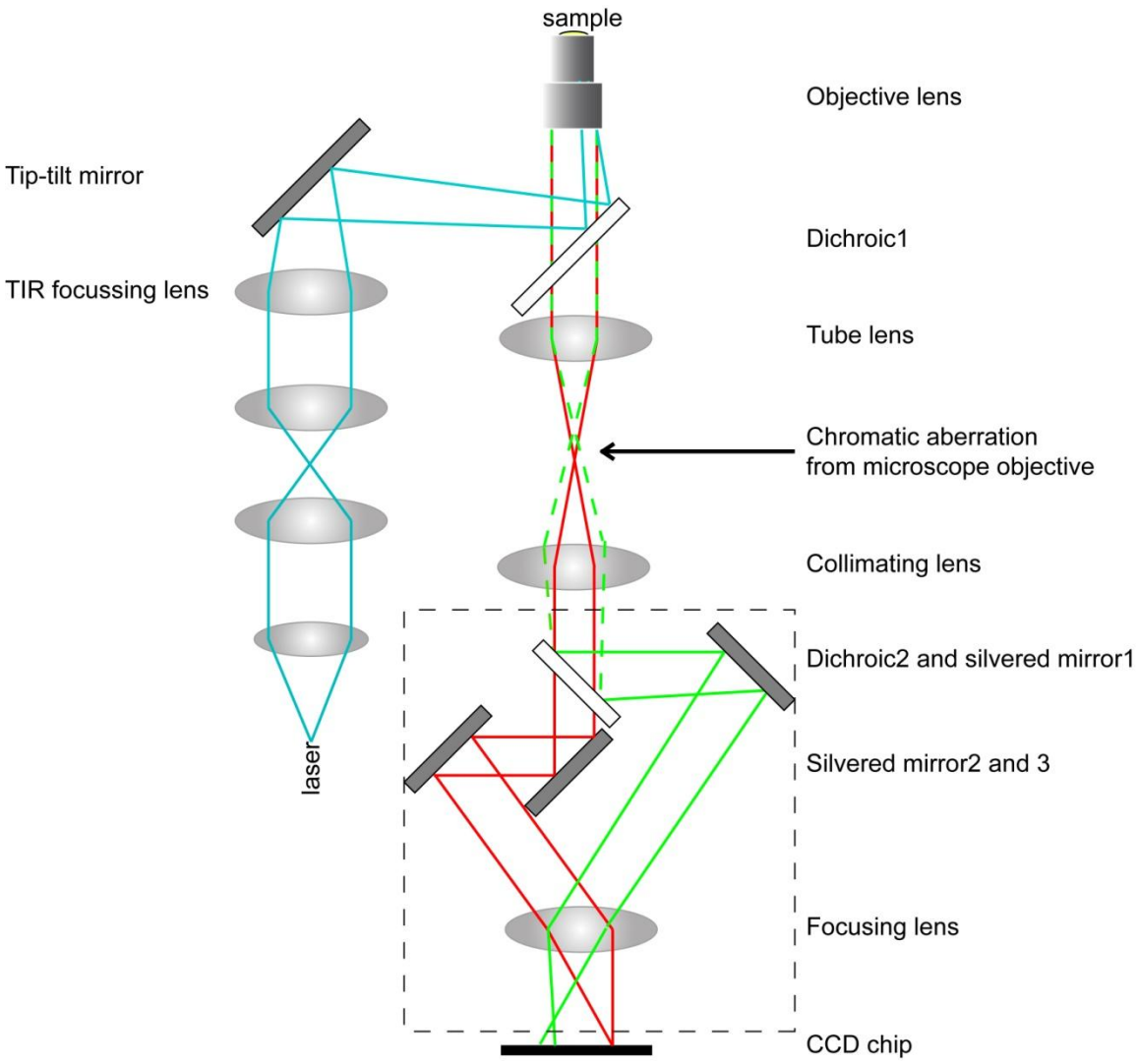

Figure 23: Chromatic aberration in the commercial dual-color optical setup. Optical components of the dual-color-device are contained in the dashed box

Once the beam has been collimated in the dual view device, it is split into its two wavelength components by a dichroic beam splitting mirror. The separated wavelength components are passed through the appropriate emission filter for each one, before they are focused again with the help of a second lens. Along their paths through the dual-color imaging device, the two wavelength components are reflected with the use of silvered mirrors such that they can be focused side-by-side on two halves on the ccd chip of a camera for visualization.

Design Goals

It is clear that chromatic aberration that is generated due the requirement of a high n.a. objective can be potentially transmitted through and even amplified with the addition of a dual-color imaging device. Also, this problem is compounded each time a new pair of wavelengths needs to be used. Our two main goals were:

1. Use optical design ideas to eliminate the chromatic aberration instead of transmitting it through the optical system.
2. Use mechanical design ideas to create a versatile setup that can easily accommodate different pairs of wavelengths.

Optical Design

The novelty of this device is in its optical configuration. Optical manipulation of the beam emerging from the microscope tube lens is required to be able to image its two wavelength component images on the adjacent halves of the ccd chip of a camera. The only way to accommodate the same image in two different colors on a single ccd chip, is to start with taking only half the image produced by the microscope, separate it into its two wavelength components and then lay the separated halves side-by-side on the ccd chip. To do this, the beam emerging from the tube lens must be partially shuttered so that only half the image from the microscope is processed through the dual-color imaging optics. We have done this by placing an aperture in the focal plane of the microscope tube lens (see Figure 24). The defining change in our optical design is that the emitted beam coming from the microscope tube lens is split into its two wavelength components by a dichroic beam splitter even before it is collimated. This allows the two wavelengths to then be collimated by two separate lenses that can be focused independently of each other. Each collimating lens can now be independently positioned such that its wavelength component is focused exactly in its back focal plane (see Figure 24). After this, the two wavelength components are reflected into the right position using silvered mirrors, passed through separate emission filters and finally re-focused by a single lens on adjacent halves of a ccd chip.

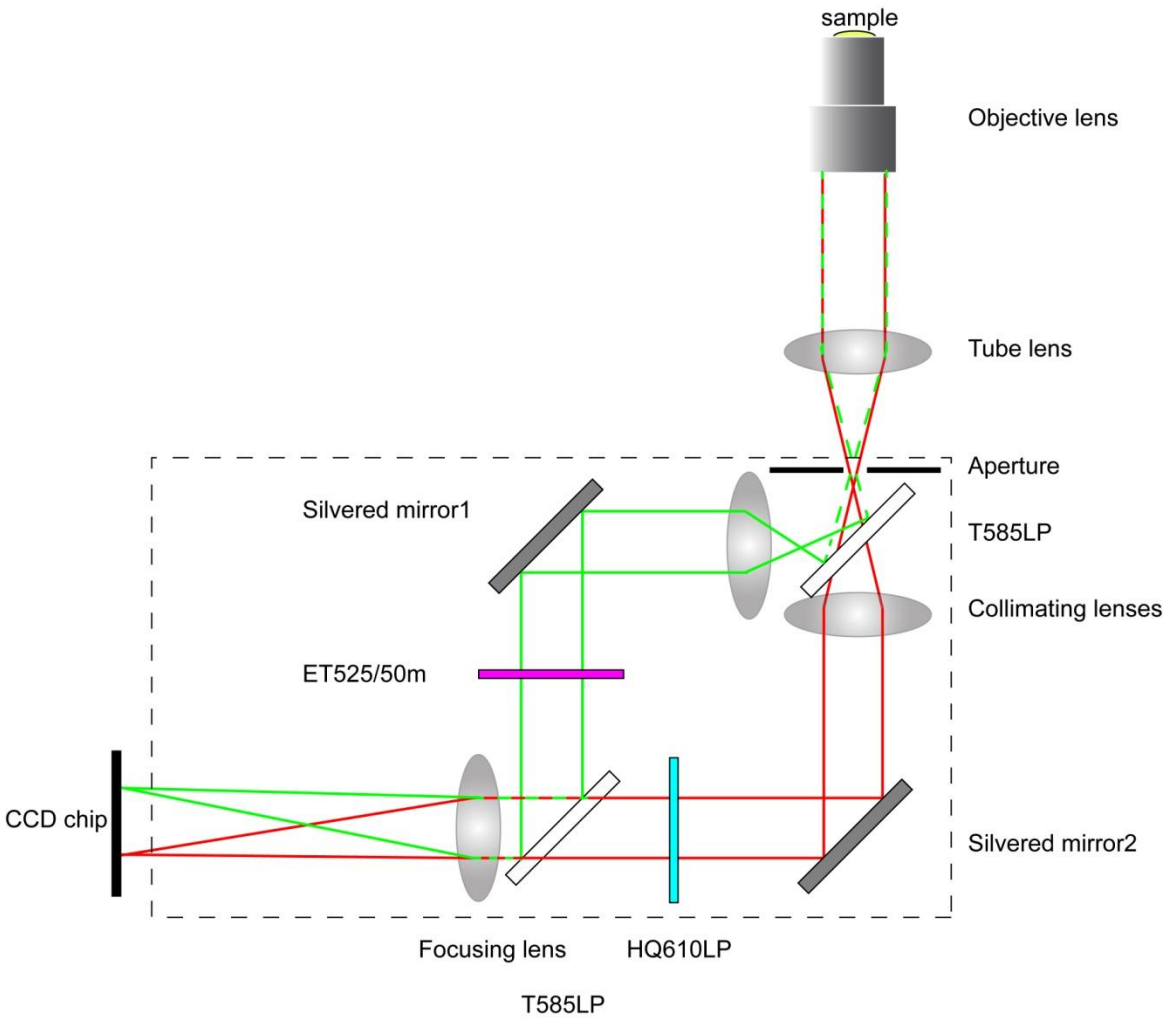

Figure 24: Novel dual-color optical setup. Optical components of the dual-color device are contained in the dashed box

Mechanical Design

The optical components for the dual-color imaging device were housed in a light-tight aluminum mounting chamber, which was mounted on the underside of the microscope table (see Figure 25). The design for the housing requires the parts to be light, yet rigid so as to avoid distortion due to bending under its own load once it is mounted under the microscope. Another requirement was to accommodate modular design for parts mating with the housing and still allow convenient access to the inside of the housing without major disassembly.

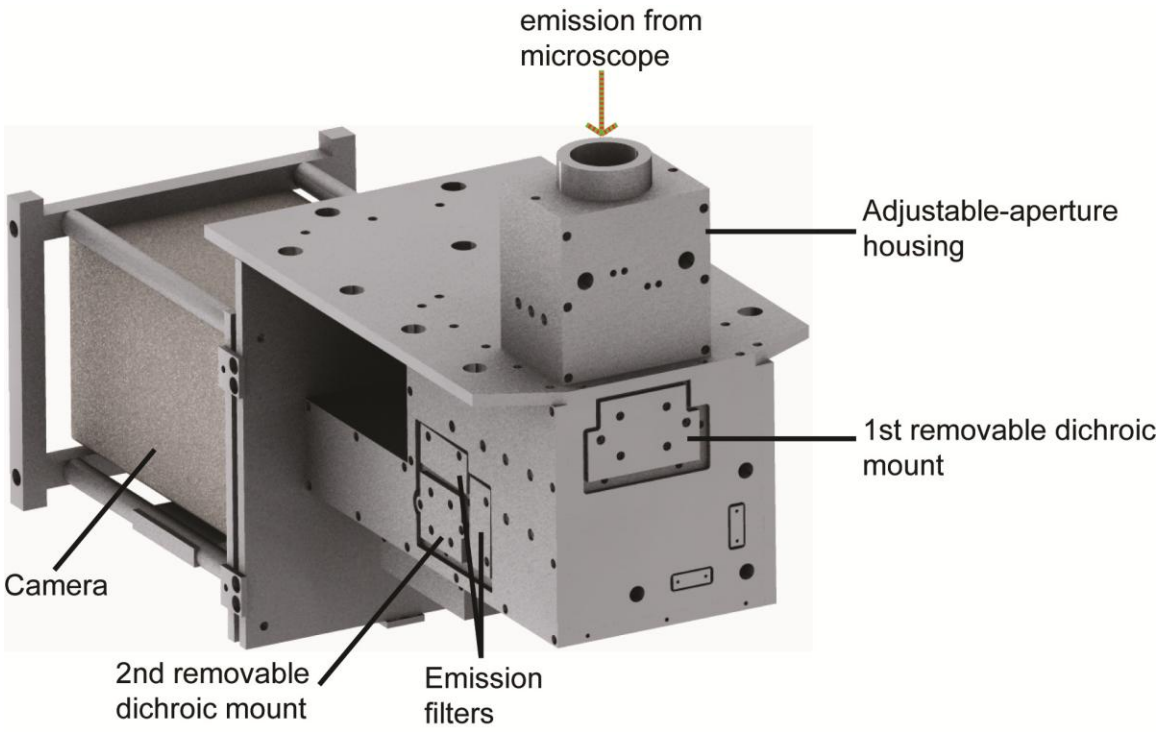

Figure 25: Mechanical design of the custom dual-color setup

The position of the device can be adjusted in x, y and z to ensure that the optical path of the microscope is aligned with that of the device and that the aperture can be positioned in the focal plane of the tube lens. The aperture itself is made of two blades, the adjustment of which allows the user to adjust the field of view between full-chip and dual-color mode. The position of each blade can be independently adjusted to place it at the desired location and at the correct angle (see Figure 26).

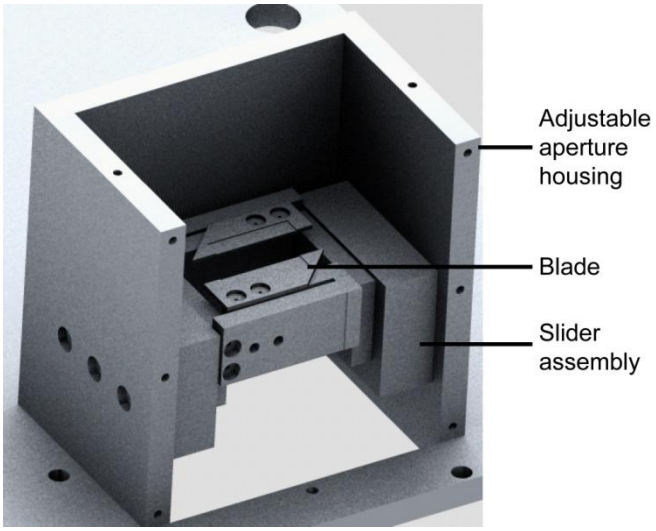

Figure 26. Mechanism for adjustment of field of view in the new dual-color setup: A cut-away view shows that the aperture comprises of two blades, the positions of which can be independently adjusted through slider assemblies

The first collimating lens for each wavelength component is mounted on a spring-assisted slider mechanism and can be adjusted independently through two separate 80TPI micrometer adjusters. The angle of the silvered mirrors can be adjusted by a tip- tilt mechanism based on the motion of three differential adjuster screws pushing on sapphire bearings against two extension springs behind the tip-tilt (see Figure 27). Each differential adjuster screw has a fine adjustment mechanism that enables a displacement of 25 μm/rev. The focusing lens is also mounted on a lens slider and its position can be adjusted with a micrometer adjuster if required for the initial alignment when two new wavelengths are used. Finally, the camera is mounted such that it lies in the focal plane of the focusing lens. The position of the camera can be adjusted in x, y and z to enable proper alignment with the optical output from the dual-color imaging device.

Removable mounts holding the two dichroic beam splitters are positioned against the setup housing with dowel pins to ensure repeatable mounting. If desired, new dichroic beam-splitters corresponding to a different pair of wavelengths can easily be switched out in this style of modular assembly (see Figure 27). The emission filters can also be switched out in a similar fashion.

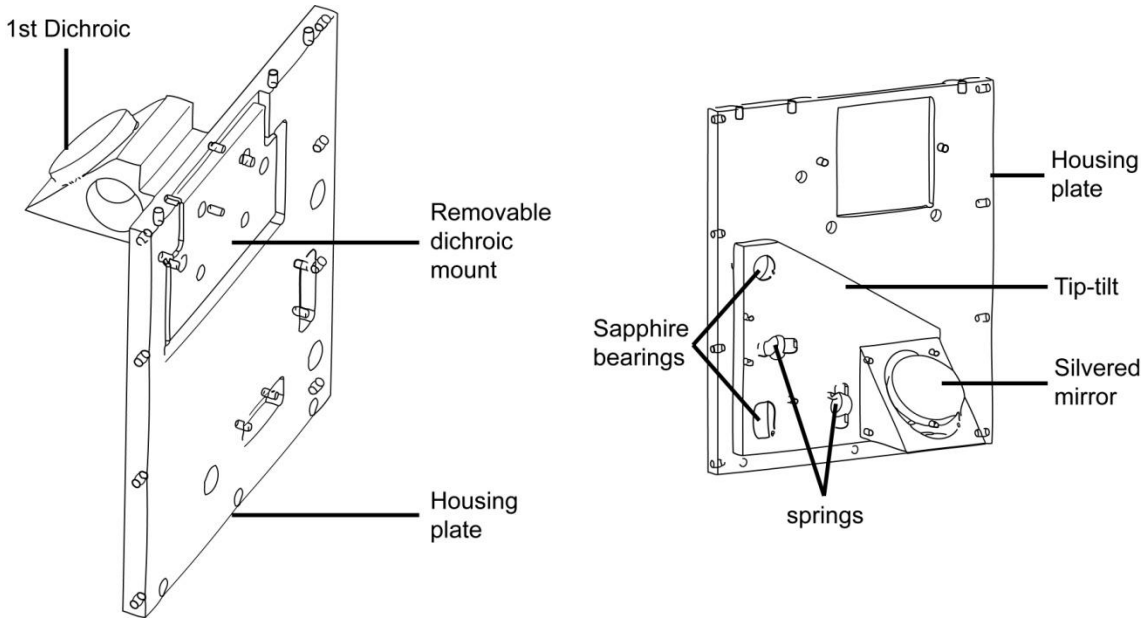

Figure 27. Mechanical design for dichroic holders and silvered mirror tip-tilt adjustment mechanism. Left: One of the two removable dichroic holders. Right: One of the two tip-tilt assemblies mounted with three bearings and two springs (one bearing is behind the mirror and cannot be seen here)

2. Sample-heater Device

Background

The function of a sample heater device on the microscope is to be able to regulate the temperature of a sample both spatially and temporally, during an experiment. There are two types of experiments that motivated the development of our sample heater device. The first is to allow *in vivo* observations of motility events under a microscope. We have previously designed and built specialized sample holders that allow the visualization of adherent cells directly in the culture plate (149). If a culture plate is sealed when it is removed from the CO_2 incubator, the sample heater would then allow us to maintain the temperature of the plate at 37ºC during observation. The CO_2 level in a typical culture dish, which is only 5-10% filled with medium, should remain relatively unchanged over a few hours. Thus, our sample heater will allow observations of cells in their physiologically relevant state.

An important aspect of performing *in vitro* biophysics experiments in the laboratory is to maintain the environment in as physiological a state as is possible. This ensures that the observations made are physiologically relevant, which is ultimately what makes such an experiment interesting. One of the challenges in working with microtubules and motor proteins is that microtubules are stable (but still dynamic) only at physiological temperature. With our sample heater, we will be able to control the temperature to allow for regular microtubule dynamics, either to study the dynamics itself or to study the behavior of motors in this physiologically relevant environment.

Commercially available sample heater devices consist of relatively bulky setups that heat a large portion of the microscope stage. This translates to more power for heating the sample, longer time for equilibration and high thermal inertia. The goal in building a customized setup was to localize the effect of heating to the sample by keeping it thermally disconnected from adjoining parts of the microscope and to provide more than one source of heat so as to set up temperature gradients. We have done this by building a 3-point heating system which heats the two ends of a sample and the center without conducting heat to other parts of the microscope. This heating arrangement gives us several advantages over the commercially available system. Due to lower thermal inertia, the temperature of the system can be cycled to allow for observations of temperature-dependent phenomena, for e.g. growth and shrinkage of microtubules. With the 3-point heating system, we can set up temperature gradients along the sample. This would allow us to observe effects of temperature on different parts of the same sample for e.g. in observing cells at different temperatures in the same culture plate. Finally, thermally isolation of the heating system from the microscope eliminates problems associated with thermal expansion of parts in the microscope- a challenging problem especially since many microscope parts are made of brass. Thermal drift from heating the microscope could easily compromise the accuracy of single-molecule observations. Temperature control is achieved through a digital temperature controller (Omega Engineering Inc., Stamford, CT) for each point of heating in the setup. This temperature controller can operate in an on/off or PID (proportional integral derivative) mode. Feedback to the temperature controller is provided through thermocouple temperature sensors- one for each independent point of heating in our setup. Thus, once the target temperature is set on

the controller, it can continuously measure the temperature of the sample and accordingly provide the appropriate output to the resistance wires for heating the sample.

Simulation for Heat Transfer

In order to establish the most basic requirements for a sample heater device, the first step was to look at a heat transfer simulation. In a simple, using a stationary heat transfer model (COMSOL Inc., Burlington, MA), it was clear that in order to maintain a minimum temperature gradient in the sample for constant temperature studies, it was required to have a three-point heating device (see Figure 28).

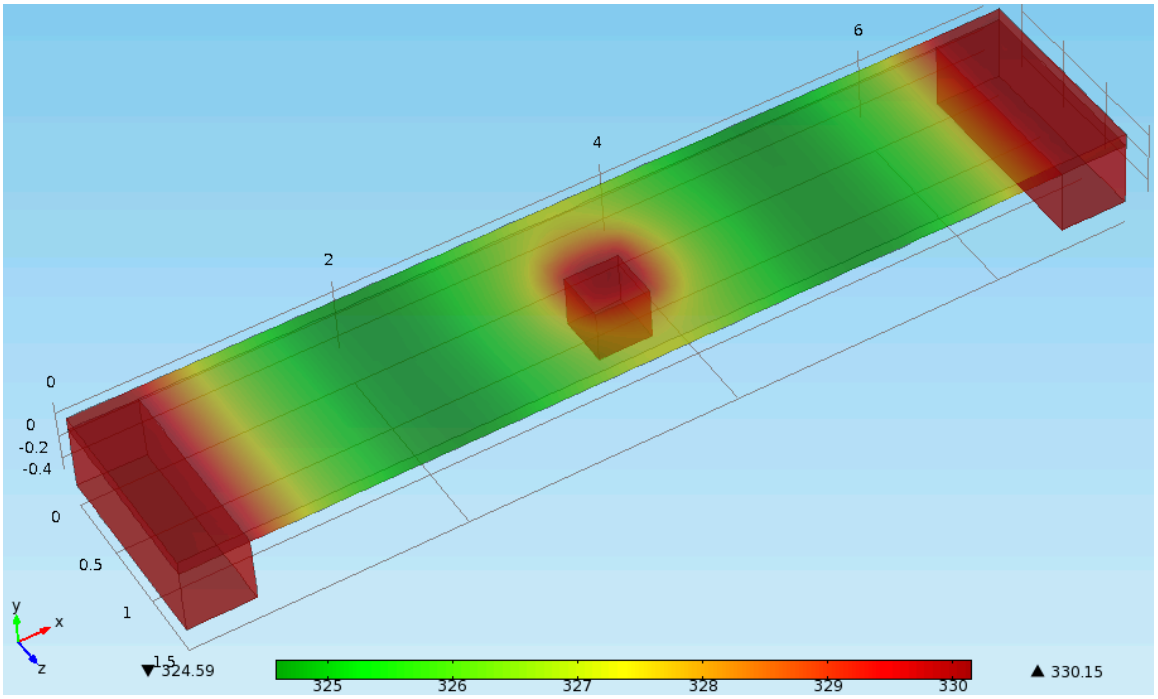

Figure 28: Heat transfer simulation for the sample heater device. Temperature is marked in degrees Kelvin.

Mechanical Design

The sample heater consists of two major mechanical components- an objective collar and a modified slide-mount. The objective collar, which mounts on our microscope objective, is made of brass with resistance-wire windings on the outside for resistance heating. The microscope objective is mounted to the microscope turret through a macor plug. With a

thermal conductivity of 1.46 W/mK, macor is a machineable glass-ceramic that has ideal properties for thermal insulation. Thus the heat transmitted to the objective is conducted only to the center of the sample and not to the rest of the microscope. To heat the ends of the sample, the modified slide mount bears a brass plate at each end against which a slide can be held down by stage clips. Resistance wire is wound on the underside of the brass plates and the brass plates are fixed on the slide mount by screws acting against compression springs. This minimizes the area of contact between the end heaters and the slide mount, again conducting minimal heat to the microscope body (Figure 29). For temperature feedback to the controller, a thermocouple for the objective heater is fixed on the objective collar and one thermocouple for each of the end heaters is fixed on each of the brass plates. All wires fixed on metal surfaces were electrically insulated using thermally conductive epoxy (Aavid Thermalloy, Concord, NH).

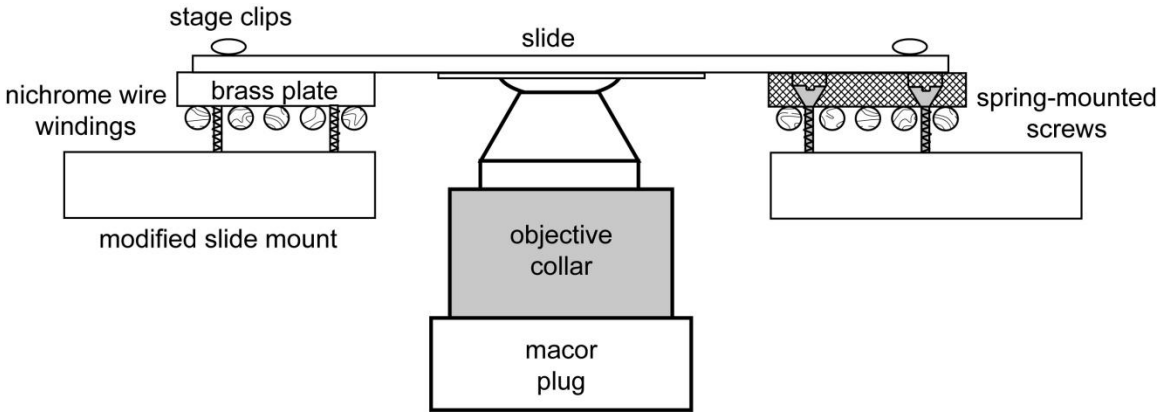

Figure 29: Mechanical design for the sample heater device. The spring-loading of the brass plates is shown in cross-section on the right hand side

Electrical Design

To achieve the desired 3-point heating system, we built an electrical layout with three separate temperature controllers connected to their respective heating points in the setup such that the temperature controllers draw current from a single power supply while receiving independent temperature feedback from their target areas in the sample. Separation of the temperature circuits allows us to setup gradients if desired. The resistance wire used for generating heat is a nichrome wire (Omega Engineering Inc.,

Stamford, CT) with a resistivity of 4.25 Ω/ft. All three heaters are connected to the same 5V dc power supply (TDK-Lamda Americas Inc., San Diego, CA) but through independent circuits. The diagram for one of these circuits is shown in Figure 30. A maximum power of 2 W is dissipated when all three heaters are actively engaged. Temperature feedback from each heating point in the setup to its respective temperature controller is provided by a T-type thermocouple wire attached with thermal epoxy to the area being heated. Thus, depending on the target temperature and heat dissipated, each circuit may draw a different amount of current to maintain its target temperature.

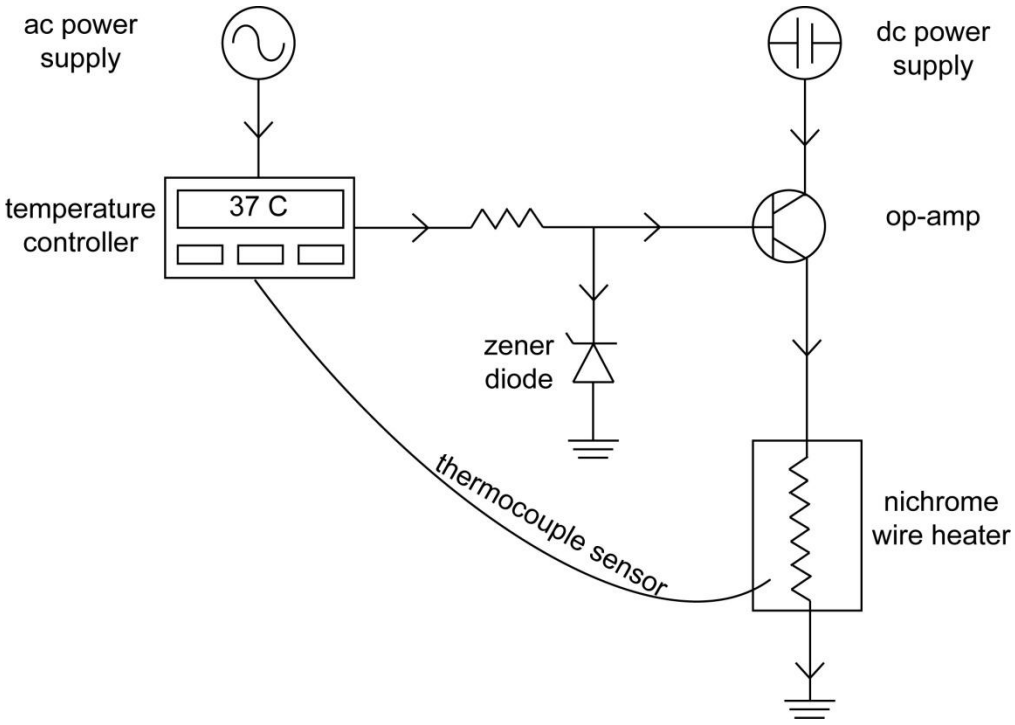

Figure 30: Electrical circuit design for the sample heater device

3. Image Processing Single-particle Tracking Program

Background

Kinesin stepping along microtubules is a stochastic process. The steps, being 8nm in size, are well below the diffraction limit of visible light and the motor may take 50 steps or 500 steps before it detaches. In order to determine mean motility parameters for such a

process, we need to look at the full range of measurements for the motility parameter of interest and study the distribution of these measurements. In single molecule motility assays, this is often done by collecting information from each motility event in an assay and plotting a histogram for the parameter of interest. The profile of the histogram then gives us an idea of the distribution of events in the assay, i.e. 5% of the motors run up to 5μm before detaching. In order to use statistical tools and calculate a mean from the fit of an appropriate mathematical function to the histogram, we require a large data set. This means tracking single molecules by hand to obtain 1000 or more data points- an activity that not only lacks creativity but can be very time consuming. When I began performing single molecule motility assays, I decided to write a simple computer program to track events and consolidate the information for individual events in a format that can be easily used as input to a commercial statistical program such as OriginLab (Northampton, MA). The requirements for such a program to be successful would be for it to

1. Accurately identify the fluorescent particle of interest

2. Track its position through several frames and

3. Store the positional information in a useful format, all within a reasonable amount of time.

Other important features would be that different sized particles can be tracked, different signal-to-noise ratios can be accommodated, photo-blinking can be overlooked and multiple movie sequences recorded in the same field of view can be analyzed sequentially without requiring user input for each of the movies.

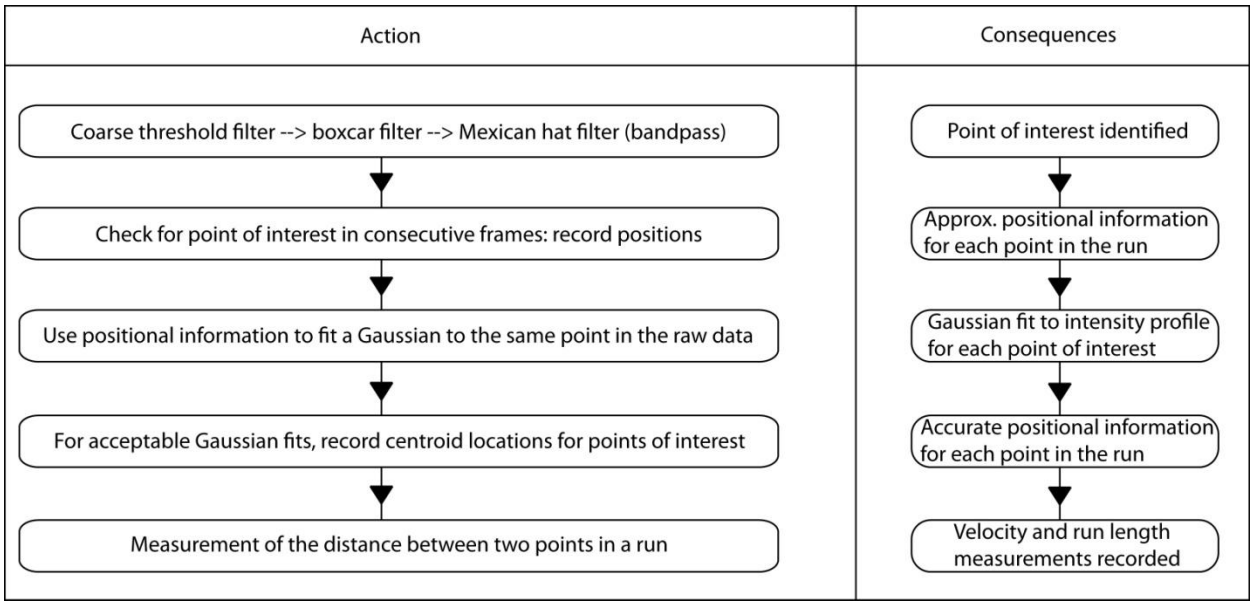

Figure 31: Algorithm for single particle tracking image-processing program in matlab

Algorithm

The process outline for identifying the first point and consecutive points in a single run is shown in Figure 31. The idea is that within a selected region of interest, the program will filter out noise below a certain threshold, identify points of interest, track each one through several frames (if they are, in fact, moving) and record the tracked position for each event. In the end the program calculates the velocity and run length for each event, generates an ASCII file with the data and also a graphical output for the distribution of events and where the events were observed on a microtubule. The running time for tracking events in a minute-long single molecule assay movie is about 1 minute. The program can also correctly identify events that are separated by photo-blinking and concatenate them together. It is easy to change thresholds for filtering, size limit for particles and if desired, criteria for recording measurements.

CHAPTER 5

Conclusions and Future Work

In cells, kinesin-1 preferentially translocates along a subset of microtubules that are decorated by a combination of PTMs. It has long been hypothesized that these PTMs are a cause for preferential motility along the microtubules. The goal of our study was to identify the means by which kinesin-1 differentiates between microtubules based on their PTMs. Our hypothesis was that intra-cellular cargo traffic along microtubules is regulated by the direct interaction of cargo-carrying kinesin with PTMs on microtubules. *In vivo*, the PTMs most commonly associated with the preferential motility of kinesin-1 are α-tubulin acetylation and detyrosination. We therefore set out to investigate the direct effects of α-tubulin acetylation and detyrosination on kinesin-1 motility. The theme of our experiments was to perform *in vitro* motility assays with purified components such that we would be able to isolate the effects of individual PTMs before looking at them in combination. This is a challenging task because the modifications seldom exist in isolation *in vivo*. This is also the aspect of studying PTMs *in vivo* that has made it difficult to ascertain the role of each one with complete certainty. We were able to independently control α-tubulin acetylation and detyrosination with the use of *in vitro* enzyme treatment. Combinatorial use of modifying enzymes allowed us to generate differentially modified pools of tubulin, which were then used to polymerize modified or unmodified microtubules.

In our study, we performed *in vitro* single-molecule motility assays using TIRF to directly observe kinesin-1 motility on modified and unmodified microtubules. The assays allow us to work with limited quantities of material to obtain large, robust data sets that can accurately represent the stochastic stepping nature of kinesin-1. Measurements of velocity, run length and binding of the motor were used as parameters to characterize changes in motility behavior. No significant change in motility behavior for kinesin-1 on

acetylated or deacetylated microtubules was observed. We measured a mean velocity of 0.67 ± 0.15 μm/s on acetylated microtubules and 0.69 ± 0.19 μm/s on deacetylated microtubules. Mean run lengths were measured to be 0.55 ± 0.33 μm on acetylated microtubules and 0.50 ± 0.43 μm on deacetylated microtubules. Mean landing rate, indicating kinesin-binding, was measured to be 3.84 ± 1.00 events/μm/min on deacetylated microtubules and 3.72 ± 1.48 on acetylated microtubules. We further extended our study to investigate the combined effects of α-tubulin acetylation and detyrosination on kinesin-1 motility. Our results indicate that there is no significant change in kinesin-1 motility directly resulting from a combination of acetylation and detyrosination. Mean velocity on acetylated detyrosinated microtubules was 0.53 ± 0.19 μm/s and on acetylated-detyrosinated microtubules, it was 0.46 ± 0.18 μm/s. The mean run length for kinesin-1 on acetylated-tyrosinated microtubules was 0.54 ± 0.42 μm and on acetylated-detyrosinated microtubules, it was 0.52 ± 0.41 μm. Mean landing rate on acetylated tyrosinated microtubules was 1.50 ± 0.40 events/ μm/ min and on acetylated-detyrosinated microtubules, the landing rate was 1.70 ± 0.51 event/ μm/ min. In contrast to previous work, the only change observed was upon addition of 10-fold diluted COS cell lysate in the assay which appeared to cause an increase in the binding for kinesin-1 to tyrosinated microtubules. From our results so far, it appears that the kinesin-1 motor domain itself is not capable of recognizing α-tubulin acetylation or detyrosination, independently or in combination, as stand-alone traffic signals. Components from the lysate such as MAPs may contribute to the changes in kinesin motility by preferentially binding to differentially modified microtubules at sub-stoichiometric ratios. As far as the direct effects of tubulin PTMs on kinesin-1, presumably there are other associated modifications, likely polyglutamylation of α- and β-tubulin CTTs that are more likely to interact with the motor due to their spatial reach. This is the only other modification found to be highly enriched in the axonal subset of microtubules where α-tubulin acetylation and detyrosination are concurrent and kinesin-1 motility is preferentially recruited.

In order to take the study further, it is likely necessary to modify the tubulin for our assays so as to incorporate α- and β-tubulin polyglutamylation. Polyglutamylation has previously been shown to influence the distribution of kinesin-13 in cells (147) and the

activity of microtubule-severing protein, spastin *in vitro* (127). It is also quite possible that specific combinations of the right PTMs and the right MAPs are required to enable preferential motility and particularly in neuronal cells- the observed compartmentalization of kinesin-1. This means that each of the modifications, independently or in combination with other modifications, could alter the binding of kinesin-1 or MAPs to affect motility along the microtubule-based transport system. Potentially, such a mechanism would provide many more levels of regulation which could be fine-tuned through both, the extent of the modifications and the concentration of the MAPs. This will have to be tested methodically, one modification and one MAP at a time.

BIBLIOGRAPHY

1. Rogers, S. L. and Gelfand, V. I. 2000. Membrane trafficking, organelle transport, and the cytoskeleton. Curr Opin Cell Biol 12: 57-62
2. Hirokawa, N. 1996. The molecular mechanism of organelle transport along microtubules: the identification and characterization of KIFs (kinesin superfamily proteins). Cell Struct Funct 21: 357-67
3. Ross, J. L., Ali, M. Y. and Warshaw, D. M. 2008. Cargo transport: molecular motors navigate a complex cytoskeleton. Curr Opin Cell Biol 20: 41-7
4. Verhey, K. J., Kaul, N. and Soppina, V. 2011. Kinesin assembly and movement in cells. Annu Rev Biophys 40: 267-88
5. Nakata, T. and Hirokawa, N. 2003. Microtubules provide directional cues for polarized axonal transport through interaction with kinesin motor head. J Cell Biol 162: 1045-55
6. Nakata, T., Terada, S. and Hirokawa, N. 1998. Visualization of the dynamics of synaptic vesicle and plasma membrane proteins in living axons. J Cell Biol 140: 659-74
7. Hwang, P. M., Fotuhi, M., Bredt, D. S., Cunningham, A. M. and Snyder, S. H. 1993. Contrasting immunohistochemical localizations in rat brain of two novel K+ channels of the Shab subfamily. J Neurosci 13: 1569-76
8. Rolls, M. M. 2011. Neuronal polarity in Drosophila: sorting out axons and dendrites. Dev Neurobiol 71: 419-29
9. Wittmann, T. and Desai, A. 2005. Microtubule cytoskeleton: a new twist at the end. Curr Biol 15: R126-9
10. Katsuki, T., Joshi, R., Ailani, D. and Hiromi, Y. 2011. Compartmentalization within neurites: its mechanisms and implications. Dev Neurobiol 71: 458-73
11. Rolls, M. M., Satoh, D., Clyne, P. J., Henner, A. L., Uemura, T. and Doe, C. Q. 2007. Polarity and intracellular compartmentalization of Drosophila neurons. Neural Dev 2: 7
12. De Vos, K. J., Grierson, A. J., Ackerley, S. and Miller, C. C. 2008. Role of axonal transport in neurodegenerative diseases. Annu Rev Neurosci 31: 151-73
13. Kamal, A., Stokin, G. B., Yang, Z., Xia, C. H. and Goldstein, L. S. 2000. Axonal transport of amyloid precursor protein is mediated by direct binding to the kinesin light chain subunit of kinesin-I. Neuron 28: 449-59
14. Gardiner, J., Barton, D., Marc, J. and Overall, R. 2007. Potential role of tubulin acetylation and microtubule-based protein trafficking in familial dysautonomia. Traffic 8: 1145-9
15. Falzone, T. L., Gunawardena, S., McCleary, D., Reis, G. F. and Goldstein, L. S. 2010. Kinesin-1 transport reductions enhance human tau hyperphosphorylation, aggregation and neurodegeneration in animal models of tauopathies. Hum Mol Genet 19: 4399-408
16. Salinas, S., Bilsland, L. G. and Schiavo, G. 2008. Molecular landmarks along the axonal route: axonal transport in health and disease. Curr Opin Cell Biol 20: 445-53
17. Yu, Y. and Feng, Y. M. 2010. The role of kinesin family proteins in tumorigenesis and progression: potential biomarkers and molecular targets for cancer therapy. Cancer 116: 5150-60

18. Schoenenberger, C. A., Mannherz, H. G. and Jockusch, B. M. 2011. Actin: from structural plasticity to functional diversity. Eur J Cell Biol 90: 797-804
19. Toomre, D., Keller, P., White, J., Olivo, J. C. and Simons, K. 1999. Dual-color visualization of trans-Golgi network to plasma membrane traffic along microtubules in living cells. J Cell Sci 112 (Pt 1): 21-33
20. Avila, J. 1992. Microtubule functions. Life Sci 50: 327-34
21. Herrmann, H., Bar, H., Kreplak, L., Strelkov, S. V. and Aebi, U. 2007. Intermediate filaments: from cell architecture to nanomechanics. Nat Rev Mol Cell Biol 8: 562-73
22. Herrmann, H., Strelkov, S. V., Burkhard, P. and Aebi, U. 2009. Intermediate filaments: primary determinants of cell architecture and plasticity. J Clin Invest 119: 1772-83
23. Pilling, A. D., Horiuchi, D., Lively, C. M. and Saxton, W. M. 2006. Kinesin-1 and Dynein are the primary motors for fast transport of mitochondria in Drosophila motor axons. Mol Biol Cell 17: 2057-68
24. Bridgman, P. C. 2004. Myosin-dependent transport in neurons. J Neurobiol 58: 164-74
25. Endow, S. A., Kull, F. J. and Liu, H. 2010. Kinesins at a glance. J Cell Sci 123: 3420-4
26. Hirokawa, N. 1982. Cross-linker system between neurofilaments, microtubules, and membranous organelles in frog axons revealed by the quick-freeze, deep-etching method. J Cell Biol 94: 129-42
27. Vale, R. D. and Milligan, R. A. 2000. The way things move: looking under the hood of molecular motor proteins. Science 288: 88-95
28. Vale, R. D., Reese, T. S. and Sheetz, M. P. 1985. Identification of a novel force-generating protein, kinesin, involved in microtubule-based motility. Cell 42: 39-50
29. Bloom, G. S., Wagner, M. C., Pfister, K. K. and Brady, S. T. 1988. Native structure and physical properties of bovine brain kinesin and identification of the ATP-binding subunit polypeptide. Biochemistry 27: 3409-16
30. Lawrence, C. J., Dawe, R. K., Christie, K. R., Cleveland, D. W., Dawson, S. C., Endow, S. A., Goldstein, L. S., Goodson, H. V., Hirokawa, N., Howard, J., Malmberg, R. L., McIntosh, J. R., Miki, H., Mitchison, T. J., Okada, Y., Reddy, A. S., Saxton, W. M., Schliwa, M., Scholey, J. M., Vale, R. D., Walczak, C. E. and Wordeman, L. 2004. A standardized kinesin nomenclature. J Cell Biol 167: 19-22
31. Verhey, K. J. and Hammond, J. W. 2009. Traffic control: regulation of kinesin motors. Nat Rev Mol Cell Biol 10: 765-77
32. Hirokawa, N., Niwa, S. and Tanaka, Y. 2010. Molecular motors in neurons: transport mechanisms and roles in brain function, development, and disease. Neuron 68: 610-38
33. Scholey, J. M., Heuser, J., Yang, J. T. and Goldstein, L. S. 1989. Identification of globular mechanochemical heads of kinesin. Nature 338: 355-7
34. Woehlke, G. and Schliwa, M. 2000. Walking on two heads: the many talents of kinesin. Nat Rev Mol Cell Biol 1: 50-8
35. Hirose, K., Lockhart, A., Cross, R. A. and Amos, L. A. 1995. Nucleotide-dependent angular change in kinesin motor domain bound to tubulin. Nature 376: 277-9
36. Alonso, M. C., Drummond, D. R., Kain, S., Hoeng, J., Amos, L. and Cross, R. A. 2007. An ATP gate controls tubulin binding by the tethered head of kinesin-1. Science 316: 120-3
37. Coy, D. L., Wagenbach, M. and Howard, J. 1999. Kinesin takes one 8-nm step for each ATP that it hydrolyzes. J Biol Chem 274: 3667-71
38. Hancock, W. O. and Howard, J. 1998. Processivity of the motor protein kinesin requires two heads. J Cell Biol 140: 1395-405
39. Clancy, B. E., Behnke-Parks, W. M., Andreasson, J. O., Rosenfeld, S. S. and Block, S. M. 2011. A universal pathway for kinesin stepping. Nat Struct Mol Biol 18: 1020-7

40. Block, S. M. 2007. Kinesin motor mechanics: binding, stepping, tracking, gating, and limping. Biophys J 92: 2986-95
41. Woehlke, G., Ruby, A. K., Hart, C. L., Ly, B., Hom-Booher, N. and Vale, R. D. 1997. Microtubule interaction site of the kinesin motor. Cell 90: 207-16
42. Kozielski, F., Sack, S., Marx, A., Thormahlen, M., Schonbrunn, E., Biou, V., Thompson, A., Mandelkow, E. M. and Mandelkow, E. 1997. The crystal structure of dimeric kinesin and implications for microtubule-dependent motility. Cell 91: 985-94
43. Wozniak, M. J. and Allan, V. J. 2006. Cargo selection by specific kinesin light chain 1 isoforms. EMBO J 25: 5457-68
44. Kikkawa, M., Ishikawa, T., Wakabayashi, T. and Hirokawa, N. 1995. Three-dimensional structure of the kinesin head-microtubule complex. Nature 376: 274-7
45. Sosa, H., Asenjo, A. B. and Peterman, E. J. 2010. Structure and dynamics of the kinesin-microtubule interaction revealed by fluorescence polarization microscopy. Methods Cell Biol 95: 505-19
46. Hoenger, A., Sablin, E. P., Vale, R. D., Fletterick, R. J. and Milligan, R. A. 1995. Three-dimensional structure of a tubulin-motor-protein complex. Nature 376: 271-4
47. Meyhofer, E. and Howard, J. 1995. The force generated by a single kinesin molecule against an elastic load. Proc Natl Acad Sci U S A 92: 574-8
48. Hoenger, A. and Milligan, R. A. 1997. Motor domains of kinesin and ncd interact with microtubule protofilaments with the same binding geometry. J Mol Biol 265: 553-64
49. Vale, R. D., Funatsu, T., Pierce, D. W., Romberg, L., Harada, Y. and Yanagida, T. 1996. Direct observation of single kinesin molecules moving along microtubules. Nature 380: 451-3
50. Lakamper, S. and Meyhofer, E. 2005. The E-hook of tubulin interacts with kinesin's head to increase processivity and speed. Biophys J 89: 3223-34
51. Hirokawa, N. and Noda, Y. 2008. Intracellular transport and kinesin superfamily proteins, KIFs: structure, function, and dynamics. Physiol Rev 88: 1089-118
52. Stephens, R. E. and Edds, K. T. 1976. Microtubules: structure, chemistry, and function. Physiol Rev 56: 709-77
53. Erickson, H. P. 1975. The structure and assembly of microtubules. Ann N Y Acad Sci 253: 60-77
54. Desai, A. and Mitchison, T. J. 1997. Microtubule polymerization dynamics. Annu Rev Cell Dev Biol 13: 83-117
55. Nogales, E., Wolf, S. G. and Downing, K. H. 1998. Structure of the alpha beta tubulin dimer by electron crystallography. Nature 391: 199-203
56. Downing, K. H. and Nogales, E. 1999. Crystallographic structure of tubulin: implications for dynamics and drug binding. Cell Struct Funct 24: 269-75
57. Wang, H. W. and Nogales, E. 2005. Nucleotide-dependent bending flexibility of tubulin regulates microtubule assembly. Nature 435: 911-5
58. Amos, L. A. and Schlieper, D. 2005. Microtubules and maps. Adv Protein Chem 71: 257-98
59. Takemura, R., Okabe, S., Umeyama, T., Kanai, Y., Cowan, N. J. and Hirokawa, N. 1992. Increased microtubule stability and alpha tubulin acetylation in cells transfected with microtubule-associated proteins MAP1B, MAP2 or tau. J Cell Sci 103 (Pt 4): 953-64
60. Panda, D., Miller, H. P. and Wilson, L. 1999. Rapid treadmilling of brain microtubules free of microtubule-associated proteins in vitro and its suppression by tau. Proc Natl Acad Sci U S A 96: 12459-64
61. Dixit, R., Ross, J. L., Goldman, Y. E. and Holzbaur, E. L. 2008. Differential regulation of dynein and kinesin motor proteins by tau. Science 319: 1086-9

62. Sudo, H. and Baas, P. W. 2011. Strategies for diminishing katanin-based loss of microtubules in tauopathic neurodegenerative diseases. Hum Mol Genet 20: 763-78
63. Morfini, G., Pigino, G., Mizuno, N., Kikkawa, M. and Brady, S. T. 2007. Tau binding to microtubules does not directly affect microtubule-based vesicle motility. J Neurosci Res 85: 2620-30
64. Cleveland, D. W. and Sullivan, K. F. 1985. Molecular biology and genetics of tubulin. Annual Review of Biochemistry 54: 331-65
65. Khodiyar, V. K., Maltais, L. J., Ruef, B. J., Sneddon, K. M., Smith, J. R., Shimoyama, M., Cabral, F., Dumontet, C., Dutcher, S. K., Harvey, R. J., Lafanechere, L., Murray, J. M., Nogales, E., Piquemal, D., Stanchi, F., Povey, S. and Lovering, R. C. 2007. A revised nomenclature for the human and rodent alpha-tubulin gene family. Genomics 90: 285-9
66. Luduena, R. F. 1998. Multiple forms of tubulin: different gene products and covalent modifications. Int Rev Cytol 178: 207-75
67. Verdier-Pinard, P., Pasquier, E., Xiao, H., Burd, B., Villard, C., Lafitte, D., Miller, L. M., Angeletti, R. H., Horwitz, S. B. and Braguer, D. 2009. Tubulin proteomics: towards breaking the code. Anal Biochem 384: 197-206
68. Callahan, R. C., Shalke, G. and Gorovsky, M. A. 1984. Developmental rearrangements associated with a single type of expressed alpha-tubulin gene in Tetrahymena. Cell 36: 441-5
69. McGrath, K. E., Yu, S. M., Heruth, D. P., Kelly, A. A. and Gorovsky, M. A. 1994. Regulation and evolution of the single alpha-tubulin gene of the ciliate Tetrahymena thermophila. Cell Motility & the Cytoskeleton 27: 272-83
70. Gaertig, J., Thatcher, T. H., McGrath, K. E., Callahan, R. C. and Gorovsky, M. A. 1993. Perspectives on tubulin isotype function and evolution based on the observation that Tetrahymena thermophila microtubules contain a single alpha- and beta-tubulin. Cell Motility & the Cytoskeleton 25: 243-53
71. Gaertig, J., Cruz, M. A., Bowen, J., Gu, L., Pennock, D. G. and Gorovsky, M. A. 1995. Acetylation of lysine 40 in alpha-tubulin is not essential in Tetrahymena thermophila. Journal of Cell Biology 129: 1301-10
72. Westermann, S. and Weber, K. 2003. Post-translational modifications regulate microtubule function. Nature reviews 4: 938-47
73. Verhey, K. J. and Gaertig, J. 2007. The tubulin code. Cell cycle (Georgetown, Tex 6: 2152-60
74. Wloga, D. and Gaertig, J. 2010. Post-translational modifications of microtubules. J Cell Sci 123: 3447-55
75. Westermann, S. and Weber, K. 2003. Post-translational modifications regulate microtubule function. Nature Reviews Molecular Cell Biology 4: 938-47
76. L'Hernault, S. W. and Rosenbaum, J. L. 1985. Chlamydomonas alpha-tubulin is posttranslationally modified by acetylation on the epsilon-amino group of a lysine. Biochemistry 24: 473-8
77. Janke, C. and Bulinski, J. C. 2011. Post-translational regulation of the microtubule cytoskeleton: mechanisms and functions. Nat Rev Mol Cell Biol 12: 773-86
78. Lowe, J., Li, H., Downing, K. H. and Nogales, E. 2001. Refined structure of alpha beta-tubulin at 3.5 A resolution. J Mol Biol 313: 1045-57
79. Burns, R. G. 1991. Alpha-, beta-, and gamma-tubulins: sequence comparisons and structural constraints. Cell Motil Cytoskeleton 20: 181-9
80. Tuszynski, J. A., Carpenter, E. J., Huzil, J. T., Malinski, W., Luchko, T. and Luduena, R. F. 2006. The evolution of the structure of tubulin and its potential consequences for the role and function of microtubules in cells and embryos. Int J Dev Biol 50: 341-58

81. Maruta, H., Greer, K. and Rosenbaum, J. L. 1986. The acetylation of alpha-tubulin and its relationship to the assembly and disassembly of microtubules. Journal of Cell Biology 103: 571-9
82. Akella, J. S., Wloga, D., Kim, J., Starostina, N. G., Lyons-Abbott, S., Morrissette, N. S., Dougan, S. T., Kipreos, E. T. and Gaertig, J. 2010. MEC-17 is an alpha-tubulin acetyltransferase. Nature 467: 218-22
83. Shida, T., Cueva, J. G., Xu, Z., Goodman, M. B. and Nachury, M. V. 2010. The major alpha-tubulin K40 acetyltransferase alphaTAT1 promotes rapid ciliogenesis and efficient mechanosensation. Proc Natl Acad Sci U S A 107: 21517-22
84. Matsuyama, A., Shimazu, T., Sumida, Y., Saito, A., Yoshimatsu, Y., Seigneurin-Berny, D., Osada, H., Komatsu, Y., Nishino, N., Khochbin, S., Horinouchi, S. and Yoshida, M. 2002. In vivo destabilization of dynamic microtubules by HDAC6-mediated deacetylation. EMBO J 21: 6820-31
85. North, B. J., Marshall, B. L., Borra, M. T., Denu, J. M. and Verdin, E. 2003. The human Sir2 ortholog, SIRT2, is an NAD+-dependent tubulin deacetylase. Mol Cell 11: 437-44
86. Hubbert, C., Guardiola, A., Shao, R., Kawaguchi, Y., Ito, A., Nixon, A., Yoshida, M., Wang, X. F. and Yao, T. P. 2002. HDAC6 is a microtubule-associated deacetylase. Nature 417: 455-8
87. Chu, C. W., Hou, F., Zhang, J., Phu, L., Loktev, A. V., Kirkpatrick, D. S., Jackson, P. K., Zhao, Y. and Zou, H. 2011. A novel acetylation of beta-tubulin by San modulates microtubule polymerization via down-regulating tubulin incorporation. Molecular Biology of the Cell 22: 448-56
88. Argarana, C. E., Barra, H. S. and Caputto, R. 1978. Release of [14C]tyrosine from tubulinyl-[14C]tyrosine by brain extract. Separation of a carboxypeptidase from tubulin-tyrosine ligase. Molecular & Cellular Biochemistry 19: 17-21
89. Murofushi, H. 1980. Purification and characterization of tubulin-tyrosine ligase from porcine brain. Journal of Biochemistry 87: 979-84
90. Schroder, H. C., Wehland, J. and Weber, K. 1985. Purification of brain tubulin-tyrosine ligase by biochemical and immunological methods. J Cell Biol 100: 276-81
91. Szyk, A., Deaconescu, A. M., Piszczek, G. and Roll-Mecak, A. 2011. Tubulin tyrosine ligase structure reveals adaptation of an ancient fold to bind and modify tubulin. Nat Struct Mol Biol 18: 1250-8
92. Alexander, J. E., Hunt, D. F., Lee, M. K., Shabanowitz, J., Michel, H., Berlin, S. C., MacDonald, T. L., Sundberg, R. J., Rebhun, L. I. and Frankfurter, A. 1991. Characterization of posttranslational modifications in neuron-specific class III beta-tubulin by mass spectrometry. Proc Natl Acad Sci U S A 88: 4685-9
93. Edde, B., Rossier, J., Le Caer, J. P., Desbruyeres, E., Gros, F. and Denoulet, P. 1990. Posttranslational glutamylation of alpha-tubulin. Science 247: 83-5
94. Rudiger, M., Plessman, U., Kloppel, K. D., Wehland, J. and Weber, K. 1992. Class II tubulin, the major brain beta tubulin isotype is polyglutamylated on glutamic acid residue 435. FEBS Lett 308: 101-5
95. Redeker, V., Levilliers, N., Schmitter, J. M., Le Caer, J. P., Rossier, J., Adoutte, A. and Bre, M. H. 1994. Polyglycylation of tubulin: a posttranslational modification in axonemal microtubules. Science 266: 1688-91
96. Bre, M. H., Redeker, V., Vinh, J., Rossier, J. and Levilliers, N. 1998. Tubulin polyglycylation: differential posttranslational modification of dynamic cytoplasmic and stable axonemal microtubules in paramecium. Mol Biol Cell 9: 2655-65
97. Redeker, V., Levilliers, N., Vinolo, E., Rossier, J., Jaillard, D., Burnette, D., Gaertig, J. and Bre, M. H. 2005. Mutations of tubulin glycylation sites reveal cross-talk between the C termini of alpha- and beta-tubulin and affect the ciliary matrix in Tetrahymena. J Biol Chem 280: 596-606

98. Regnard, C., Audebert, S., Desbruyeres, Denoulet, P. and Edde, B. 1998. Tubulin polyglutamylase: partial purification and enzymatic properties. Biochemistry 37: 8395-404
99. Regnard, C., Desbruyeres, E., Denoulet, P. and Edde, B. 1999. Tubulin polyglutamylase: isozymic variants and regulation during the cell cycle in HeLa cells. J Cell Sci 112 (Pt 23): 4281-9
100. Janke, C., Rogowski, K., Wloga, D., Regnard, C., Kajava, A. V., Strub, J. M., Temurak, N., van Dijk, J., Boucher, D., van Dorsselaer, A., Suryavanshi, S., Gaertig, J. and Edde, B. 2005. Tubulin polyglutamylase enzymes are members of the TTL domain protein family. Science 308: 1758-62
101. van Dijk, J., Rogowski, K., Miro, J., Lacroix, B., Edde, B. and Janke, C. 2007. A targeted multienzyme mechanism for selective microtubule polyglutamylation. Mol Cell 26: 437-48
102. Kimura, Y., Kurabe, N., Ikegami, K., Tsutsumi, K., Konishi, Y., Kaplan, O. I., Kunitomo, H., Iino, Y., Blacque, O. E. and Setou, M. 2010. Identification of tubulin deglutamylase among Caenorhabditis elegans and mammalian cytosolic carboxypeptidases (CCPs). J Biol Chem 285: 22936-41
103. Berezniuk, I., Vu, H. T., Lyons, P. J., Sironi, J. J., Xiao, H., Burd, B., Setou, M., Angeletti, R. H., Ikegami, K. and Fricker, L. D. 2012. Cytosolic Carboxypeptidase 1 Is Involved in Processing alpha- and beta-Tubulin. J Biol Chem 287: 6503-17
104. Rogowski, K., Juge, F., van Dijk, J., Wloga, D., Strub, J. M., Levilliers, N., Thomas, D., Bre, M. H., Van Dorsselaer, A., Gaertig, J. and Janke, C. 2009. Evolutionary divergence of enzymatic mechanisms for posttranslational polyglycylation. Cell 137: 1076-87
105. Wloga, D., Webster, D. M., Rogowski, K., Bre, M. H., Levilliers, N., Jerka-Dziadosz, M., Janke, C., Dougan, S. T. and Gaertig, J. 2009. TTLL3 Is a tubulin glycine ligase that regulates the assembly of cilia. Dev Cell 16: 867-76
106. Janke, C. and Kneussel, M. 2010. Tubulin post-translational modifications: encoding functions on the neuronal microtubule cytoskeleton. Trends Neurosci 33: 362-72
107. Hammond, J. W., Cai, D. and Verhey, K. J. 2008. Tubulin modifications and their cellular functions. Current Opinion in Cell Biology 20: 71-6
108. Ikegami, K. and Setou, M. 2010. Unique post-translational modifications in specialized microtubule architecture. Cell Struct Funct 35: 15-22
109. Cai, D., McEwen, D. P., Martens, J. R., Meyhofer, E. and Verhey, K. J. 2009. Single molecule imaging reveals differences in microtubule track selection between Kinesin motors. PLoS Biol 7: e1000216
110. Hammond, J. W., Cai, D. and Verhey, K. J. 2008. Tubulin modifications and their cellular functions. Current opinion in cell biology 20: 71-6
111. Lakamper, S. and Meyhofer, E. 2006. Back on track - on the role of the microtubule for kinesin motility and cellular function. Journal of muscle research and cell motility 27: 161-71
112. Arce, C. A., Rodriguez, J. A., Barra, H. S. and Caputo, R. 1975. Incorporation of L-tyrosine, L-phenylalanine and L-3,4-dihydroxyphenylalanine as single units into rat brain tubulin. European Journal of Biochemistry 59: 145-9
113. Craig, A. M. and Banker, G. 1994. Neuronal polarity. Annu Rev Neurosci 17: 267-310
114. Craig, A. M., Jareb, M. and Banker, G. 1992. Neuronal polarity. Curr Opin Neurobiol 2: 602-6
115. Dotti, C. G. and Simons, K. 1990. Polarized sorting of viral glycoproteins to the axon and dendrites of hippocampal neurons in culture. Cell 62: 63-72
116. Verhey, K. J., Meyer, D., Deehan, R., Blenis, J., Schnapp, B. J., Rapoport, T. A. and Margolis, B. 2001. Cargo of kinesin identified as JIP scaffolding proteins and associated signaling molecules. J Cell Biol 152: 959-70
117. Reed, N. A., Cai, D., Blasius, T. L., Jih, G. T., Meyhofer, E., Gaertig, J. and Verhey, K. J. 2006. Microtubule acetylation promotes kinesin-1 binding and transport. Curr Biol 16: 2166-72

118. Jacobson, C., Schnapp, B. and Banker, G. A. 2006. A change in the selective translocation of the Kinesin-1 motor domain marks the initial specification of the axon. Neuron 49: 797-804
119. Huang, C. F. and Banker, G. 2011. The Translocation Selectivity of the Kinesins that Mediate Neuronal Organelle Transport. Traffic
120. Cambray-Deakin, M. A. and Burgoyne, R. D. 1987. Posttranslational modifications of alpha-tubulin: acetylated and detyrosinated forms in axons of rat cerebellum. J Cell Biol 104: 1569-74
121. Cambray-Deakin, M. A. and Burgoyne, R. D. 1987. Acetylated and detyrosinated alpha-tubulins are co-localized in stable microtubules in rat meningeal fibroblasts. Cell Motil Cytoskeleton 8: 284-91
122. Dunn, S., Morrison, E. E., Liverpool, T. B., Molina-Paris, C., Cross, R. A., Alonso, M. C. and Peckham, M. 2008. Differential trafficking of Kif5c on tyrosinated and detyrosinated microtubules in live cells. J Cell Sci 121: 1085-95
123. Sudo, H. and Baas, P. W. 2010. Acetylation of microtubules influences their sensitivity to severing by katanin in neurons and fibroblasts. J Neurosci 30: 7215-26
124. Peris, L., Thery, M., Faure, J., Saoudi, Y., Lafanechere, L., Chilton, J. K., Gordon-Weeks, P., Galjart, N., Bornens, M., Wordeman, L., Wehland, J., Andrieux, A. and Job, D. 2006. Tubulin tyrosination is a major factor affecting the recruitment of CAP-Gly proteins at microtubule plus ends. Journal of Cell Biology 174: 839-49
125. Bieling, P., Kandels-Lewis, S., Telley, I. A., van Dijk, J., Janke, C. and Surrey, T. 2008. CLIP-170 tracks growing microtubule ends by dynamically recognizing composite EB1/tubulin-binding sites. J Cell Biol 183: 1223-33
126. Konishi, Y. and Setou, M. 2009. Tubulin tyrosination navigates the kinesin-1 motor domain to axons. Nat Neurosci 12: 559-67
127. Lacroix, B., van Dijk, J., Gold, N. D., Guizetti, J., Aldrian-Herrada, G., Rogowski, K., Gerlich, D. W. and Janke, C. 2010. Tubulin polyglutamylation stimulates spastin-mediated microtubule severing. J Cell Biol 189: 945-54
128. Dompierre, J. P., Godin, J. D., Charrin, B. C., Cordelieres, F. P., King, S. J., Humbert, S. and Saudou, F. 2007. Histone deacetylase 6 inhibition compensates for the transport deficit in Huntington's disease by increasing tubulin acetylation. Journal of Neuroscience 27: 3571-83
129. Bobrowska, A., Paganetti, P., Matthias, P. and Bates, G. P. 2011. Hdac6 knock-out increases tubulin acetylation but does not modify disease progression in the R6/2 mouse model of Huntington's disease. PLoS One 6: e20696
130. Zilberman, Y., Ballestrem, C., Carramusa, L., Mazitschek, R., Khochbin, S. and Bershadsky, A. 2009. Regulation of microtubule dynamics by inhibition of the tubulin deacetylase HDAC6. J Cell Sci 122: 3531-41
131. Kim, M. S., Kwon, H. J., Lee, Y. M., Baek, J. H., Jang, J. E., Lee, S. W., Moon, E. J., Kim, H. S., Lee, S. K., Chung, H. Y., Kim, C. W. and Kim, K. W. 2001. Histone deacetylases induce angiogenesis by negative regulation of tumor suppressor genes. Nat Med 7: 437-43
132. Johnstone, R. W. 2002. Histone-deacetylase inhibitors: novel drugs for the treatment of cancer. Nat Rev Drug Discov 1: 287-99
133. Koeller, K. M., Haggarty, S. J., Perkins, B. D., Leykin, I., Wong, J. C., Kao, M. C. and Schreiber, S. L. 2003. Chemical genetic modifier screens: small molecule trichostatin suppressors as probes of intracellular histone and tubulin acetylation. Chem Biol 10: 397-410
134. Ikegami, K., Heier, R. L., Taruishi, M., Takagi, H., Mukai, M., Shimma, S., Taira, S., Hatanaka, K., Morone, N., Yao, I., Campbell, P. K., Yuasa, S., Janke, C., Macgregor, G. R. and Setou, M. 2007. Loss of alpha-tubulin polyglutamylation in ROSA22 mice is associated with abnormal targeting of KIF1A and modulated synaptic function. Proceedings of the National Academy of Sciences of the United States of America 104: 3213-8

135. Akhmanova, A. and Hammer, J. A., 3rd. 2010. Linking molecular motors to membrane cargo. Curr Opin Cell Biol 22: 479-87
136. Gagnon, J. A. and Mowry, K. L. 2011. Molecular motors: directing traffic during RNA localization. Crit Rev Biochem Mol Biol 46: 229-39
137. Schuh, M. 2011. An actin-dependent mechanism for long-range vesicle transport. Nat Cell Biol 13: 1431-6
138. Gennerich, A. and Vale, R. D. 2009. Walking the walk: how kinesin and dynein coordinate their steps. Curr Opin Cell Biol 21: 59-67
139. Hirokawa, N. 2011. From electron microscopy to molecular cell biology, molecular genetics and structural biology: intracellular transport and kinesin superfamily proteins, KIFs: genes, structure, dynamics and functions. J Electron Microsc (Tokyo) 60 Suppl 1: S63-92
140. Yildiz, A., Tomishige, M., Gennerich, A. and Vale, R. D. 2008. Intramolecular strain coordinates kinesin stepping behavior along microtubules. Cell 134: 1030-41
141. Coppin, C. M., Finer, J. T., Spudich, J. A. and Vale, R. D. 1996. Detection of sub-8-nm movements of kinesin by high-resolution optical-trap microscopy. Proc Natl Acad Sci U S A 93: 1913-7
142. Bulinski, J. C., Richards, J. E. and Piperno, G. 1988. Posttranslational modifications of alpha tubulin: detyrosination and acetylation differentiate populations of interphase microtubules in cultured cells. Journal of Cell Biology 106: 1213-20
143. Schatten, G., Simerly, C., Asai, D. J., Szoke, E., Cooke, P. and Schatten, H. 1988. Acetylated alpha-tubulin in microtubules during mouse fertilization and early development. Dev Biol 130: 74-86
144. Rosenbaum, J. 2000. Cytoskeleton: functions for tubulin modifications at last. Curr Biol 10: R801-3
145. Fukushima, N., Furuta, D., Hidaka, Y., Moriyama, R. and Tsujiuchi, T. 2009. Post-translational modifications of tubulin in the nervous system. J Neurochem 109: 683-93
146. Zekert, N. and Fischer, R. 2009. The Aspergillus nidulans kinesin-3 UncA motor moves vesicles along a subpopulation of microtubules. Mol Biol Cell 20: 673-84
147. Ikegami, K., Heier, R. L., Taruishi, M., Takagi, H., Mukai, M., Shimma, S., Taira, S., Hatanaka, K., Morone, N., Yao, I., Campbell, P. K., Yuasa, S., Janke, C., Macgregor, G. R. and Setou, M. 2007. Loss of alpha-tubulin polyglutamylation in ROSA22 mice is associated with abnormal targeting of KIF1A and modulated synaptic function. Proceedings of the National Academy of Sciences of the United States of America 104: 3213-8
148. McGrath, K. E., Yu, S. M., Heruth, D. P., Kelly, A. A. and Gorovsky, M. A. 1994. Regulation and evolution of the single alpha-tubulin gene of the ciliate Tetrahymena thermophila. Cell Motil Cytoskeleton 27: 272-83
149. Cai, D., Verhey, K. J. and Meyhofer, E. 2007. Tracking single Kinesin molecules in the cytoplasm of mammalian cells. Biophys J 92: 4137-44
150. Gaertig, J. and Wloga, D. 2008. Ciliary tubulin and its post-translational modifications. Curr Top Dev Biol 85: 83-113
151. Nicastro, D., Schwartz, C., Pierson, J., Gaudette, R., Porter, M. E. and McIntosh, J. R. 2006. The molecular architecture of axonemes revealed by cryoelectron tomography. Science 313: 944-8
152. Pigino, G., Maheshwari, A., Bui, K. H., Shingyoji, C., Kamimura, S. and Ishikawa, T. 2012. Comparative structural analysis of eukaryotic flagella and cilia from Chlamydomonas, Tetrahymena, and sea urchins. J Struct Biol
153. Castoldi, M. and Popov, A. V. 2003. Purification of brain tubulin through two cycles of polymerization-depolymerization in a high-molarity buffer. Protein Expr Purif 32: 83-8

154. Gilbert, S. P., Webb, M. R., Brune, M. and Johnson, K. A. 1995. Pathway of processive ATP hydrolysis by kinesin. Nature 373: 671-6
155. Redeker, V. 2010. Mass spectrometry analysis of C-terminal posttranslational modifications of tubulins. Methods Cell Biol 95: 77-103
156. Hammond, J. W., Huang, C. F., Kaech, S., Jacobson, C., Banker, G. and Verhey, K. J. 2010. Posttranslational modifications of tubulin and the polarized transport of kinesin-1 in neurons. Mol Biol Cell 21: 572-83
157. Tannenbaum, J. and Slepecky, N. B. 1997. Localization of microtubules containing posttranslationally modified tubulin in cochlear epithelial cells during development. Cell Motil Cytoskeleton 38: 146-62
158. Poole, C. A., Zhang, Z. J. and Ross, J. M. 2001. The differential distribution of acetylated and detyrosinated alpha-tubulin in the microtubular cytoskeleton and primary cilia of hyaline cartilage chondrocytes. J Anat 199: 393-405
159. Akisaka, T., Yoshida, H. and Takigawa, T. 2011. Differential distribution of posttranslationally modified microtubules in osteoclasts. J Histochem Cytochem 59: 630-8
160. Kreitzer, G., Liao, G. and Gundersen, G. G. 1999. Detyrosination of tubulin regulates the interaction of intermediate filaments with microtubules in vivo via a kinesin-dependent mechanism. Molecular Biology of the Cell 10: 1105-18
161. Chapin, S. J. and Bulinski, J. C. 1991. Preparation and functional assay of pure populations of tyrosinated and detyrosinated tubulin. Methods Enzymol 196: 254-64
162. Gundersen, G. G., Kalnoski, M. H. and Bulinski, J. C. 1984. Distinct populations of microtubules: tyrosinated and nontyrosinated alpha tubulin are distributed differently in vivo. Cell 38: 779-89
163. Marx, A., Muller, J., Mandelkow, E. M., Hoenger, A. and Mandelkow, E. 2006. Interaction of kinesin motors, microtubules, and MAPs. J Muscle Res Cell Motil 27: 125-37
164. Thorn, K. S., Ubersax, J. A. and Vale, R. D. 2000. Engineering the processive run length of the kinesin motor. J Cell Biol 151: 1093-100
165. Wang, Z. and Sheetz, M. P. 2000. The C-terminus of tubulin increases cytoplasmic dynein and kinesin processivity. Biophys J 78: 1955-64
166. Kinosita, K., Jr., Itoh, H., Ishiwata, S., Hirano, K., Nishizaka, T. and Hayakawa, T. 1991. Dual-view microscopy with a single camera: real-time imaging of molecular orientations and calcium. J Cell Biol 115: 67-73